High Frequency Gravitational Wave Detection with Bulk Acoustic Wave Devices: From Technology to First Data

THE UNIVERSITY OF WESTERN AUSTRALIA

Maxim Goryachev
Eugene Ivanov
Mike Tobar

EQUS
Australian Research Council Centre of Excellence for Engineered Quantum Systems

Outline

Bulk Acoustic Wave (BAW) Technology
BAW as a GW Antenna
Current Status and First Results
Perspectives
Test of Fundamental Physics @ UWA

Quantum & Frequency Metrology

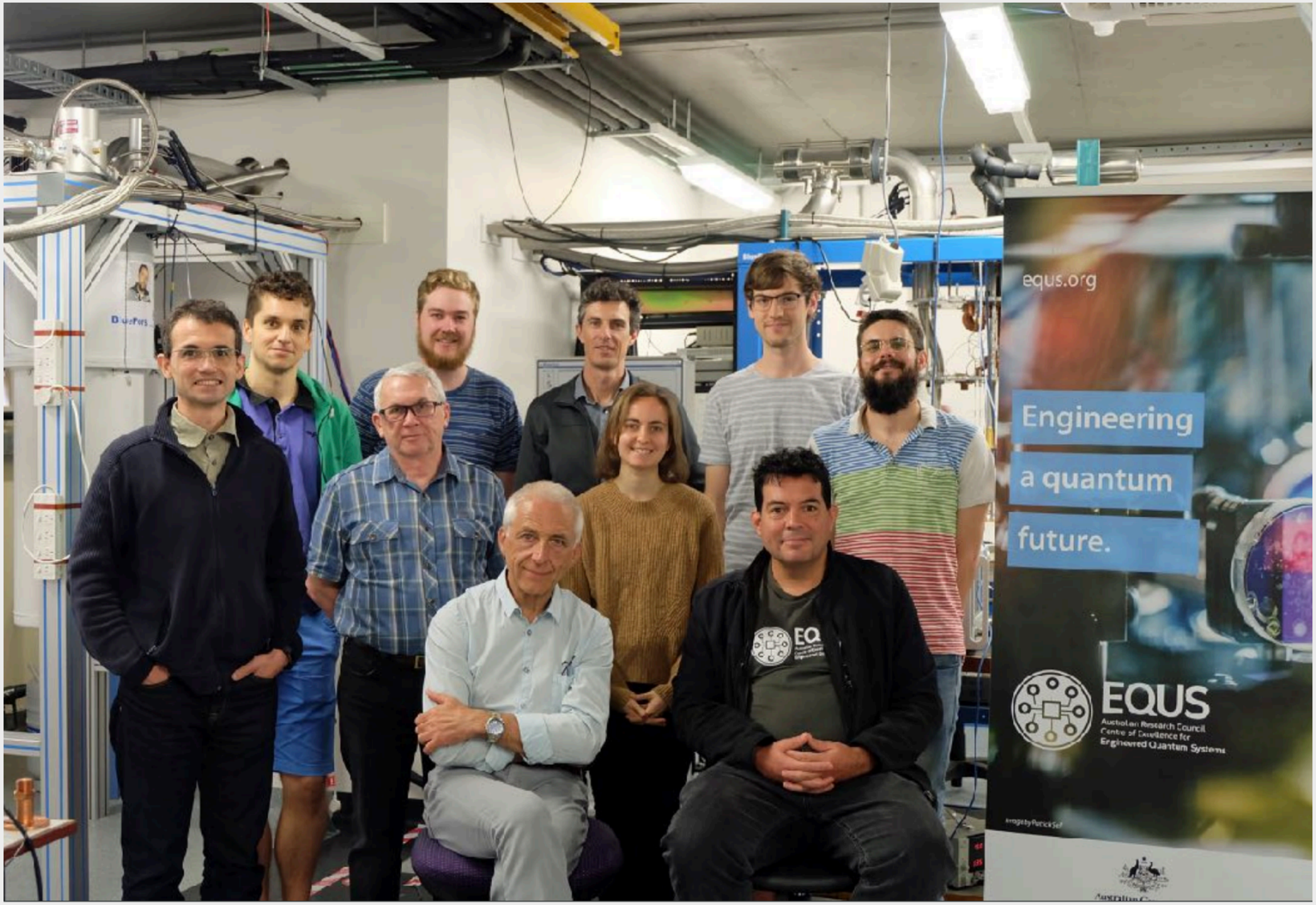

Centre for Dark Matter Particle Physics

EQUS
Australian Research Council
Centre of Excellence for
Engineered Quantum Systems

NIOBE

Resonant Bar Gravitational Wave detector

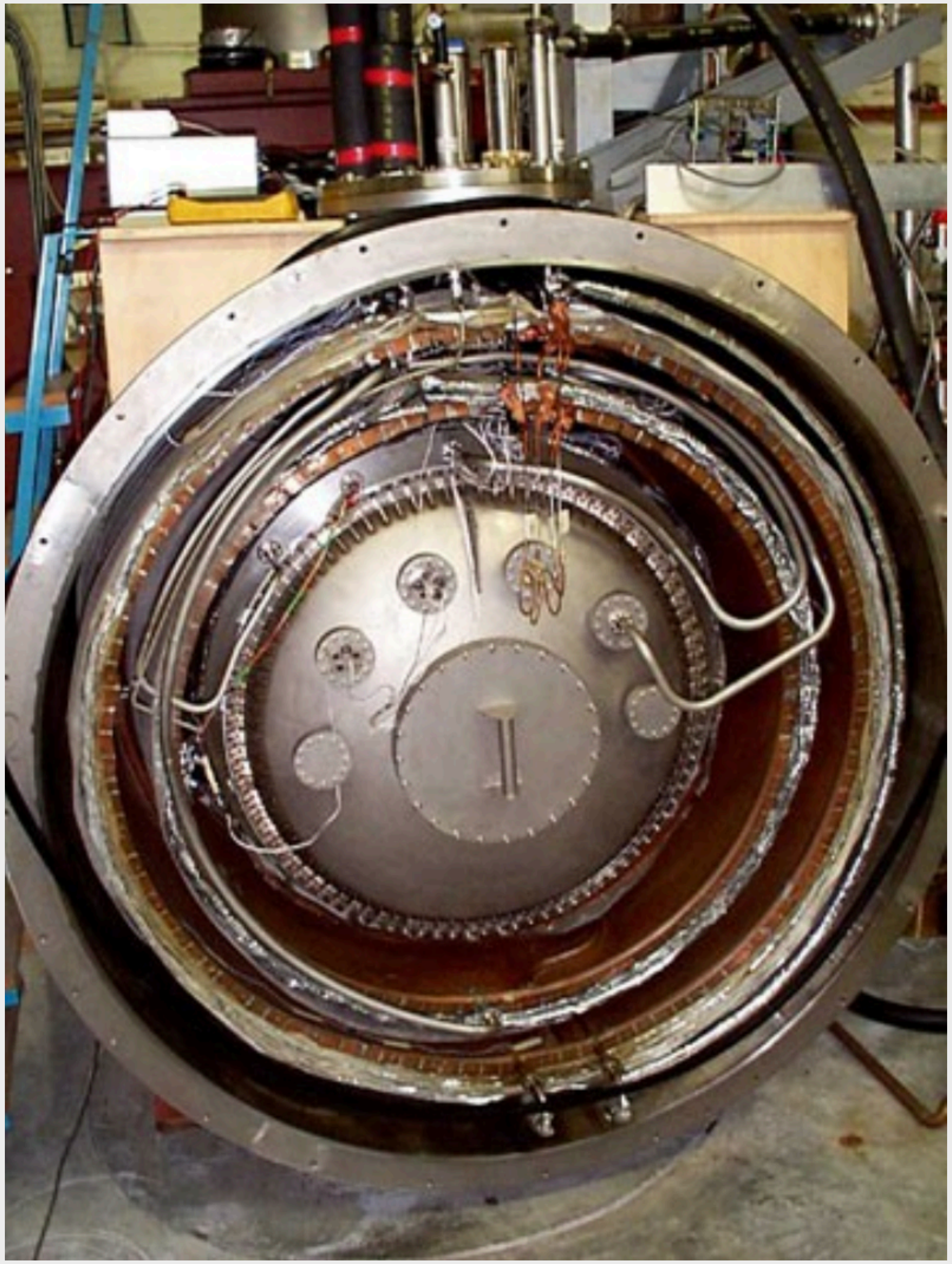

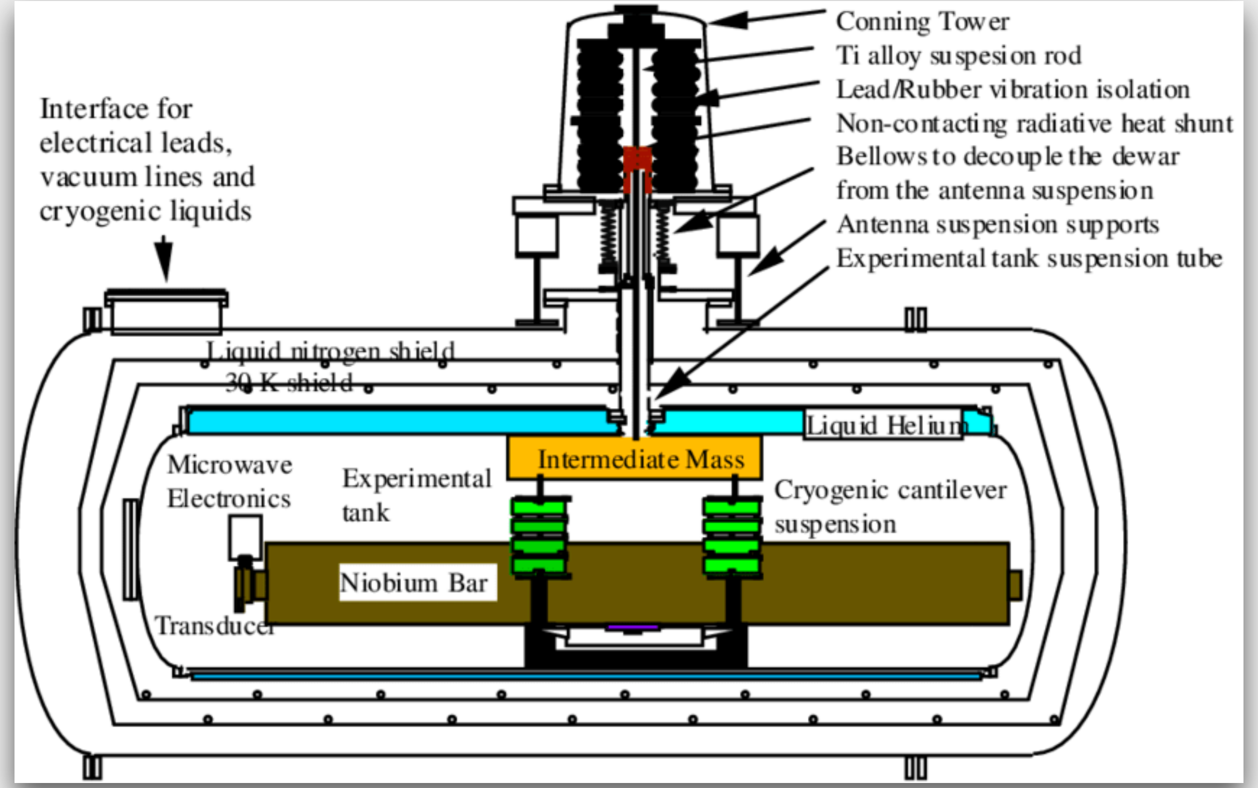

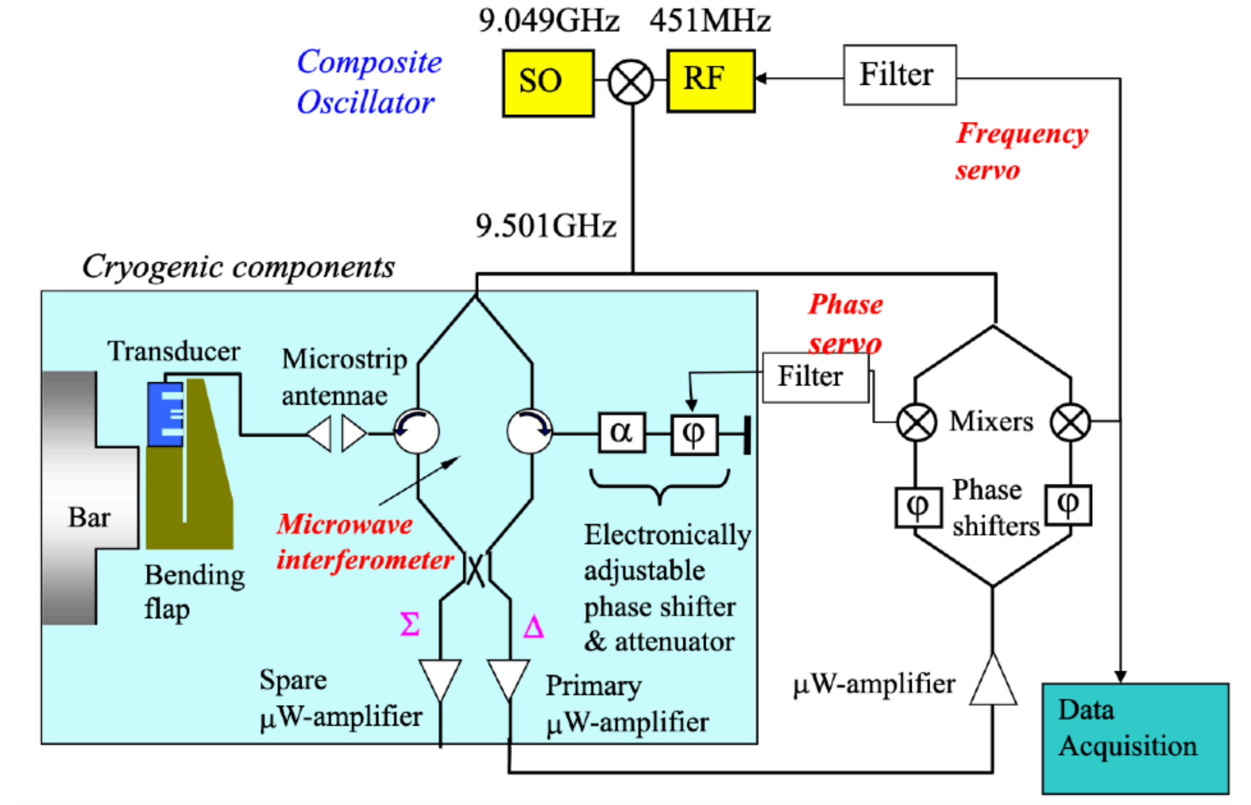

Phys. Rev. Lett 74, 1908 (1995)

Quantum & Frequency Metrology

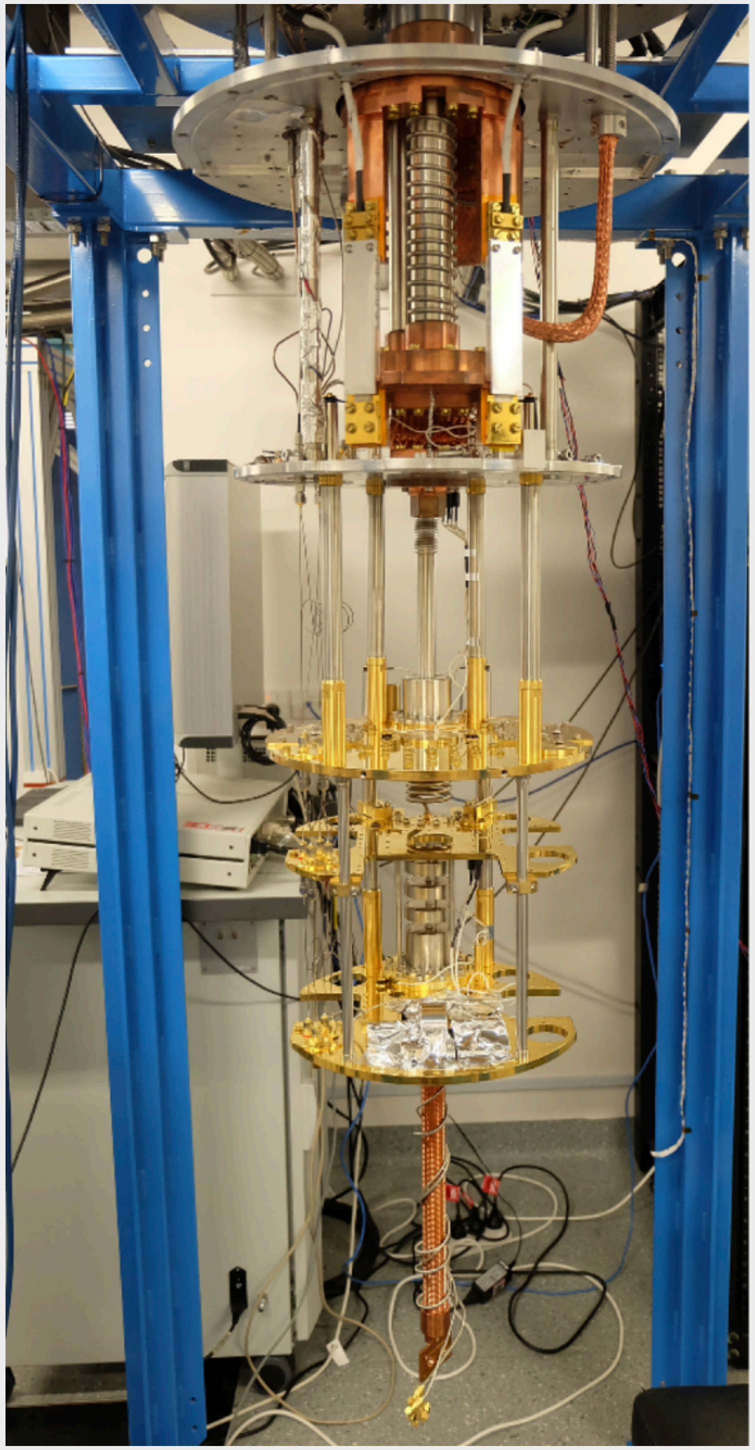

Centre for Dark Matter
Particle Physics

EQUS
Australian Research Council
Centre of Excellence for
Engineered Quantum Systems

Outline

- Bulk Acoustic Wave (BAW) Technology
- BAW as a GW Antenna
- Current Status and First Results
- Perspectives
- Test of Fundamental Physics @ UWA

Detection Approach

displacement | current | voltage | data

$$h(t) \longrightarrow u(t) + n \longrightarrow i(t) + n \longrightarrow A(i(t) + n) + n_A \longrightarrow A(i(\tau) + n) + n_A$$

Resonant Bar | Transducer | Amplifier | Down Conversion | Data Logging

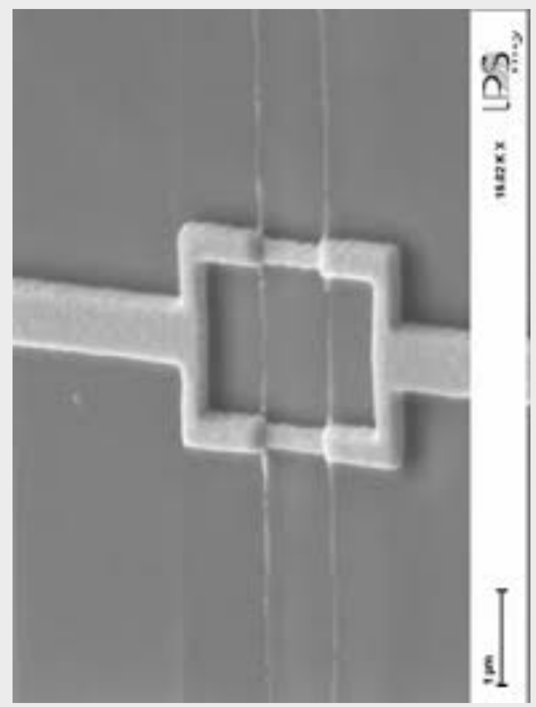

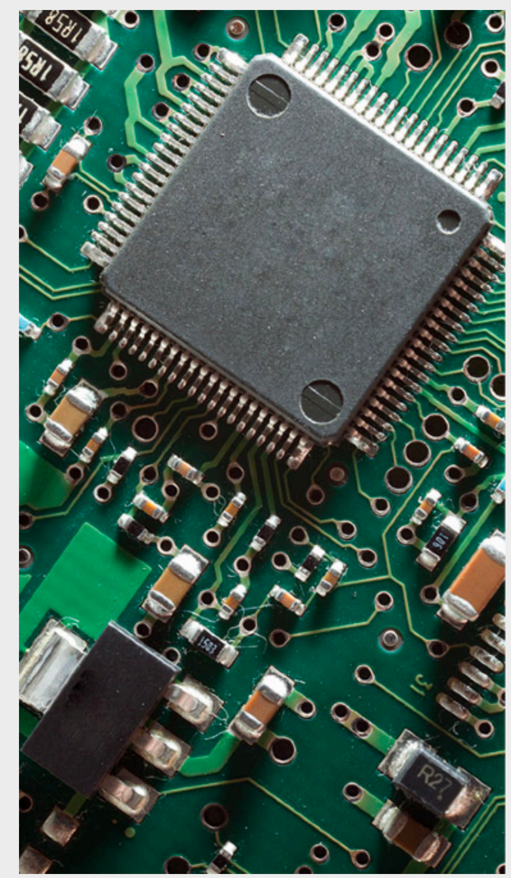

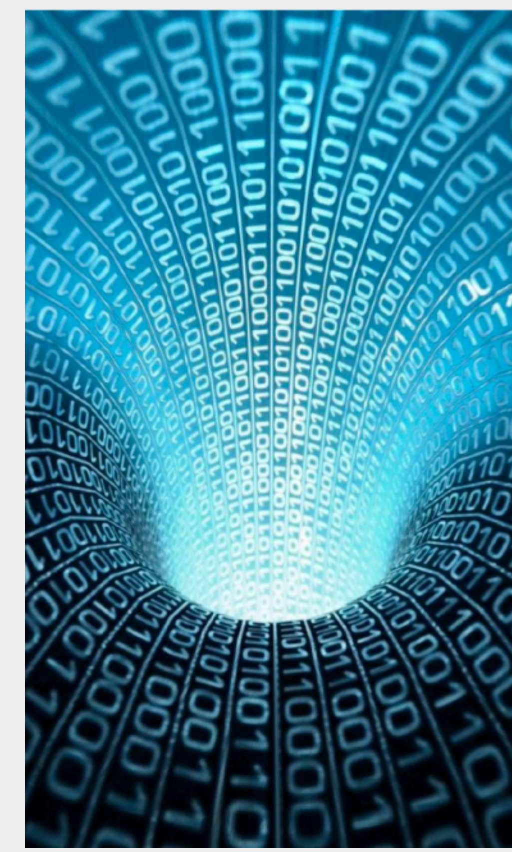

BAW Cavity

SQUID

FPGA

EQUS
Australian Research Council
Centre of Excellence for
Engineered Quantum Systems

Detection Approach

displacement | current | voltage | data

$$h(t) \longrightarrow u(t) + n \longrightarrow i(t) + n \longrightarrow A(i(t) + n) + n_A \longrightarrow A(i(\tau) + n) + n_A$$

Resonant Bar | Transducer | Amplifier | Down Conversion | Data Logging

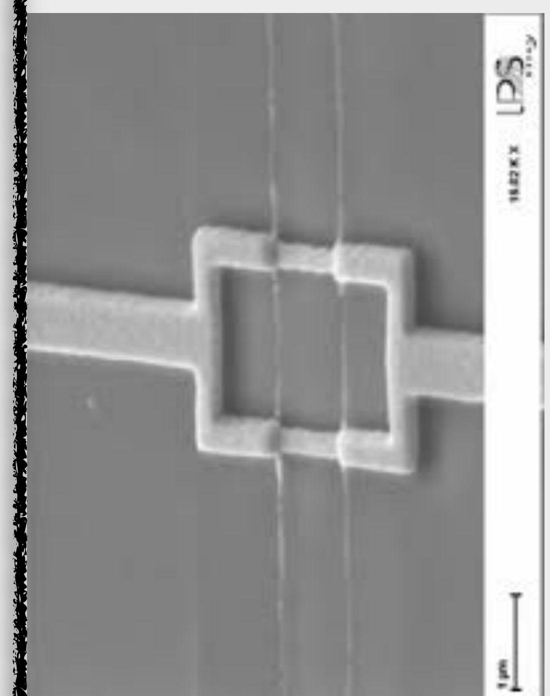

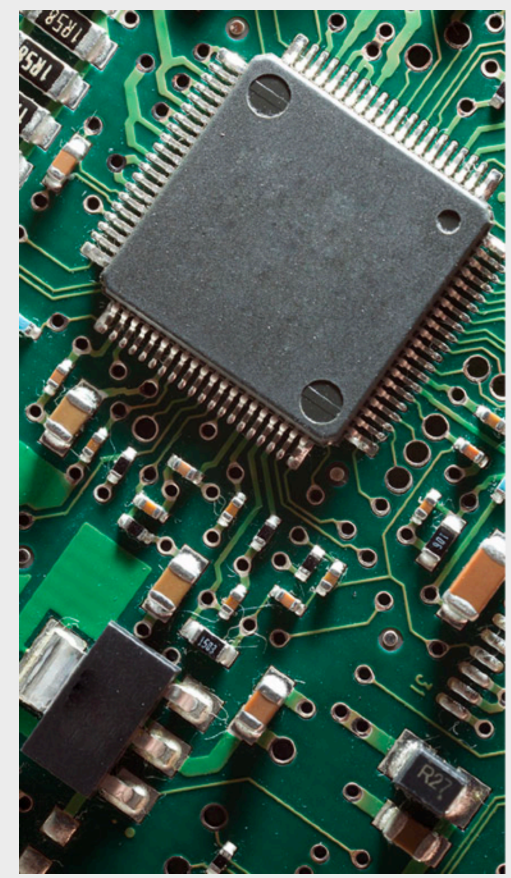

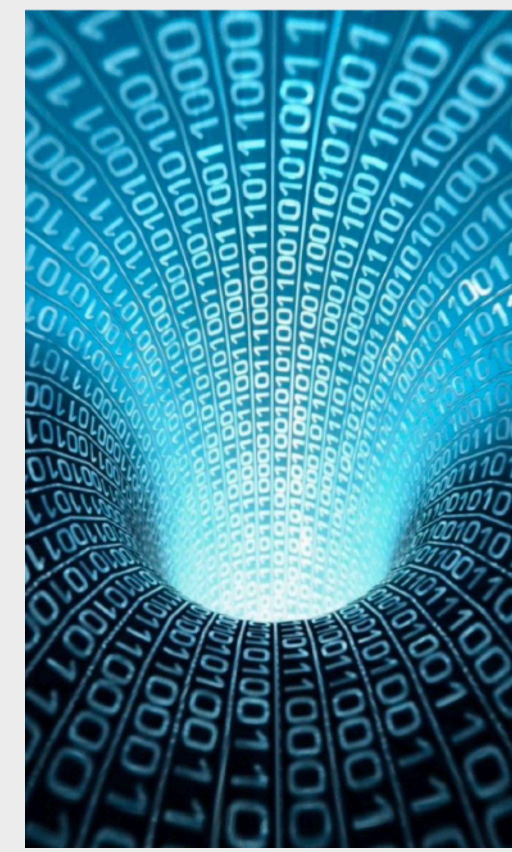

BAW Cavity | SQUID | FPGA

EQUS
Australian Research Council
Centre of Excellence for
Engineered Quantum Systems

Bulk Acoustic Wave Devices

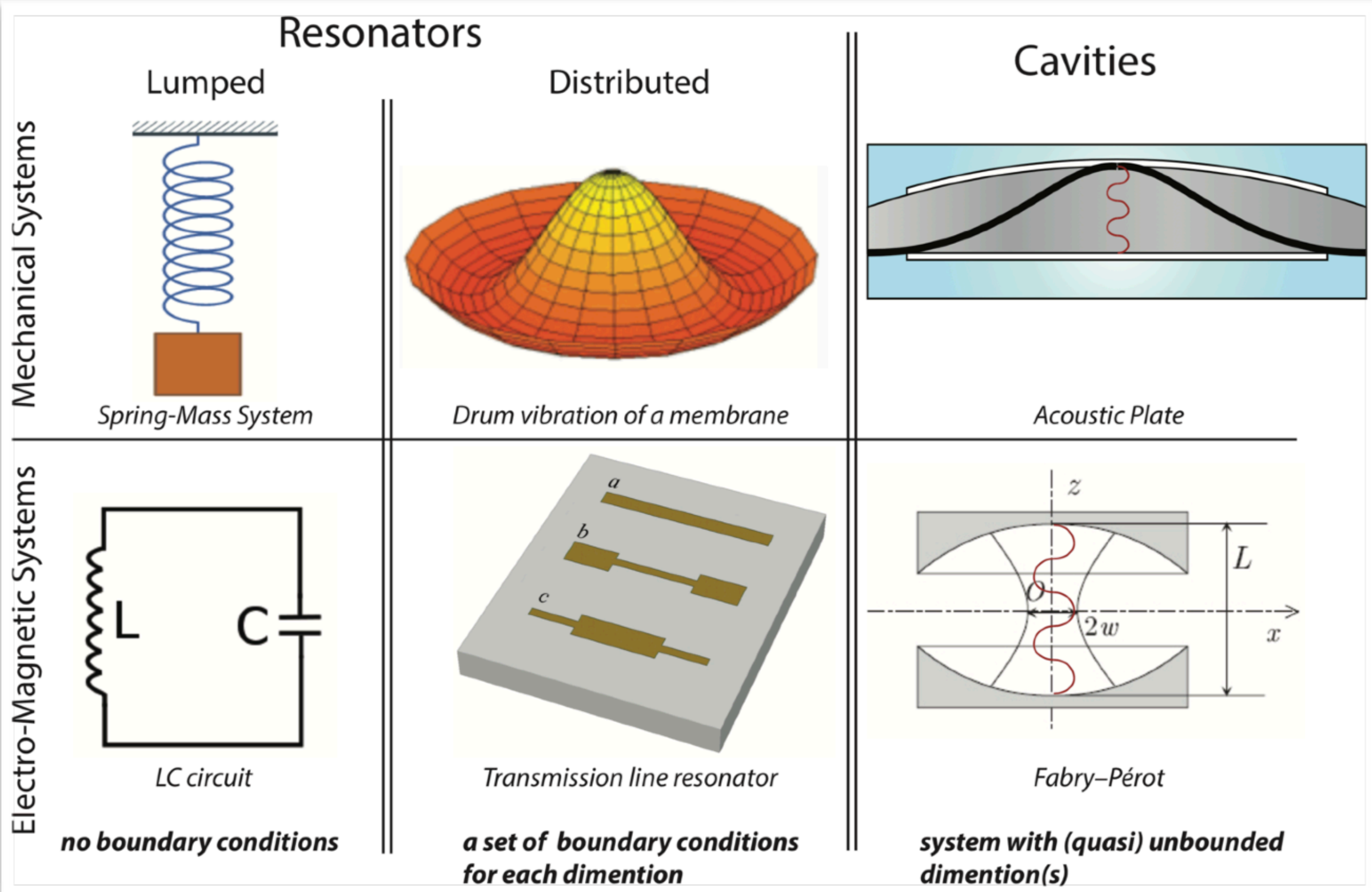

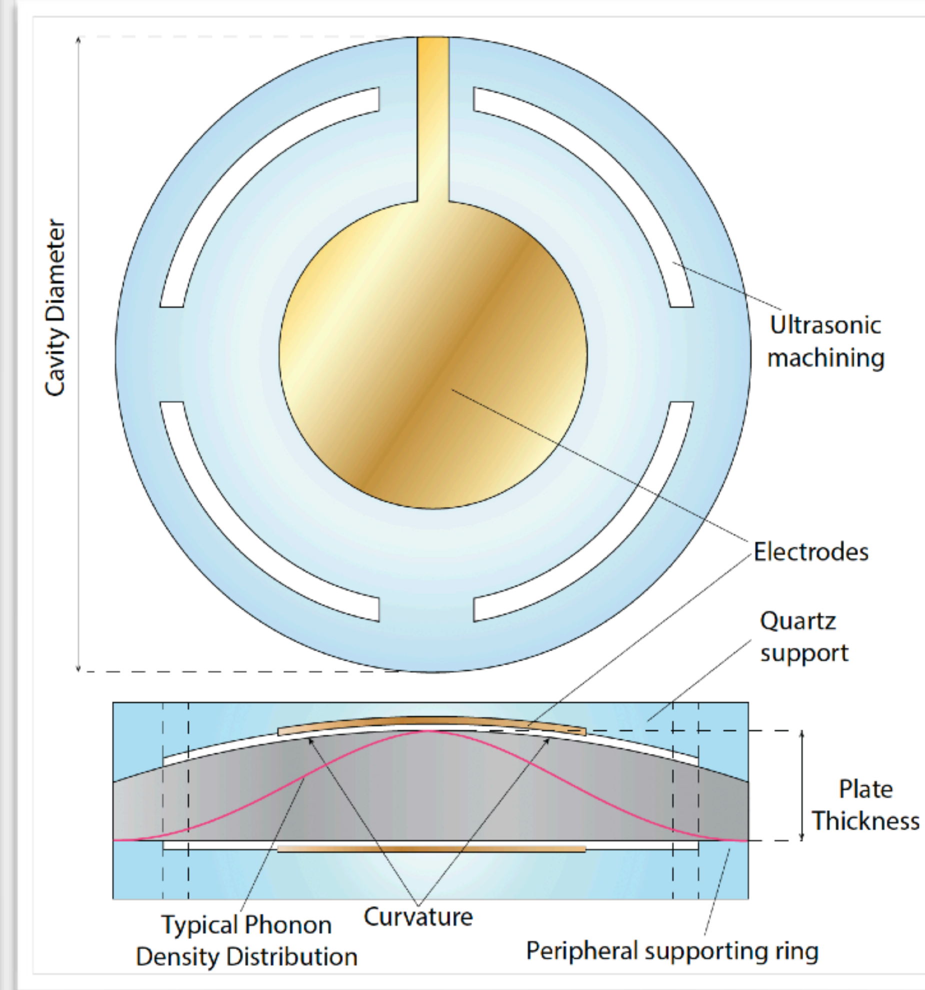

- Frequency range: 1-1000 MHz
- Tree mode family types: 2 transverse and 1 longitudinal
- Piezoelectric Coupling
- Established technology (>70 years for time keeping applications)
- Record high Quality factors ~ 10^{10}

Scientific Reports Vol. 3, 2132 (2013)

EQUS
Australian Research Council Centre of Excellence for Engineered Quantum Systems

Bulk Acoustic Wave Devices

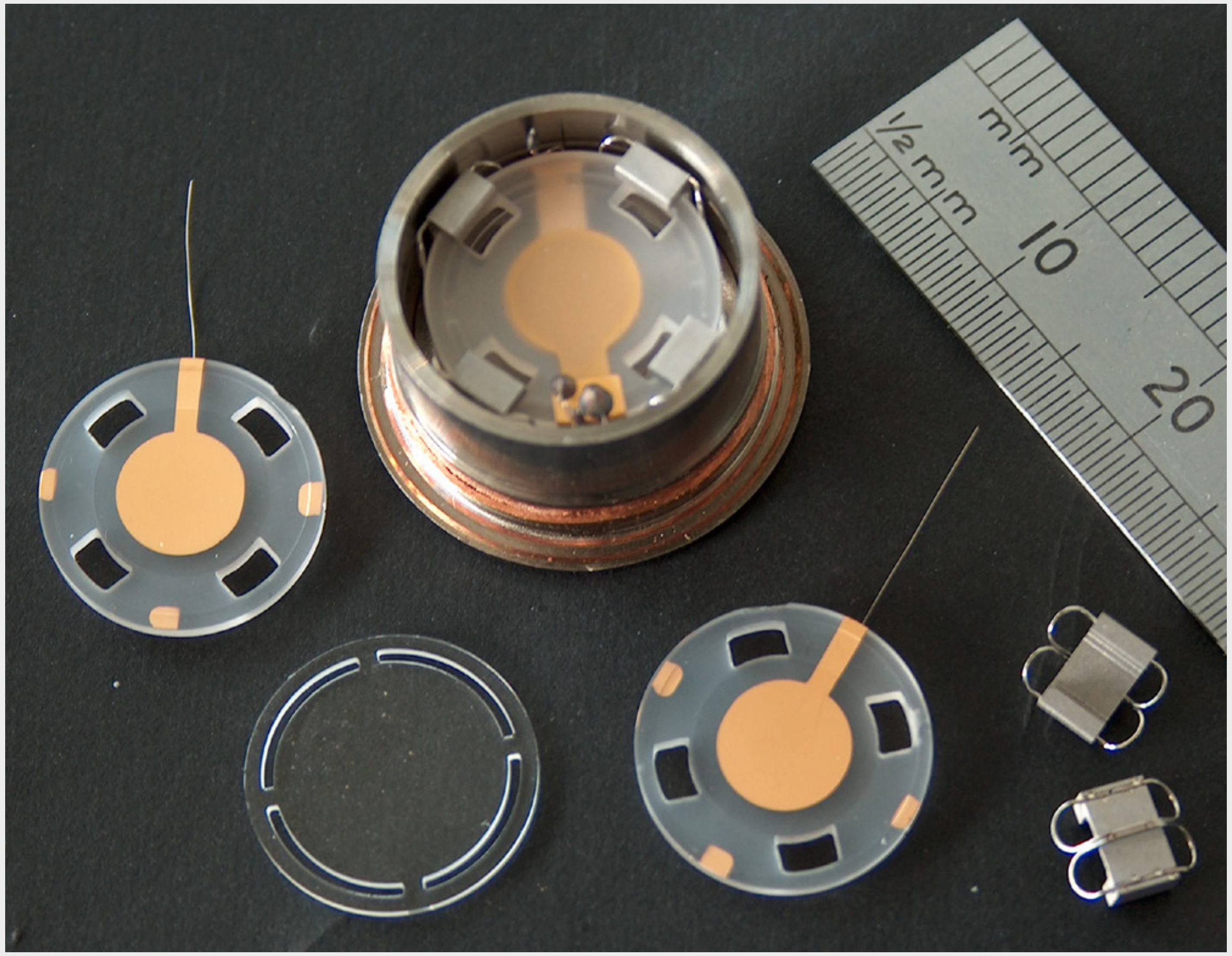

- Top High Quality α-quartz,
- BVA-technology,
- SC-cut,
- plano-covex...

Room temperature

A BAW quartz resonators optimized for the 5th overtone of the C-mode (slow shear) at $5 - 10$ MHz in the Akhiezer regime $(Q \times f = constant)$.

Cryogenic temperature

Acoustic cavity traps longitudinally polarised phonons (of up to 227th OT) in Landau-Rumer regime $(Q = constant)$.

EQUS
Australian Research Council
Centre of Excellence for
Engineered Quantum Systems

Types of Losses

When losses due to phonon-tunnelling to the environment are minimised,

$$\frac{1}{Q_{total}} = \frac{1}{Q_{phonon-phonon}} + \frac{1}{Q_{TLS}} + \frac{1}{Q_{scattering}} + \frac{1}{Q_{thermoelastic}} + \text{etc} \quad (1)$$

Phonon-Phonon Dissipation (Landau-Rumer),

acoustic phonon scattering by thermal phonons over crystal anharmonicity

TLS Absorption

coupling to TLS attributed to impurity ions, e.g. Al^{3+}, Na^{+}, Li^{+}, H^{+}, etc

Scattering Losses

due to acoustic phonon scattering on surface roughness and on small impurities in bulk (Rayleigh scattering)

Thermoelastic Dissipation

due to thermal currents induced by medium compression/decompression...

Scientific Reports Vol. 3, 2132 (2013)

EQUS
Australian Research Council
Centre of Excellence for
Engineered Quantum Systems

Observation of Phonon Loss Regimes

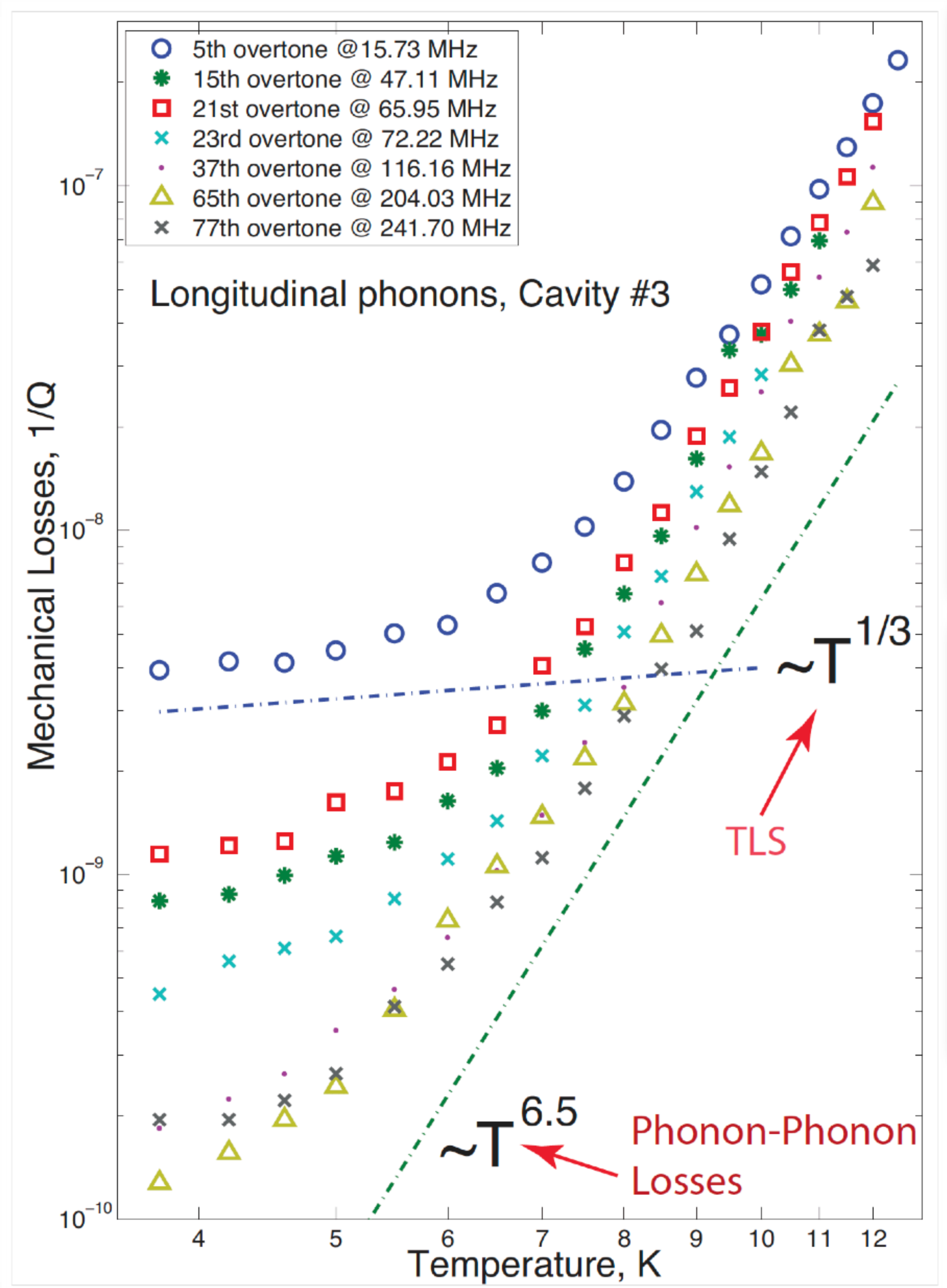

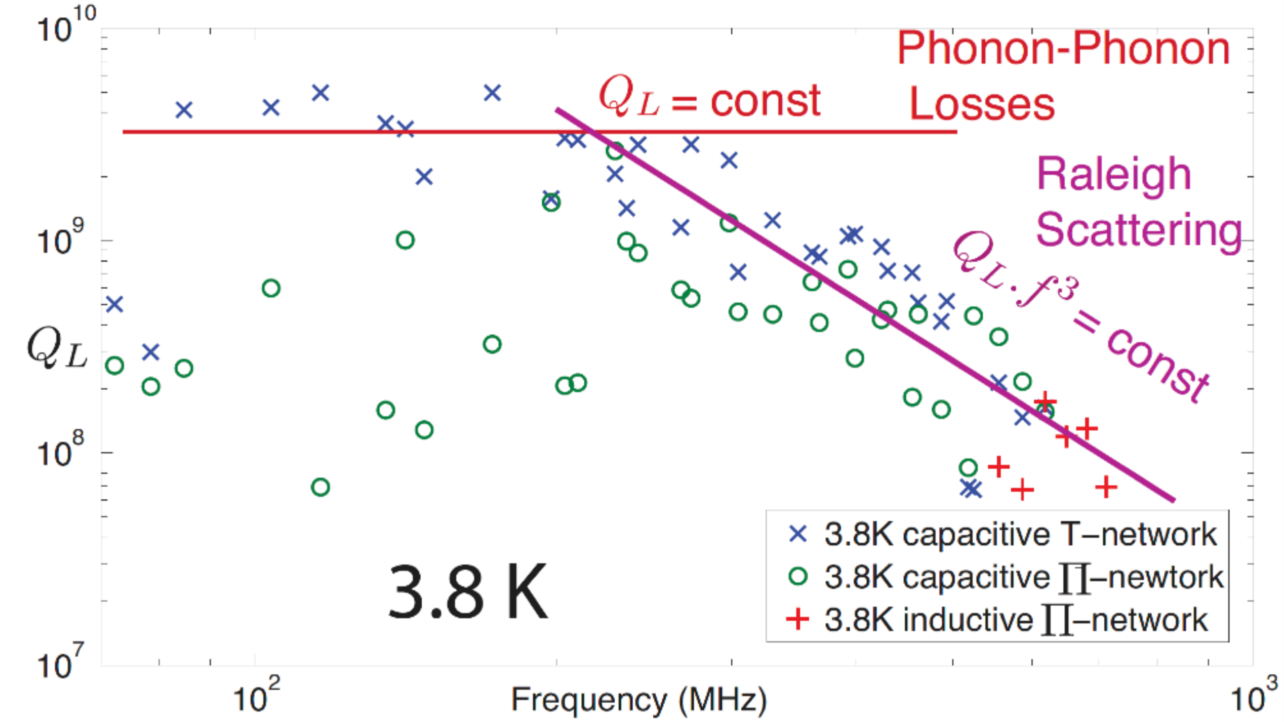

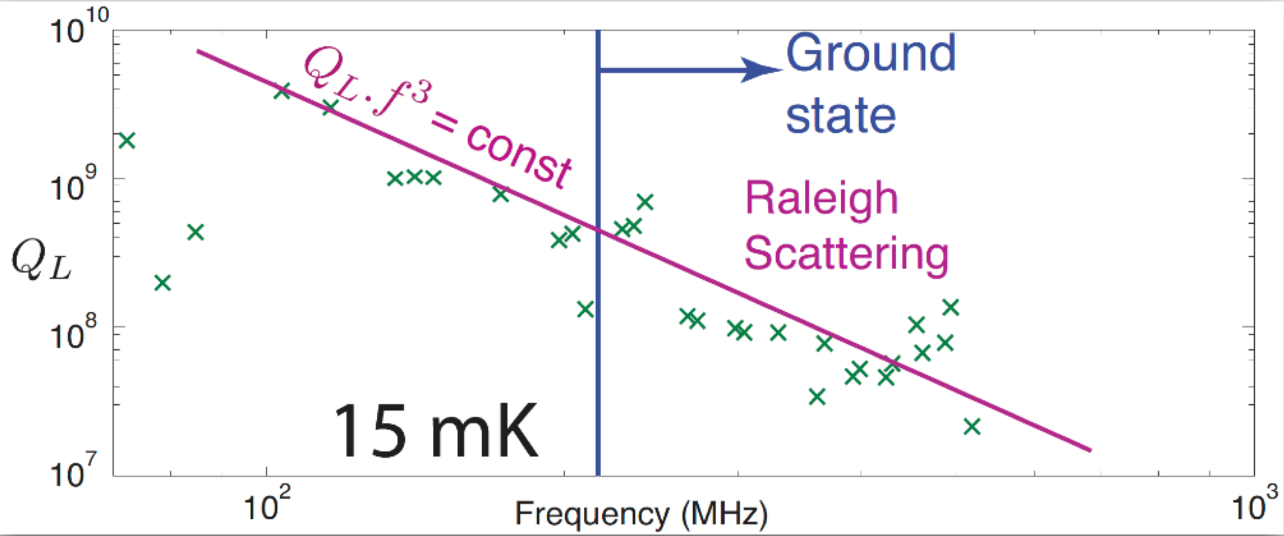

- $Q_{L,max} = 5 \times 10^9$,
- $Q_L \times f = 8.6 \times 10^{17}$ Hz,
- OTs up to 227^{th} (712.46 MHz),

Q = 8x10⁹

Scientific Reports Vol. 3, 2132 (2013)

Phys. Rev. Lett. 111, 085502 (2013)

EQUS Australian Research Council Centre of Excellence for Engineered Quantum Systems

Comparing to Other Technologies

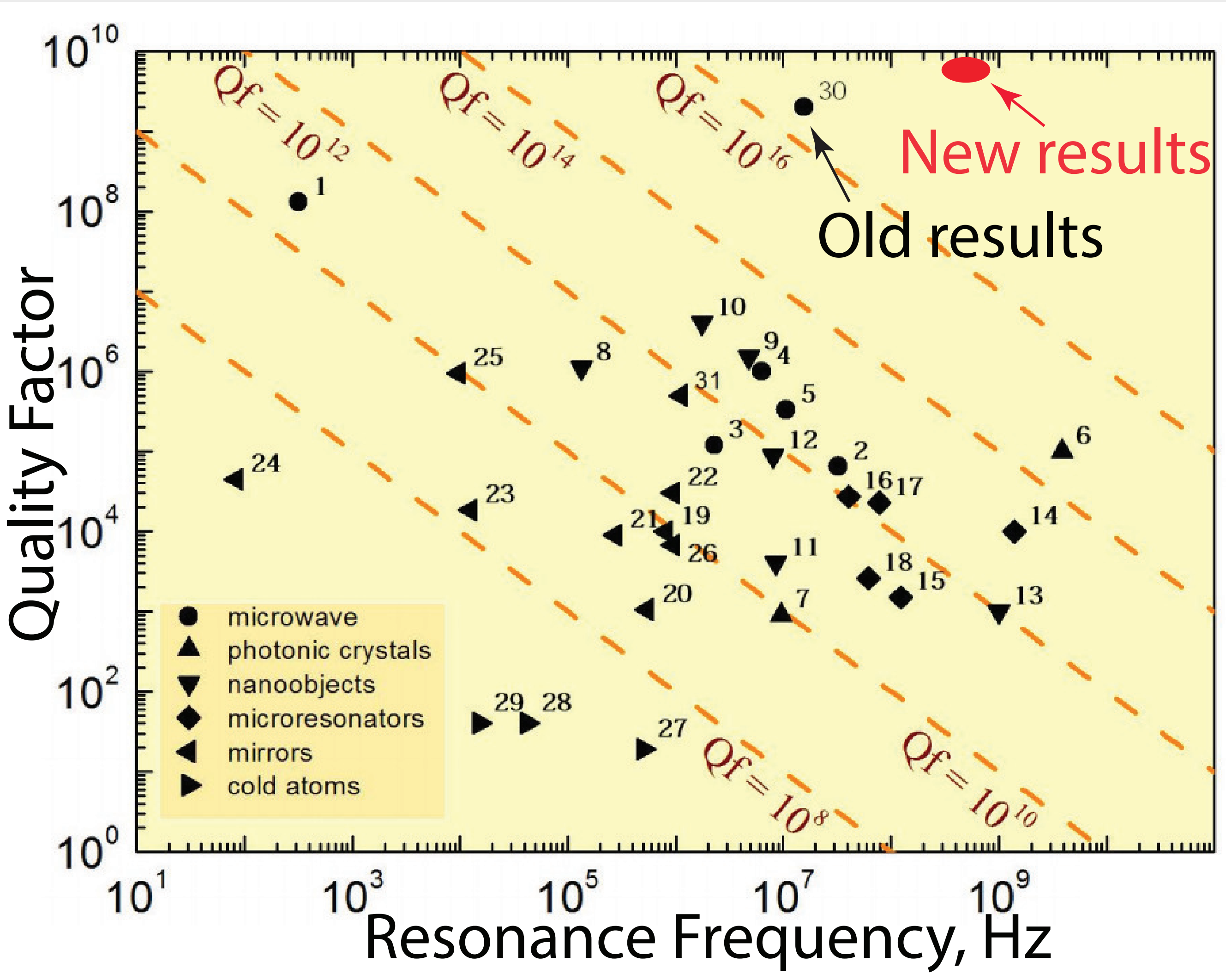

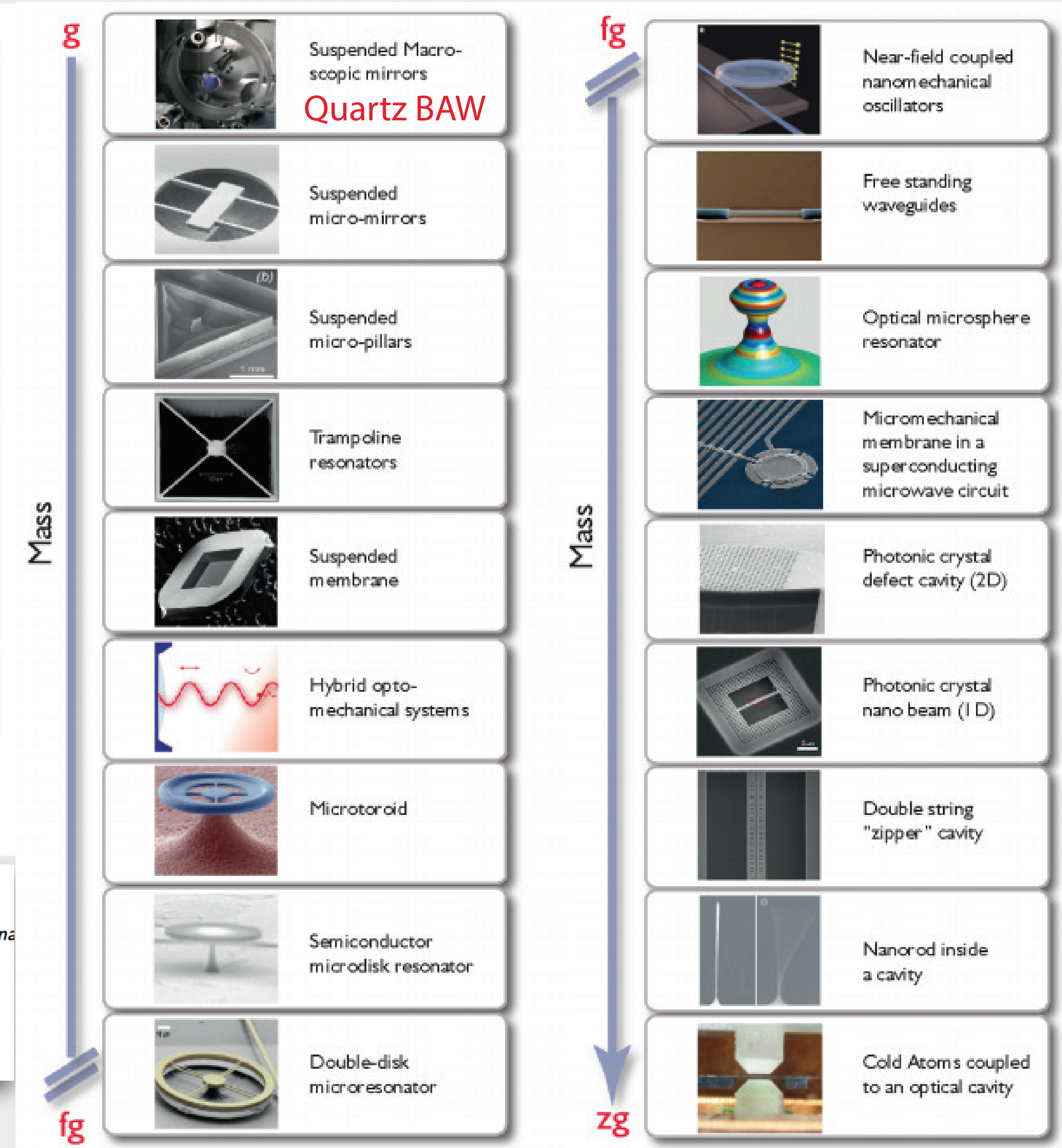

Cavity Optomechanics

Markus Aspelmeyer*
Vienna Center for Quantum Science and Technology (VCQ), Faculty of Physics, University of Vienna, 1090 Vienna Austria
Tobias J. Kippenberg†
Ecole Polytechnique Fédérale de Lausanne (EPFL), 1015 Lausanne, Switzerland
Florian Marquardt‡
University of Erlangen-Nürnberg, Institute for Theoretical Physics, Staudtstr. 7, 91058 Erlangen, Germany; and Max Planck Institute for the Science of Light, Erlangen, Germany

arXiv:1303.0733

Effective mass

$$m_{\mathrm{eff}} = \int_V \rho \frac{u^2_{nmp}(x, y)}{u^2_{\max}} \mathrm{d}v,$$

$$m_{n,0,0} = \rho\pi h_0 L^2 \frac{\mathrm{Erf}\left(\sqrt{n}\,\eta_x\right)\mathrm{Erf}\left(\sqrt{n}\,\eta_y\right)}{\eta_x \eta_y n} = \frac{\overline{m}}{\xi_n},$$

$$\sqrt{\left\langle \hat{x}^2_{\mathrm{flat},1} \right\rangle} \approx 4.7\times 10^{-20}\mathrm{m},$$
$$\sqrt{\left\langle \hat{p}^2_{\mathrm{flat},1} \right\rangle} \approx 10^{-15}\,\frac{\mathrm{m}\times\mathrm{kg}}{\mathrm{sec}},$$
$$\overline{m} = 0.93\ \mathrm{g},$$

NJP Vol. 16, 083007 (2014)

Comparing to Other Technologies

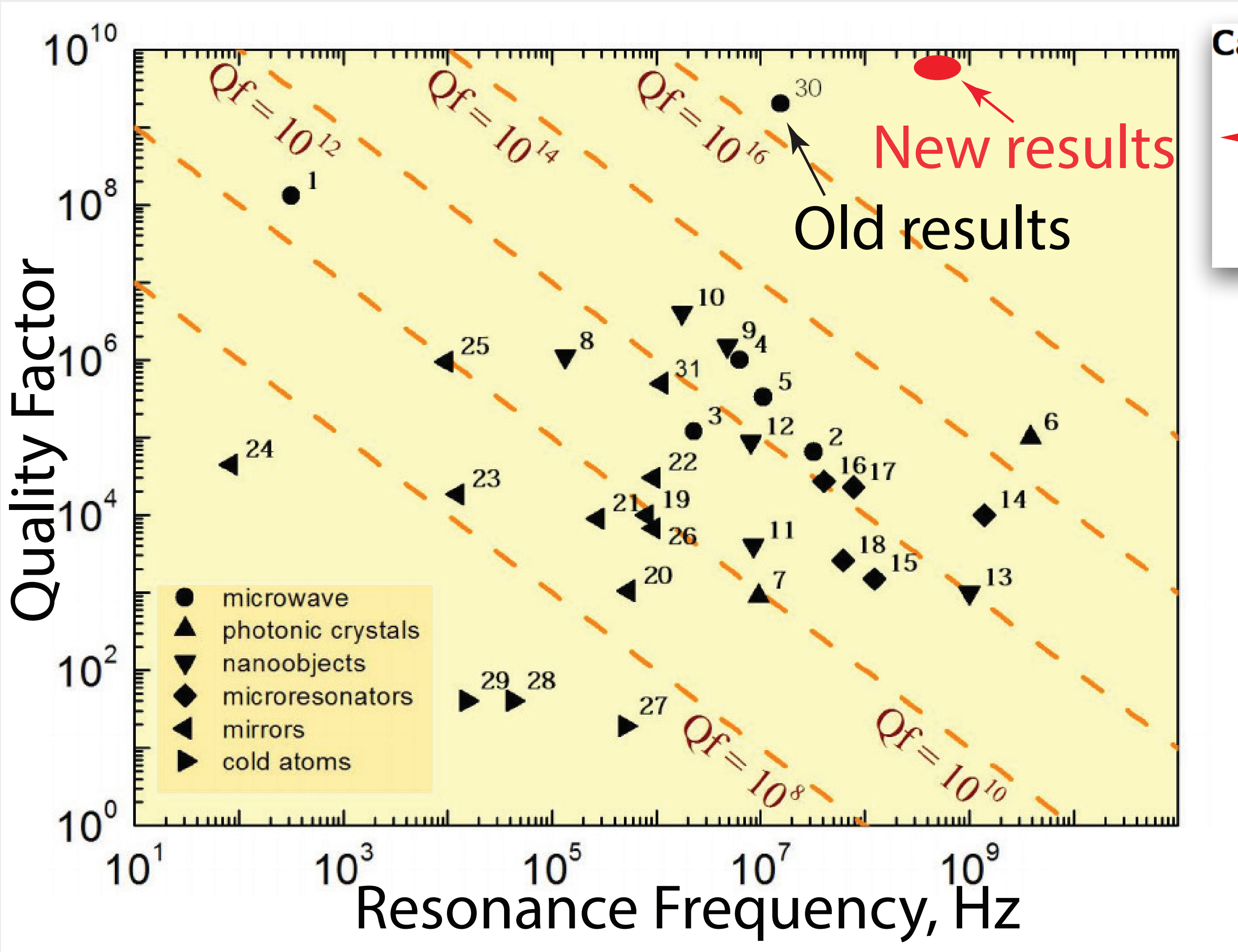

Cavity Optomechanics

Markus Aspelmeyer*
Vienna Center for Quantum Science and Technology (VCQ), Faculty of Physics, University of Vienna, 1090 Vienna Austria
Tobias J. Kippenberg†
Ecole Polytechnique Fédérale de Lausanne (EPFL), 1015 Lausanne, Switzerland
Florian Marquardt‡
University of Erlangen-Nürnberg, Institute for Theoretical Physics, Staudtstr. 7, 91058 Erlangen, Germany; and Max Planck Institute for the Science of Light, Erlangen, Germany

arXiv:1303.0733

Q/T = const

Bose-Einstein statistics:

$$n_{\mathrm{TH}} \sim \frac{1}{e^{\frac{\hbar\omega}{k_B T}} - 1}, \text{ in TD equilibrium}$$

Example:

at 15 mK, $n_{TH} = 1$ for 217 MHz

Experiment	Freq., (Hz)	Q-factor	T (K)	n_{TH}	$Q(n_{\mathrm{TH}} = 1)$
Silicon	1.96×10^4	2×10^9	4	4.3×10^6	677
Sapphire	5.33×10^4	6×10^8	4	1.6×10^6	554
Silica	7.0×10^7	10^4	0.6	179	81
Spoke	7.8×10^7	2.2×10^4	0.65	1.7	83
FBAR	6.07×10^9	260	0.025	9×10^{-6}	260
Al	1.06×10^7	3.3×10^5	0.015	29.1	1.6×10^4
Silicon beam	3.68×10^9	4×10^5	20	113	5.1×10^3
Nb-Al-SiN beam	6.3×10^6	10^6	0.10	330	4.4×10^3
Quartz BAW			0.015	< 1	0.7×10^9
Quartz BAW (NEW)	204×10^6	8×10^9	3.75	382	

EQUS
Australian Research Council Centre of Excellence for Engineered Quantum Systems

Further Directions of Research

Coupling to light & mw

Mechanical Resonator ⟷ Optical Interface

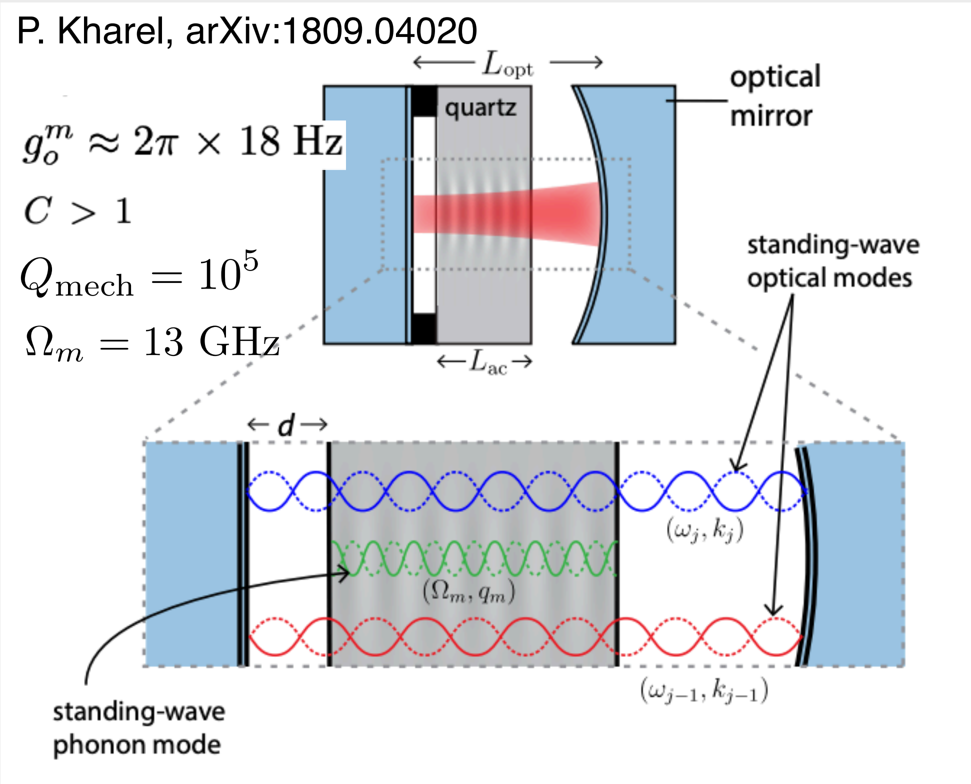

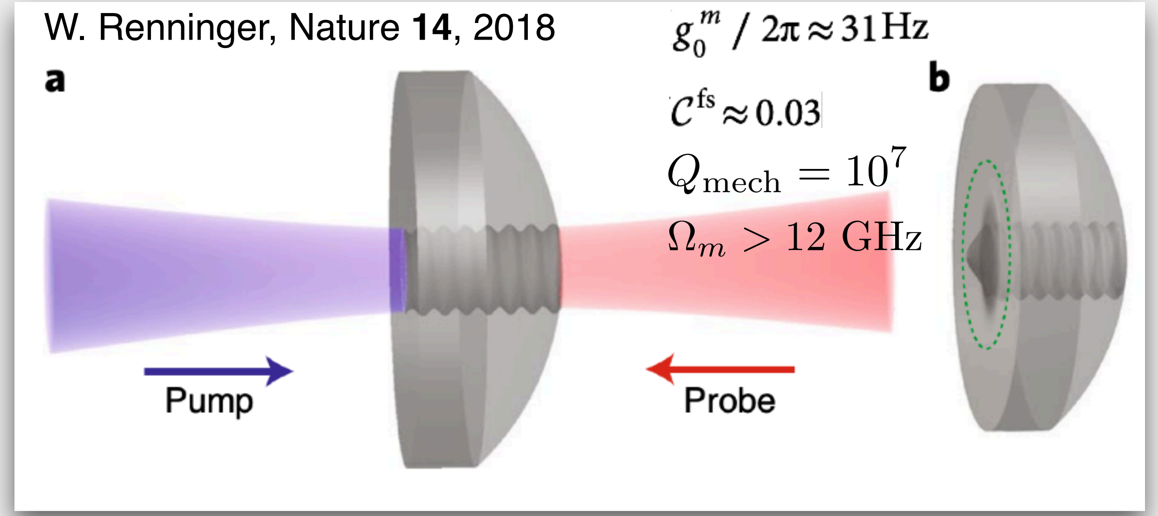

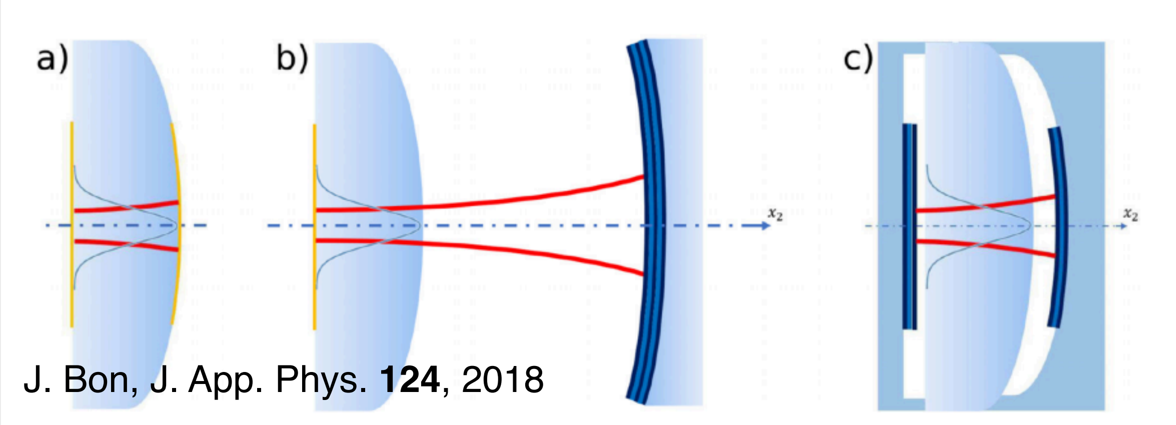

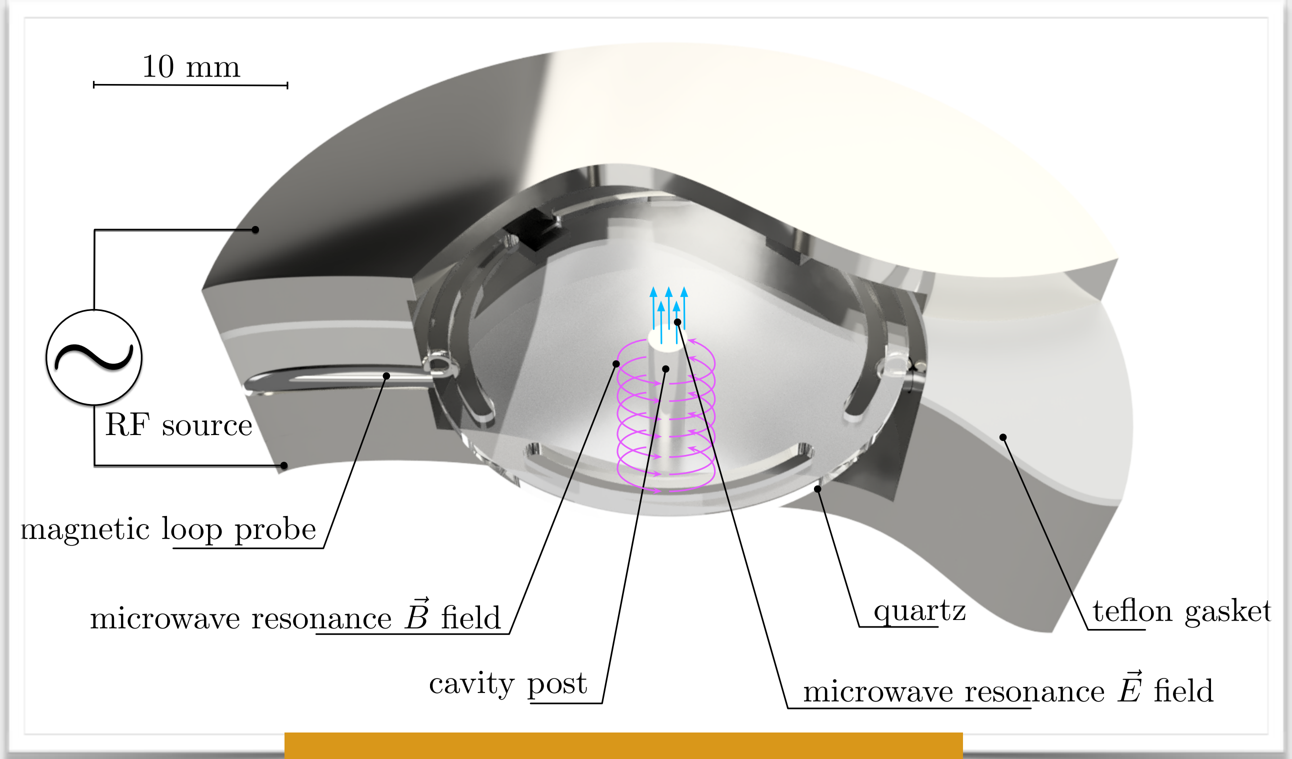

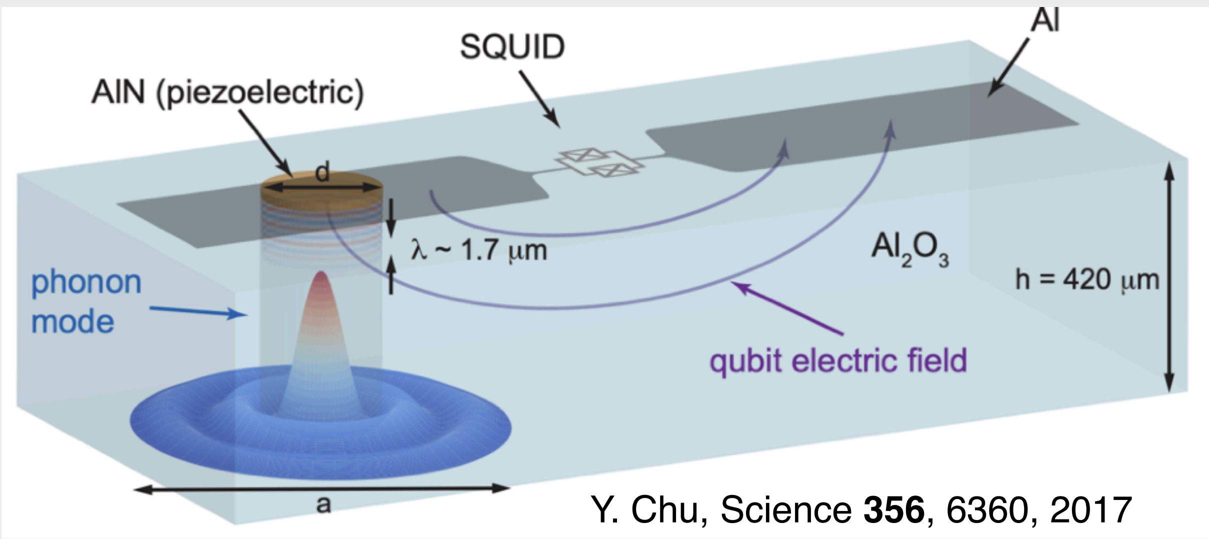

arXiv:1907.10753

Further Directions of Research

Further understanding of loss mechanisms (<1K)

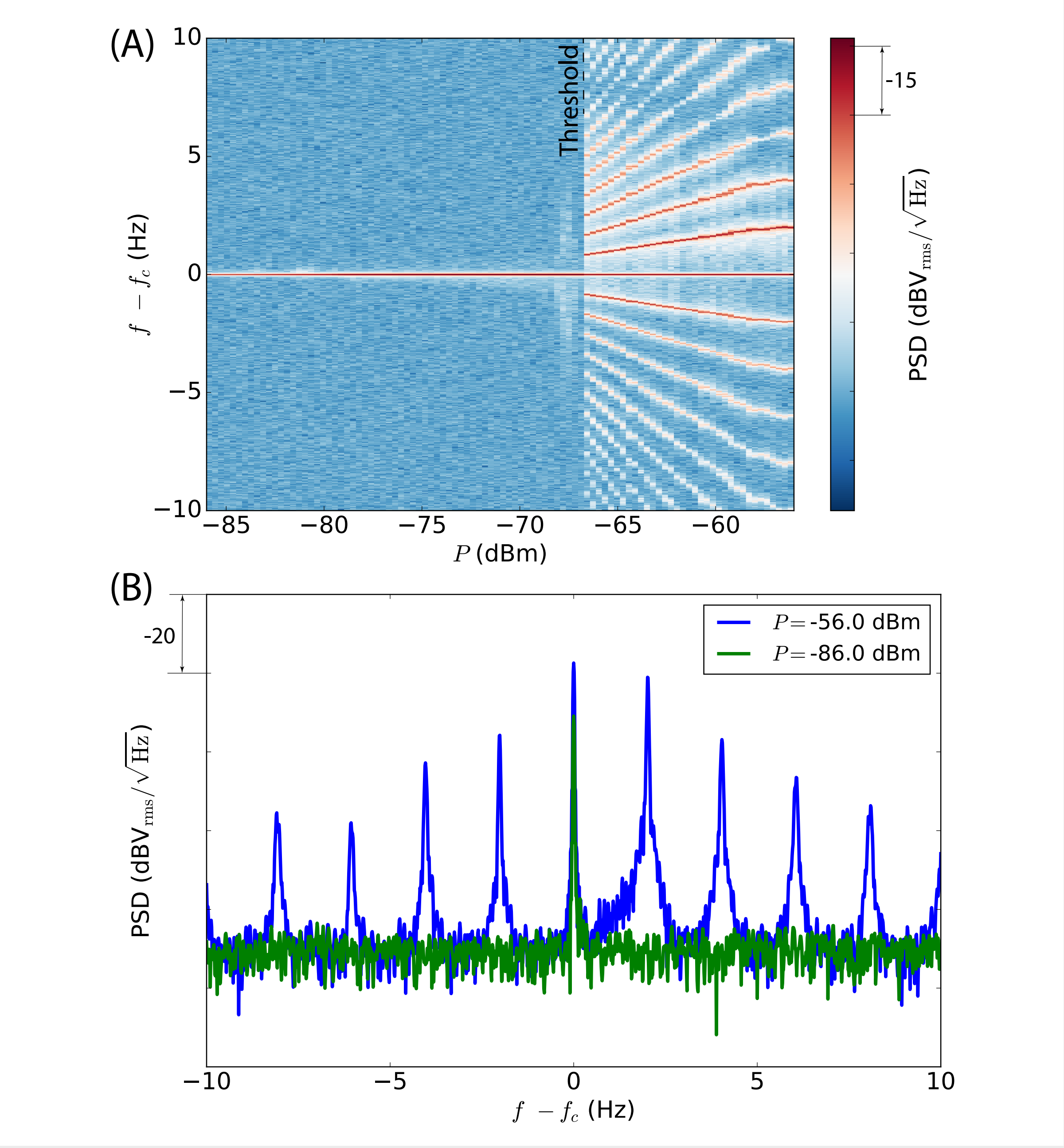

Nonlinearities
Magnetic field sensitivity

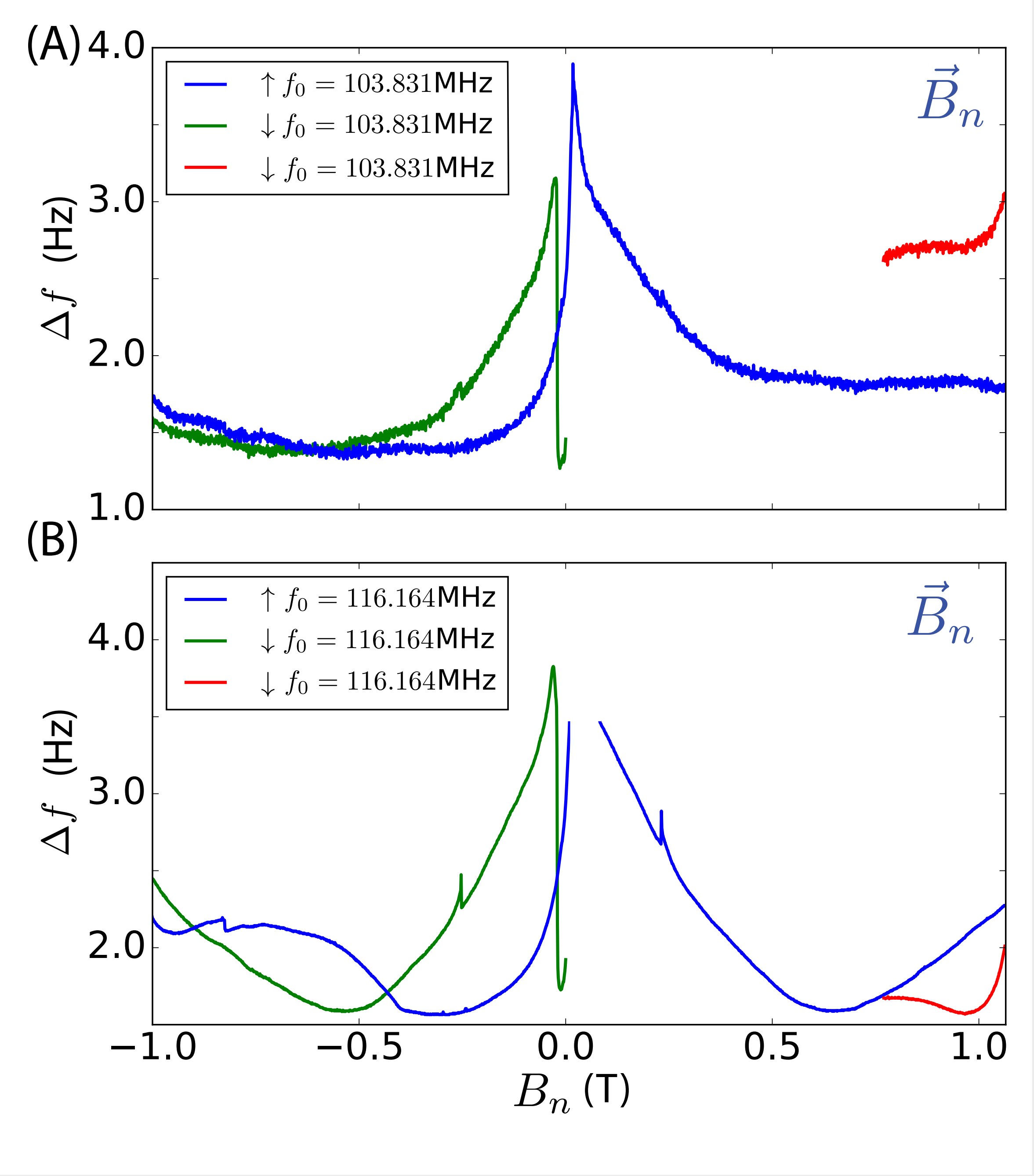

arXiv:1902.02001

EQUS
Australian Research Council Centre of Excellence for Engineered Quantum Systems

Pros and Cons of BAWs

- ✓ Highest Q (High Sensitivity)
- ✓ Internal (Peizoelectric) coupling to SQUIDs
- ✓ Allows parametric detection methods
- ✓ Large number of sensitive modes (>100)
- ✓ Modes scattered over wide frequency range (1-700MHz)
- ✓ Well established technology (mass production)
- ✓ Relatively inexpensive
- ✓ Small scale (~ 1 inch size)
- ✓ Relatively large effective mass (~1g)
- ✓ High Precision (insensitive to external influences)

- ✗ Poor accuracy

EQUS
Australian Research Council
Centre of Excellence for
Engineered Quantum Systems

Outline

BAW Technology

BAW as a GW Antenna

Current Status and First Results

Perspectives

Test of Fundamental Physics @ UWA

BAW Cavity as a GW Antenna

Gravitational wave detection with high frequency phonon trapping acoustic cavities

Maxim Goryachev and Michael E. Tobar
Phys. Rev. D **90**, 102005 – Published 24 November 2014

There are a number of theoretical predictions for astrophysical and cosmological objects, which emit high frequency ($10^6 - 10^9$ Hz) gravitation waves (GW) or contribute somehow to the stochastic high frequency GW background. Here we propose a new sensitive detector in this frequency band, which is based on existing cryogenic ultrahigh quality factor quartz bulk acoustic wave cavity technology, coupled to near-quantum-limited SQUID amplifiers at 20 mK. We show that spectral strain sensitivities reaching 10^{-22} per $\sqrt{\mathrm{Hz}}$ per mode is possible, which in principle can cover the frequency range with multiple (>100) modes with quality factors varying between 10^6 and 10^{10} allowing wide bandwidth detection. Due to its compactness and well-established manufacturing process, the system is easily scalable into arrays and distributed networks that can also impact the overall sensitivity and introduce coincidence analysis to ensure no false detections.

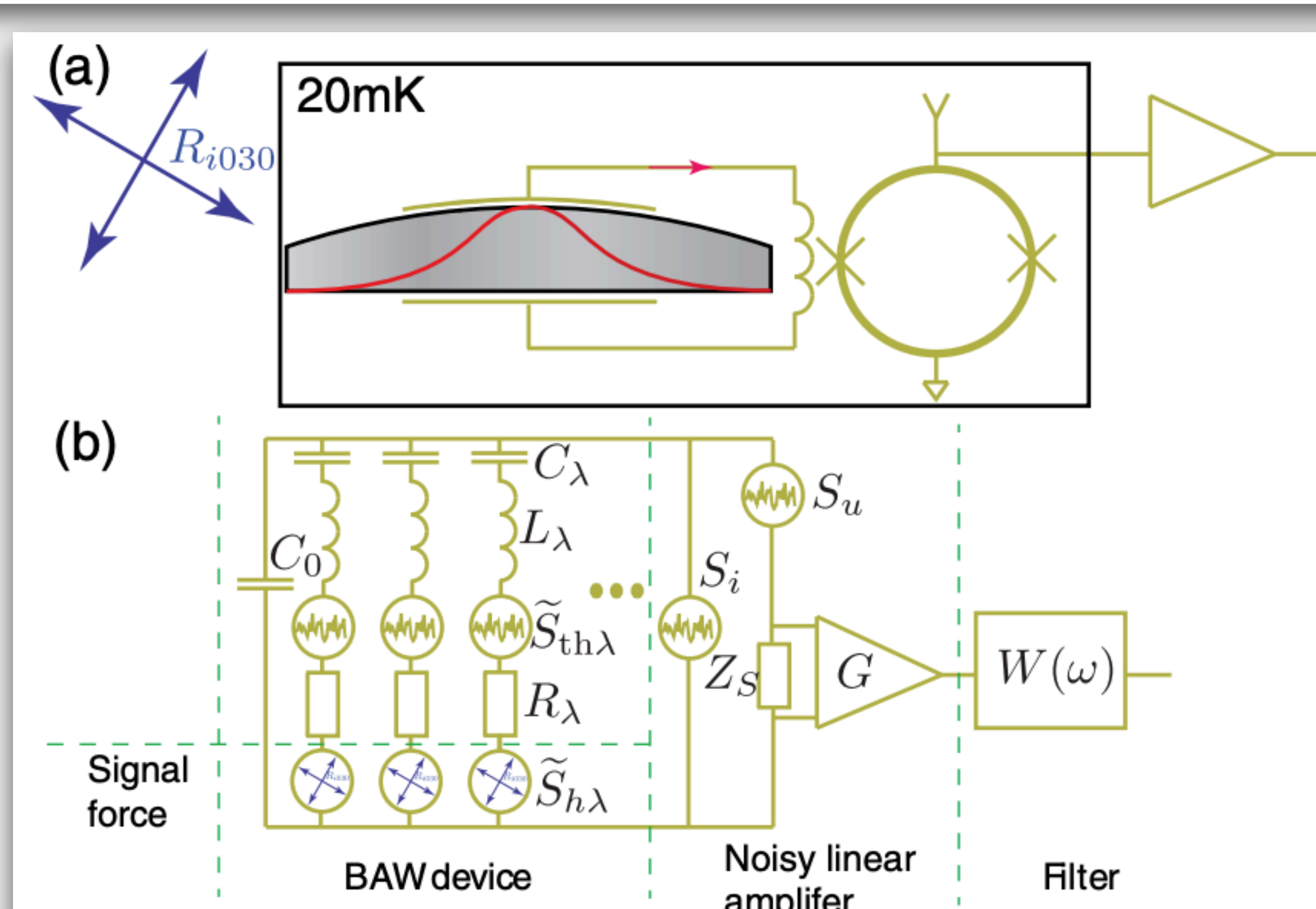

EQUS
Australian Research Council Centre of Excellence for Engineered Quantum Systems

BAW Cavity as a GW Antenna

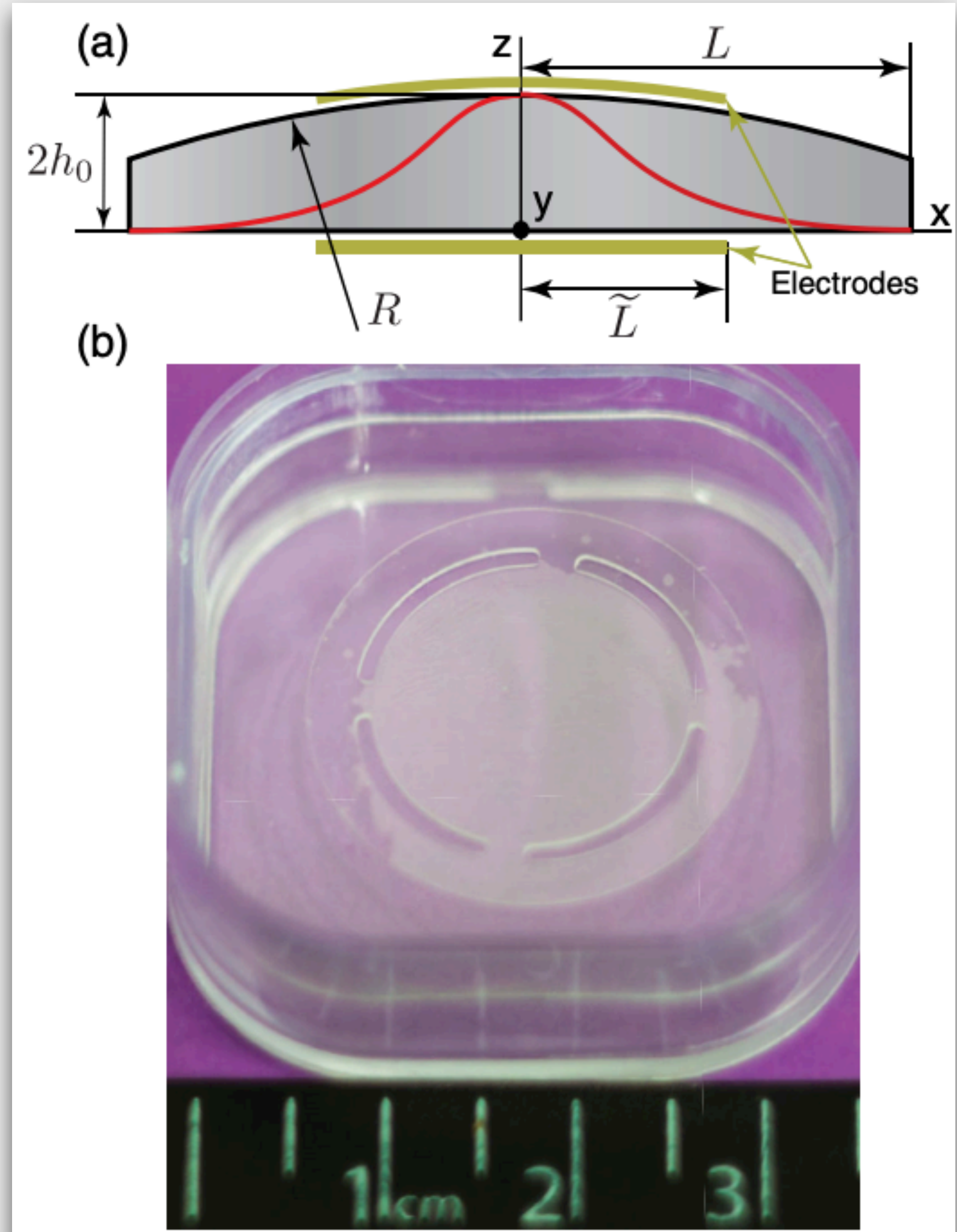

$$u_\lambda(\mathbf{x},t) = B_\lambda(t)U_\lambda(\mathbf{x}), \qquad \int_\mathcal{V} dv \rho U_\lambda U_{\lambda'} = \delta_{\lambda\lambda'} m_\lambda,$$

EOM for a Bar Detector

$$\ddot{B}_\lambda + \tau_\lambda^{-1}\dot{B}_\lambda + \omega_\lambda^2 B = -c^2 R_{i0j0} \int_\mathcal{V} dv \frac{\rho}{m_\lambda} U_\lambda^i(\mathbf{x}) x^j,$$

mode bandwidth

resonance frequency

curvature tensor

overlap

coupling coefficient

$$\xi_\lambda = h_0 \tilde{\xi}_\lambda = \int_\mathcal{V} dv \frac{\rho}{m_\lambda} U_\lambda^i(\mathbf{x}) x^j,$$

$$\tilde{\xi}_{Xn00} = \frac{\xi_{Xn00}}{h_0} = \frac{8}{n\pi} \frac{\mathrm{Erf}(\sqrt{n}\eta_x)\mathrm{Erf}(\sqrt{n}\eta_y)}{\mathrm{Erf}(\sqrt{2n}\eta_x)\mathrm{Erf}(\sqrt{2n}\eta_y)}.$$

trapping coefficient

$$\eta_x = \frac{L}{2}\sqrt{\frac{\chi_x}{h_0\sqrt{RL}}}, \qquad \eta_y = \frac{L}{2}\sqrt{\frac{\chi_y}{h_0\sqrt{RL}}}.$$

Phys.Rev.D 90, 102005 (2014)

EQUS Australian Research Council Centre of Excellence for Engineered Quantum Systems

BAW Cavity as a GW Antenna

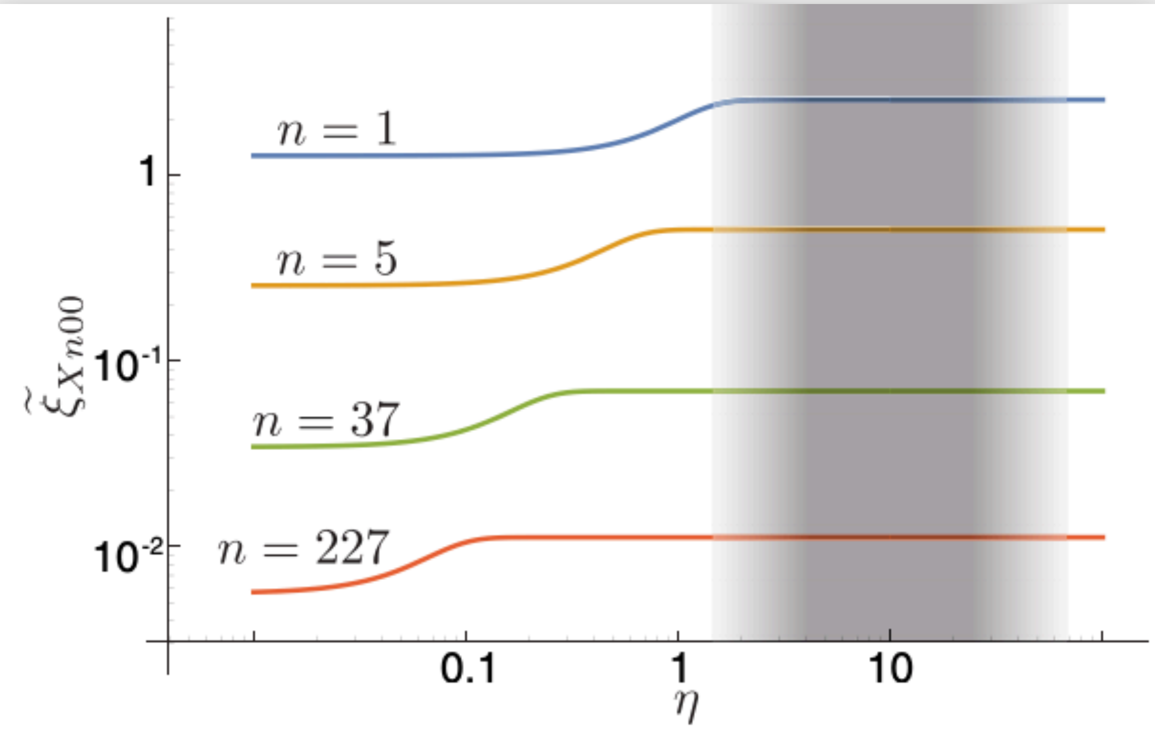

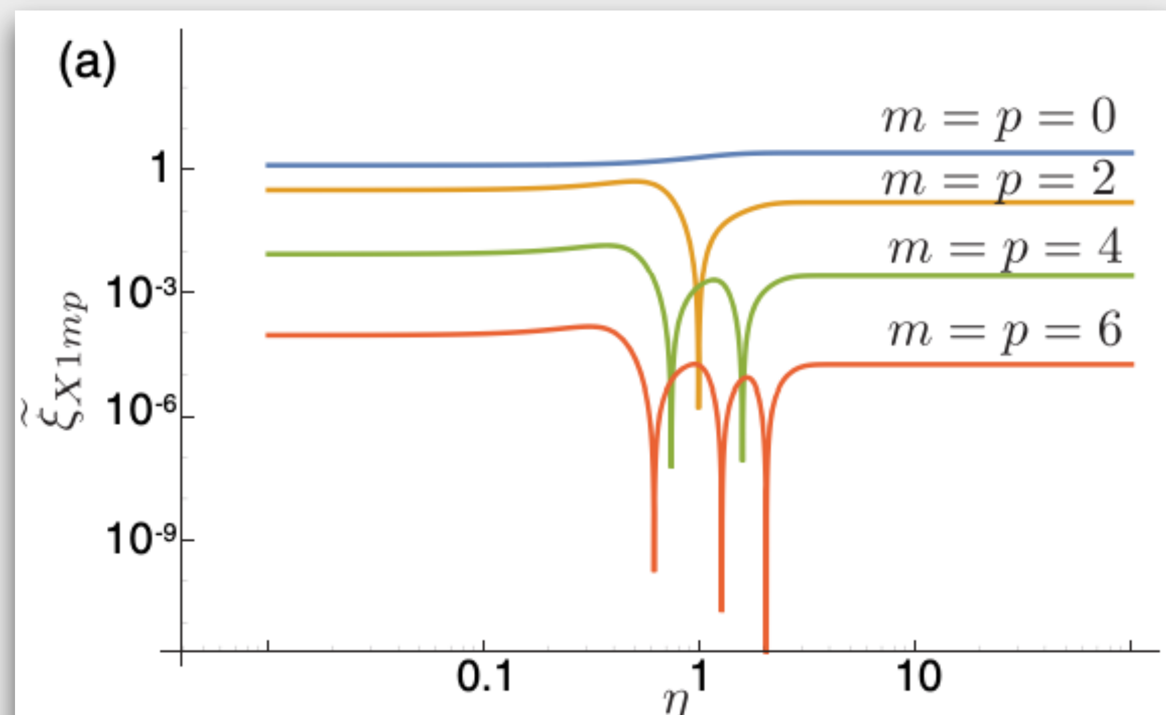

$$u_\lambda(\mathbf{x}, t) = B_\lambda(t) U_\lambda(\mathbf{x}), \qquad \int_{\mathcal{V}} dv \rho U_\lambda U_{\lambda'} = \delta_{\lambda\lambda'} m_\lambda,$$

$$\ddot{B}_\lambda + \tau_\lambda^{-1} \dot{B}_\lambda + \omega_\lambda^2 B = -c^2 R_{i0j0} \int_{\mathcal{V}} dv \frac{\rho}{m_\lambda} U_\lambda^i(\mathbf{x}) x^j,$$

mode bandwidth

resonance frequency

curvature tensor

overlap

coupling coefficient

$$\xi_\lambda = h_0 \tilde{\xi}_\lambda = \int_{\mathcal{V}} dv \frac{\rho}{m_\lambda} U_\lambda^i(\mathbf{x}) x^j,$$

$$\tilde{\xi}_{Xn00} = \frac{\xi_{Xn00}}{h_0} = \frac{8}{n\pi} \frac{\mathrm{Erf}(\sqrt{n}\eta_x)\mathrm{Erf}(\sqrt{n}\eta_y)}{\mathrm{Erf}(\sqrt{2n}\eta_x)\mathrm{Erf}(\sqrt{2n}\eta_y)}.$$

trapping coefficient

$$\eta_x = \frac{L}{2}\sqrt{\frac{\chi_x}{h_0\sqrt{RL}}}, \qquad \eta_y = \frac{L}{2}\sqrt{\frac{\chi_y}{h_0\sqrt{RL}}}.$$

Phys.Rev.D 90, 102005 (2014)

EQUS
Australian Research Council
Centre of Excellence for
Engineered Quantum Systems

Detection Limit in Acoustic Antenna

Rev.Sci.Inst. 66, 2751 (1995)

Nyquist Spectral Density of Force Fluctuations

The acoustic losses in a two-mode resonant bar antenna cause a white spectral density of force to excite the resonant system according to Nyquist's theorem. The single sided spectral density of force (N^2/Hz), exciting a mechanical oscillator in equilibrium with the surroundings of temperature T, is given by

$$S^{+}_{fn}=4kTh_n=4kT\omega_n m_n/Q_n . \qquad (13)$$

$$m_{n,0,0} \sim n^{-1}$$

$$\omega_{n,0,0} \sim n$$

$$h^{+}(f)=\frac{\pi S^{+}_{ns}(f)}{4fL},$$

Thus, the spectral strain sensitivity due to acoustic losses can be shown to be given by[13]

$$h^{+}_{th\ 1}(f)=\frac{\pi}{Lf}\sqrt{\frac{2kT}{\omega_1 Q_1 m_1}}.$$

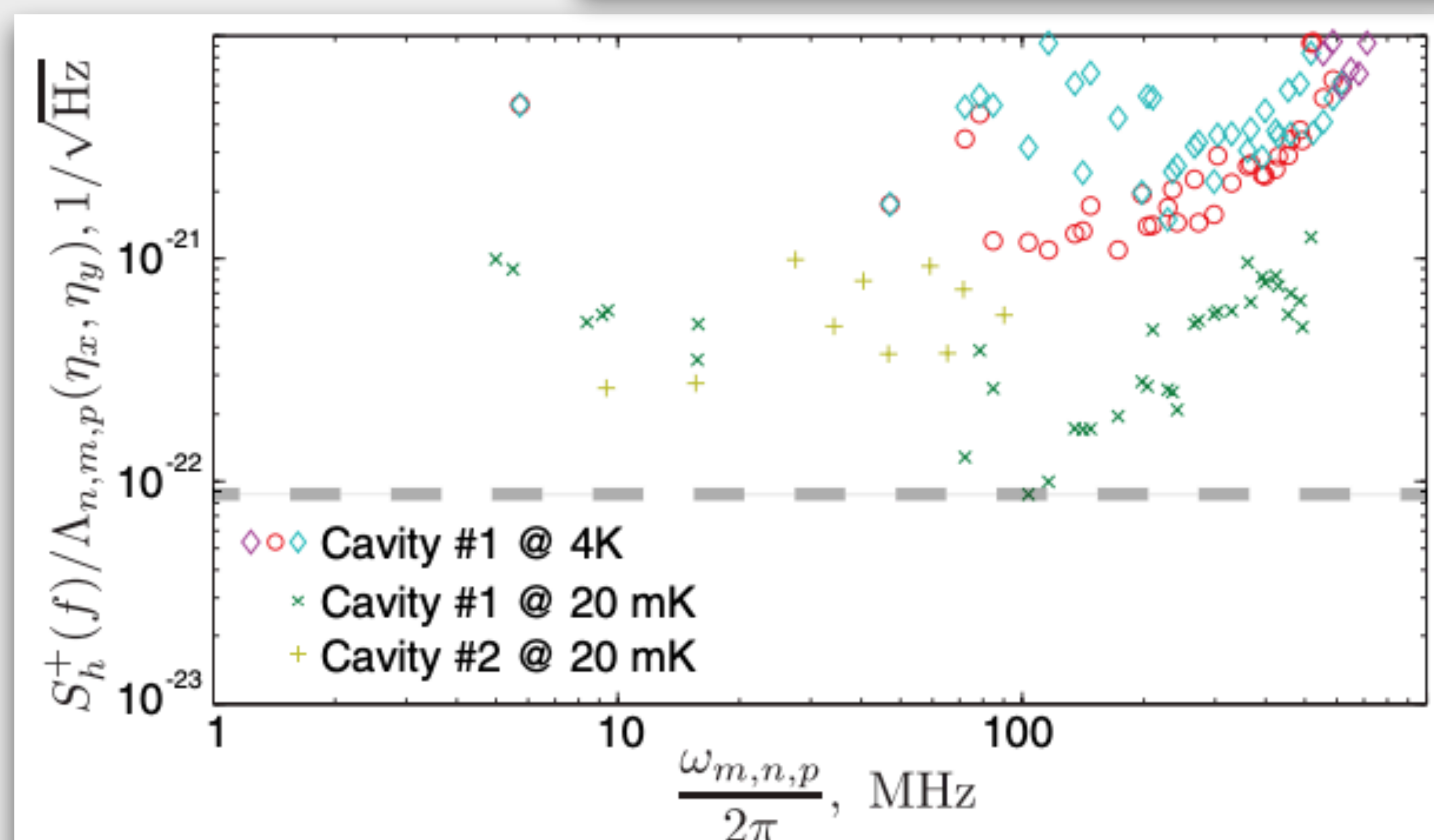

$$S_h^+ = 1.7\times 10^{-22}\frac{\sqrt{\eta_x\eta_y \mathrm{Erf}(\sqrt{2n}\eta_x)\mathrm{Erf}(\sqrt{2n}\eta_y)}}{\mathrm{Erf}(\sqrt{n}\eta_x)\mathrm{Erf}(\sqrt{n}\eta_y)}$$

$$= 1.7\times 10^{-22}\Lambda_{n,0,0}(\eta_x,\eta_y),\ \frac{[\mathrm{strain}]}{\sqrt{\mathrm{Hz}}},$$

Phys.Rev.D 90, 102005 (2014)

EQUS
Australian Research Council Centre of Excellence for Engineered Quantum Systems

Detection Limit in Acoustic Antenna

Rev.Sci.Inst. 66, 2751 (1995)

Nyquist Spectral Density of Force Fluctuations

The acoustic losses in a two-mode resonant bar antenna cause a white spectral density of force to excite the resonant system according to Nyquist's theorem. The single sided spectral density of force (N^2/Hz), exciting a mechanical oscillator in equilibrium with the surroundings of temperature T, is given by

$$S_{fn}^{+}=4kTh_n=4kT\omega_n m_n/Q_n. \qquad (13)$$

$$\boxed{\begin{aligned} m_{n,0,0} &\sim n^{-1} \\ \omega_{n,0,0} &\sim n \end{aligned}}$$

$$h^{+}(f)=\frac{\pi S_{ns}^{+}(f)}{4fL},$$

Thus, the spectral strain sensitivity due to acoustic losses can be shown to be given by[15]

$$h_{th\ 1}^{+}(f)=\frac{\pi}{Lf}\sqrt{\frac{2kT}{\omega_1 Q_1 m_1}}.$$

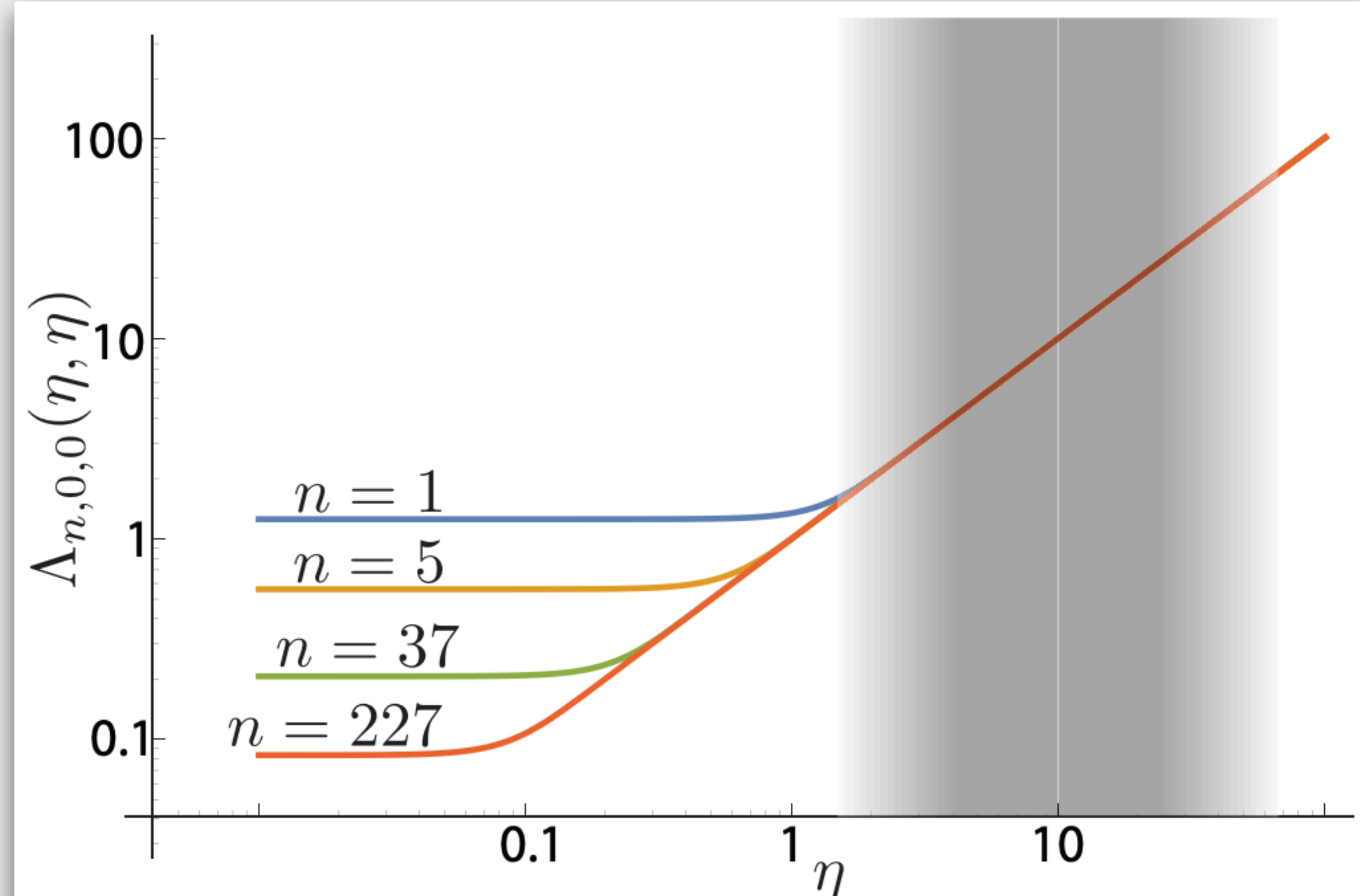

$$\begin{aligned} S_h^{+} &= 1.7\times10^{-22}\,\frac{\sqrt{\eta_x\eta_y\mathrm{Erf}(\sqrt{2n}\eta_x)\mathrm{Erf}(\sqrt{2n}\eta_y)}}{\mathrm{Erf}(\sqrt{n}\eta_x)\mathrm{Erf}(\sqrt{n}\eta_y)} \\ &= 1.7\times10^{-22}\Lambda_{n,0,0}(\eta_x,\eta_y),\ \frac{[\text{strain}]}{\sqrt{\text{Hz}}}, \end{aligned}$$

Phys.Rev.D 90, 102005 (2014)

EQUS
Australian Research Council
Centre of Excellence for
Engineered Quantum Systems

Detection Limit in Acoustic Antenna

Rev.Sci.Inst. 66, 2751 (1995)

Nyquist Spectral Density of Force Fluctuations

The acoustic losses in a two-mode resonant bar antenna cause a white spectral density of force to excite the resonant system according to Nyquist's theorem. The single sided spectral density of force (N^2/Hz), exciting a mechanical oscillator in equilibrium with the surroundings of temperature T, is given by

$$S_{fn}^{+} = 4kTh_n = 4kT\omega_n m_n / Q_n . \qquad (13)$$

$$\boxed{\begin{aligned} m_{n,0,0} &\sim n^{-1} \\ \omega_{n,0,0} &\sim n \end{aligned}}$$

Thus, the spectral strain sensitivity due to acoustic losses can be shown to be given by:

$h^{+}(f) =$

Resonant bar antenna
would be infinitely broadband if it is limited
only by resonance own
(narrowband) noise

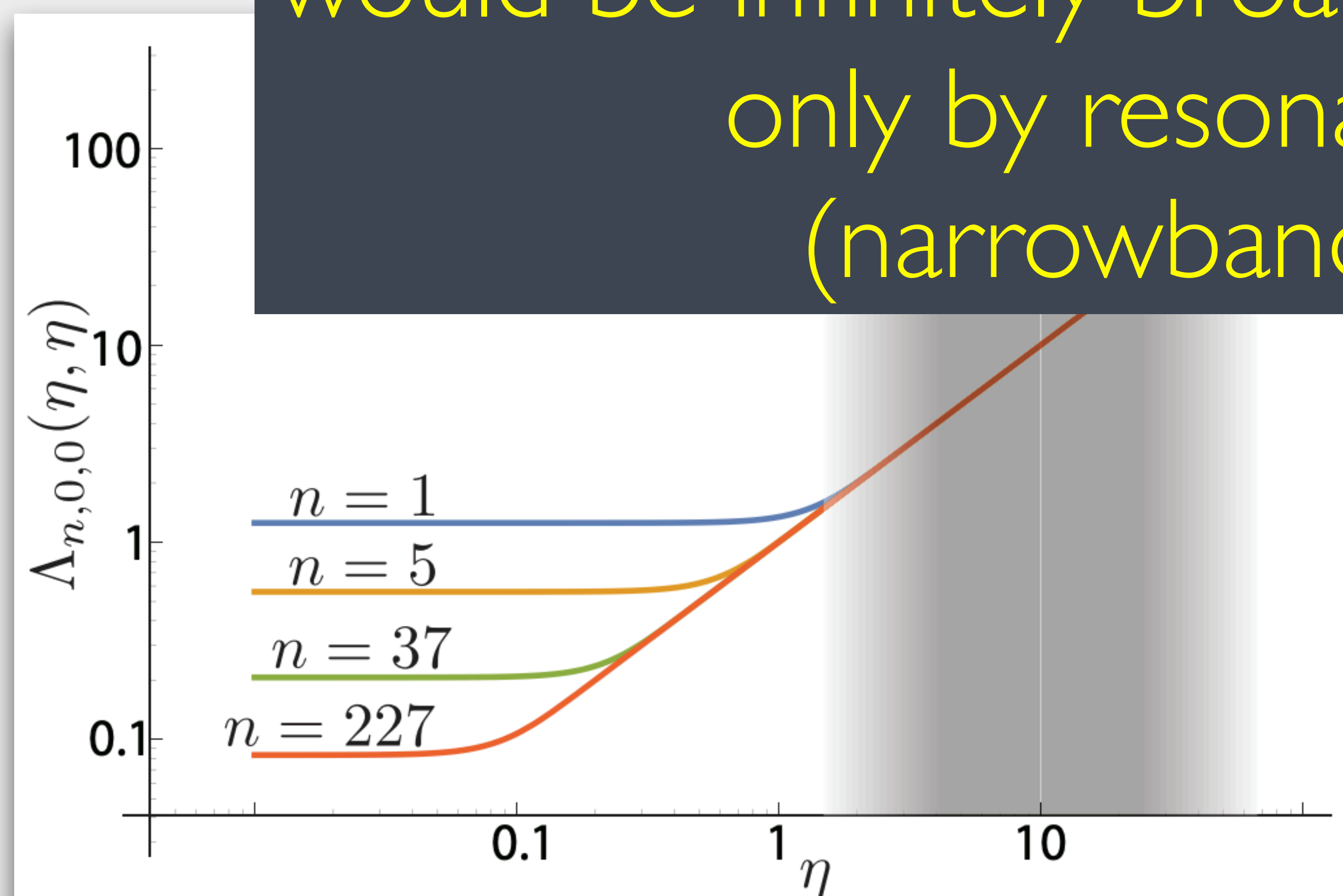

$\mathrm{Erf}(\sqrt{2n}\eta_y)$

$\sqrt{n}\eta_y)$

$\sqrt{\mathrm{Hz}}$

Phys.Rev.D 90, 102005 (2014)

EQUS
Australian Research Council
Centre of Excellence for
Engineered Quantum Systems

BAW Cavity as a GW Antenna

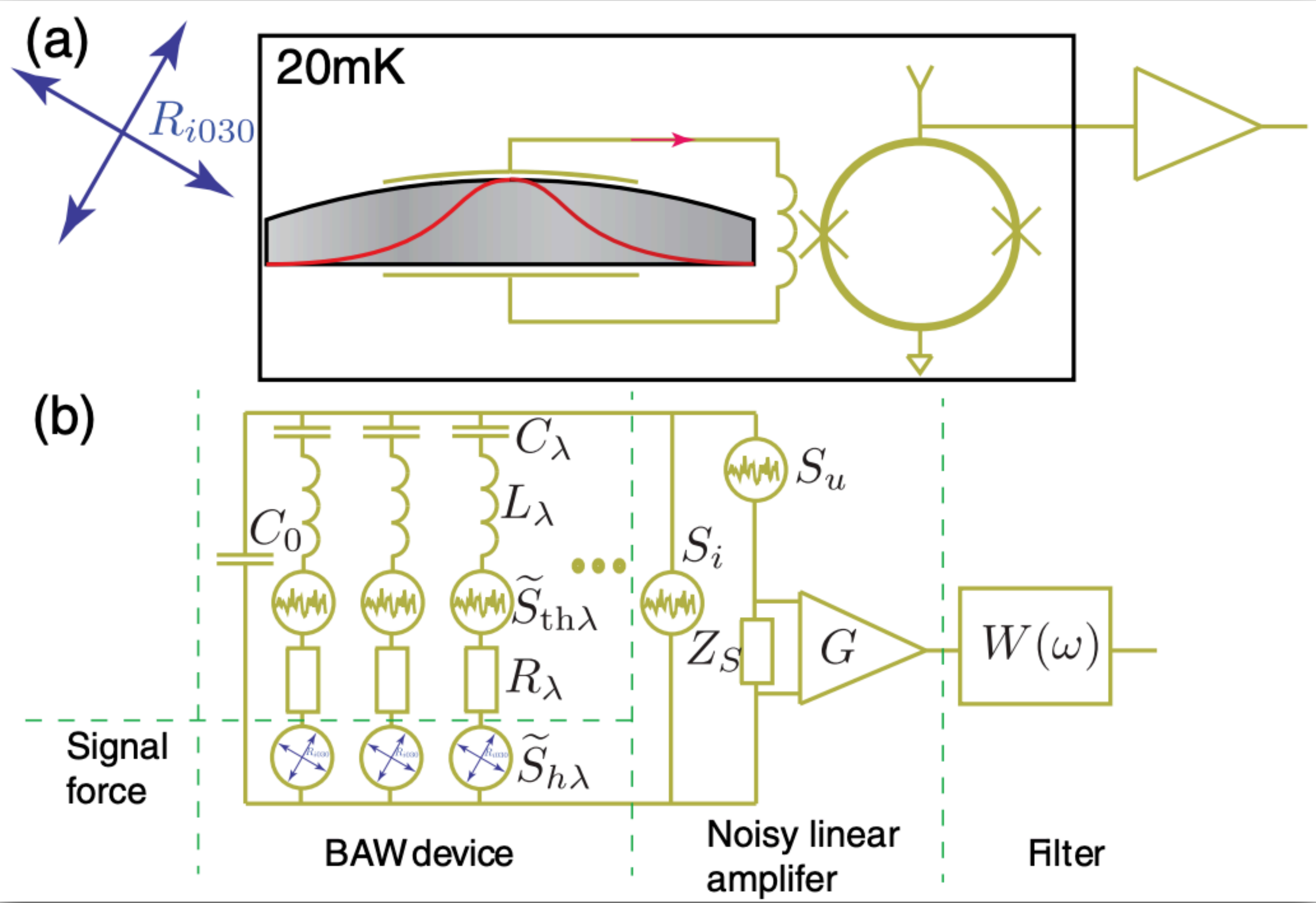

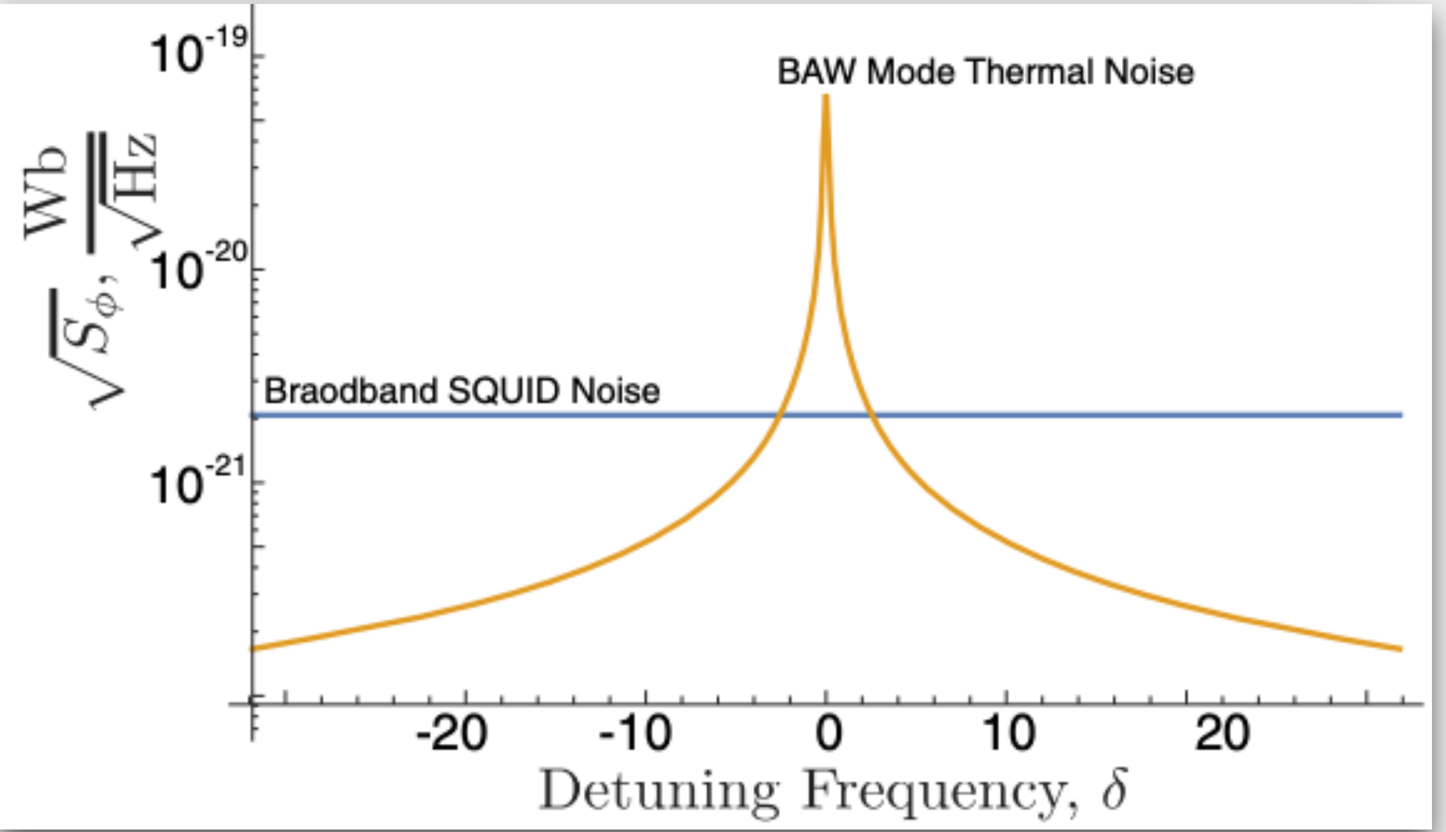

SQUID BA noise

$$S_f = \kappa_\lambda^2 |Z_{BA}|^2 S_i.$$

could be neglected

SQUID additive noise

$$S_\lambda = \frac{1}{\kappa_\lambda^2 \omega_\lambda^2 |Z_\lambda|^2} \tilde{S}_\lambda = \frac{S_u}{\kappa_\lambda^2 \omega_\lambda^2 |Z_S|^2} = \frac{S_\phi}{\kappa_\lambda^2 |Z_S|^2},$$

$\sqrt{S_\phi}$ $10^{-6} \phi_0 / \sqrt{\mathrm{Hz}}$

sets the minimal detectable signal from BAW

Phys.Rev.D 90, 102005 (2014)

EQUS Australian Research Council Centre of Excellence for Engineered Quantum Systems

BAW Cavity as a GW Antenna

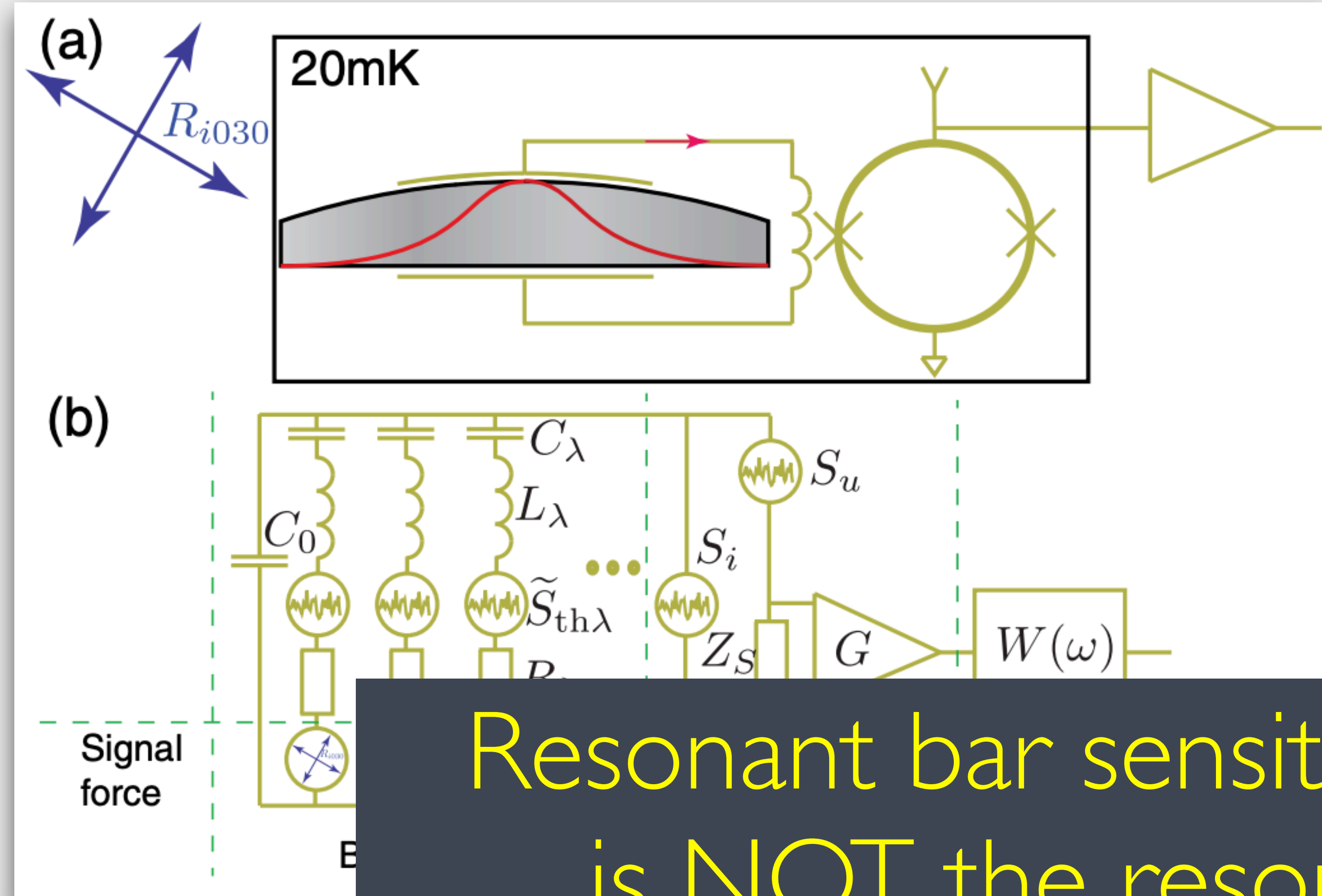

SQUID BA noise

$$S_f = \kappa_\lambda^2 |Z_{BA}|^2 S_i.$$

could be neglected

SQUID additive noise

$$S_\phi = \frac{1}{\ldots} \quad \tilde{S} = \frac{S_u}{\ldots} = \frac{S_\phi}{\kappa_\lambda^2 |Z_S|^2},$$

Resonant bar sensitive frequency range is NOT the resonance bandwidth

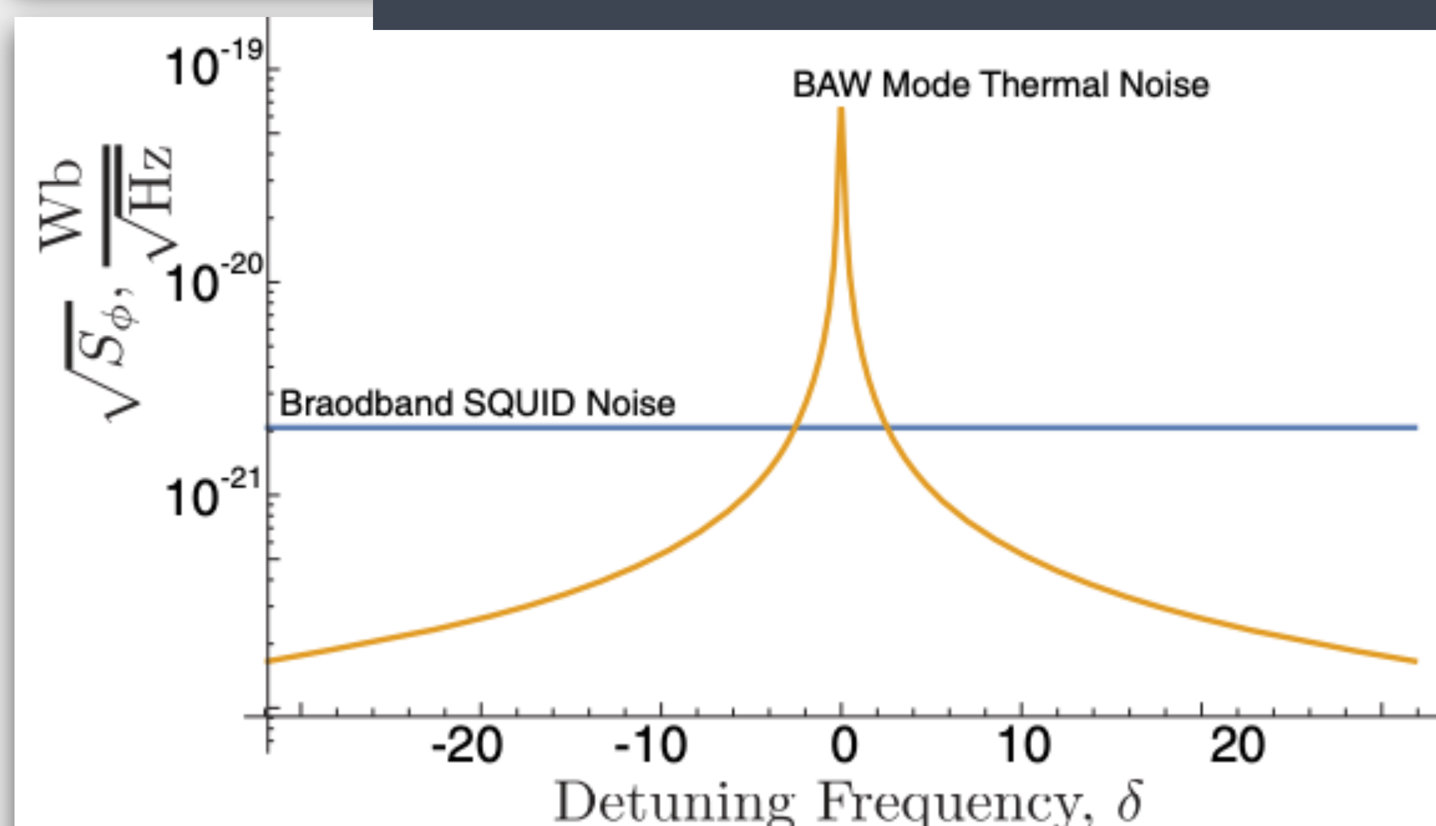

sets the minimal detectable signal from BAW

Phys.Rev.D 90, 102005 (2014)

EQUS
Australian Research Council
Centre of Excellence for
Engineered Quantum Systems

BAW Cavity as a GW Antenna

Observation of the Fundamental Nyquist Noise Limit in an Ultra-High Q-Factor Cryogenic Bulk Acoustic Wave Cavity

Maxim Goryachev,[1,*] Eugene N. Ivanov,[1] Frank van Kann,[2] Serge Galliou,[3] and Michael E. Tobar[1]

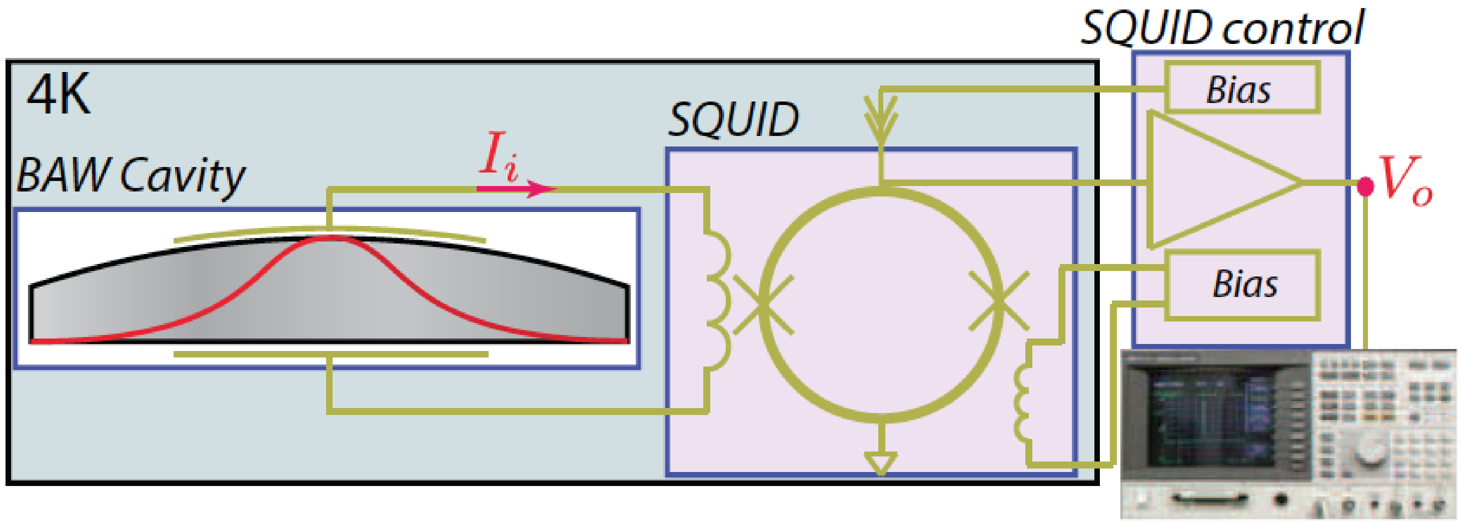

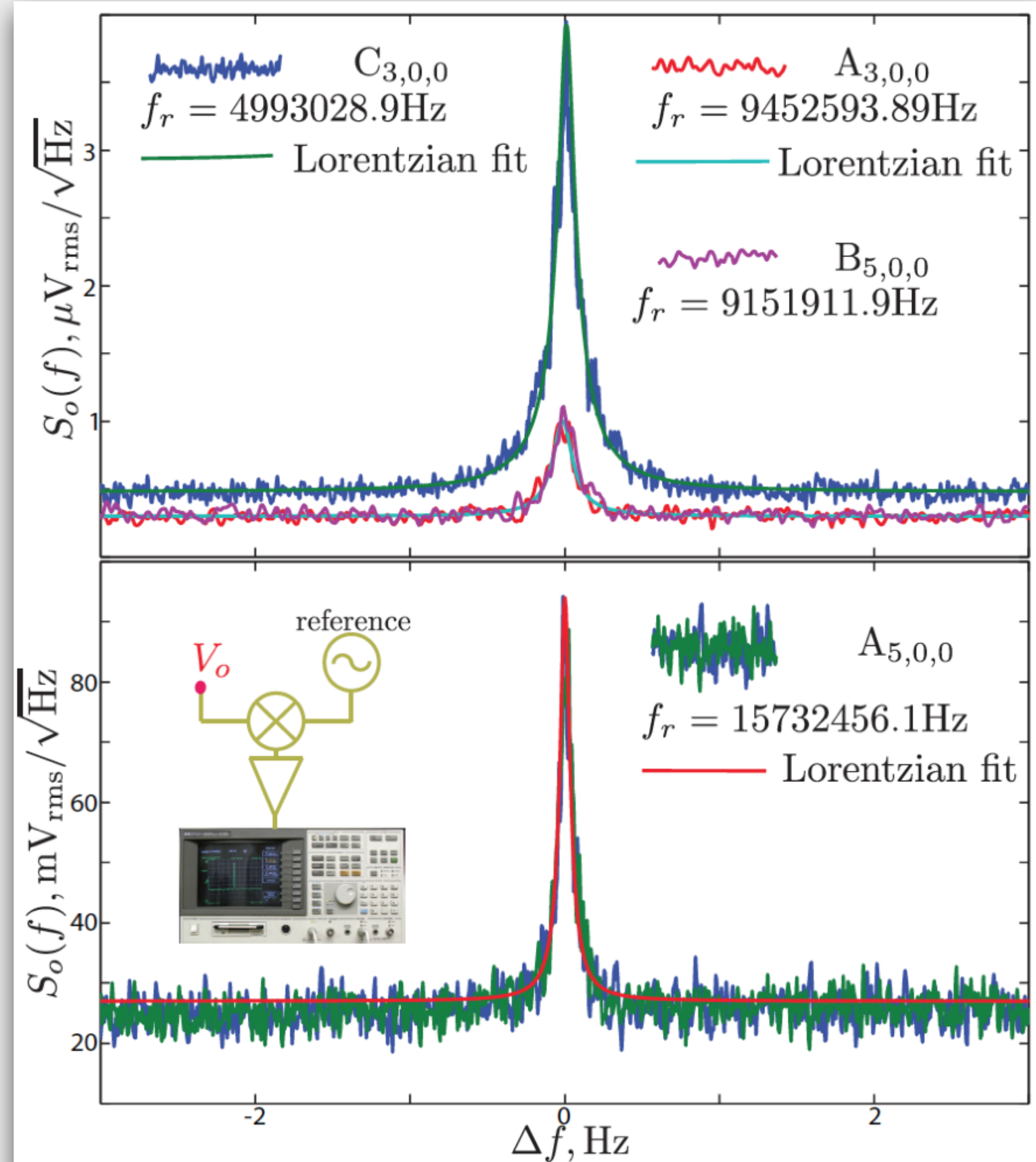

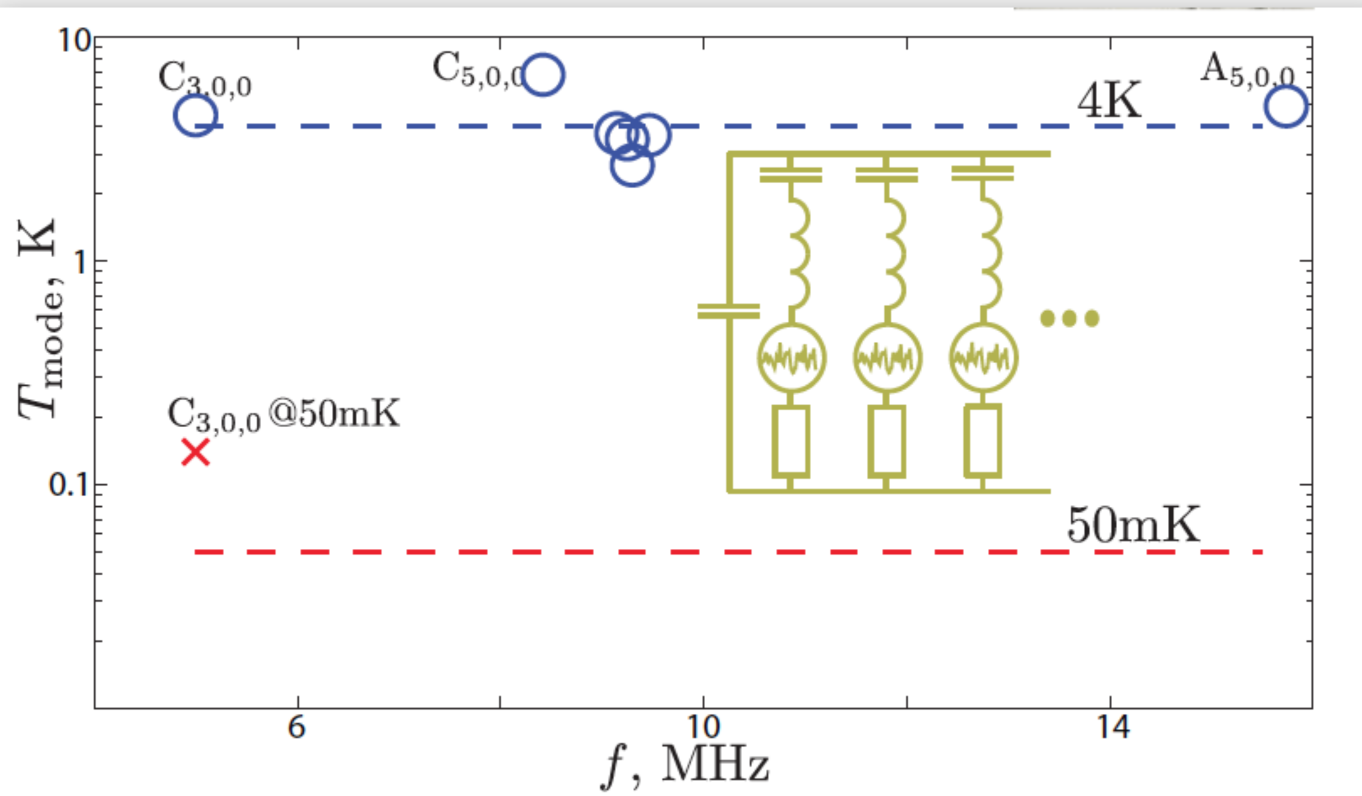

$X_{n,m,p}$	f_r, MHz	$Q_{fit}, 10^7$	$V_p, \frac{\mu V}{\sqrt{Hz}}$	R_x, Ω	$Q_Z, 10^7$
$C_{3,0,0}$	4.993	4.9	4	3	4.4
$C_{5,0,0}$	8.392			5.36	10.7
$B_{3,0,0}$	5.505			2.9	4.84
$B_{5,0,0}$	9.152	10	1.1	5.9	6.4
$B_{5,m,p}$	9.247	10		7.9	11.9
$B_{5,m,p}$	9.287	10	0.87	5.92	25.8
$A_{3,0,0}$	9.452	9.4	1	6	6
$A_{5,0,0}$	15.732	26		2.3	30
$C_{3,0,0}$ @50mK	4.993	2.9	0.74	2.3	3

Appl.Phys.Lett 105, 153505

Outline

- BAW Technology
- BAW as a GW Antenna
- Current Status and First Results
- Perspectives
- Test of Fundamental Physics @ UWA

Current Status

Control and Signal Processing

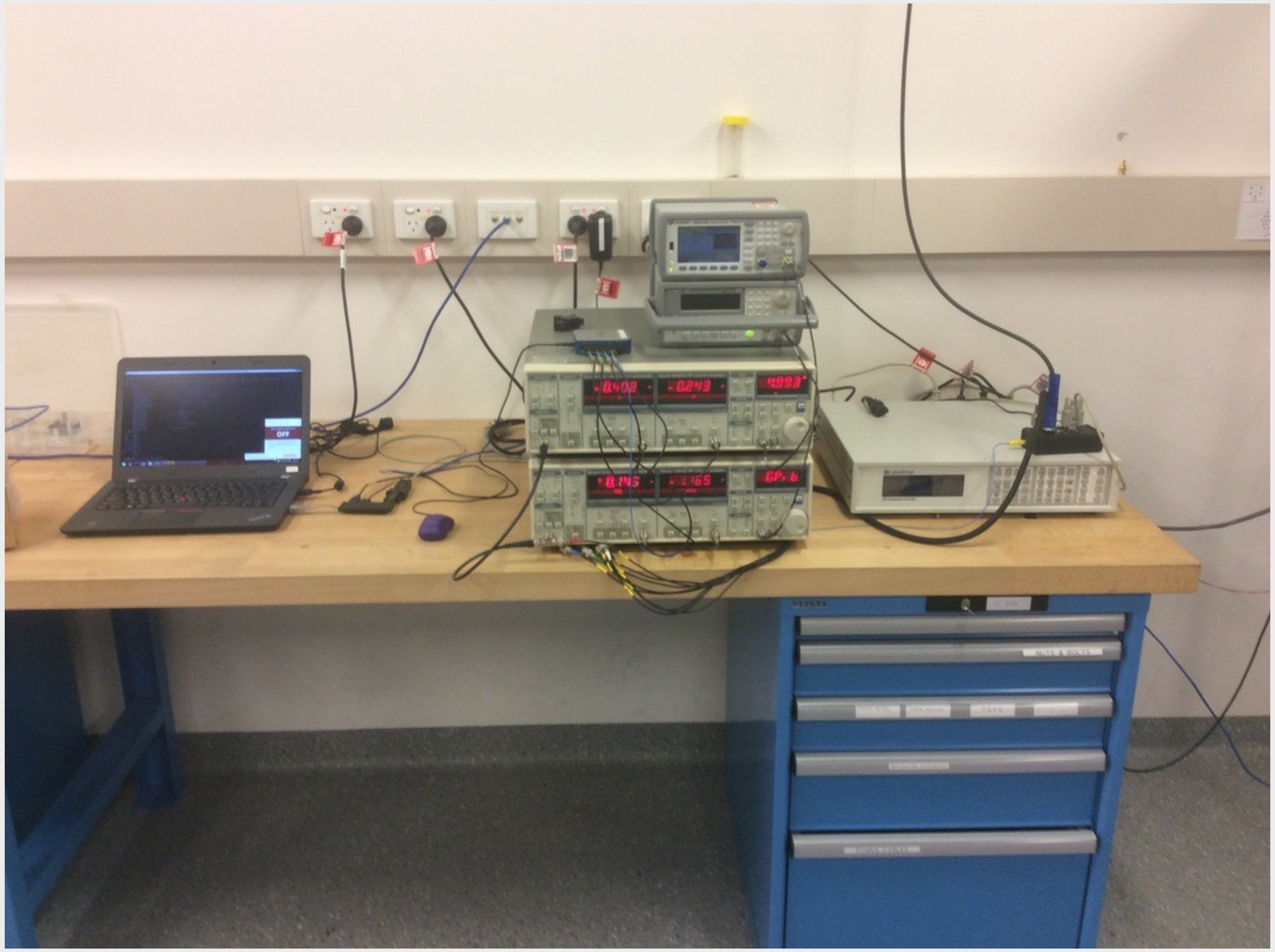

Two standalone lockin amplifiers
Two Signal generators
Locked to an H-maser
Temperature controller
SQUID control
Python data logging

Cryogenic Part

3.4K cryocooler
SQUID electronics

BAW and SQUID sit in a bulk Nb shield

EQUS
Australian Research Council
Centre of Excellence for
Engineered Quantum Systems

Current Status

Control and Signal Processing

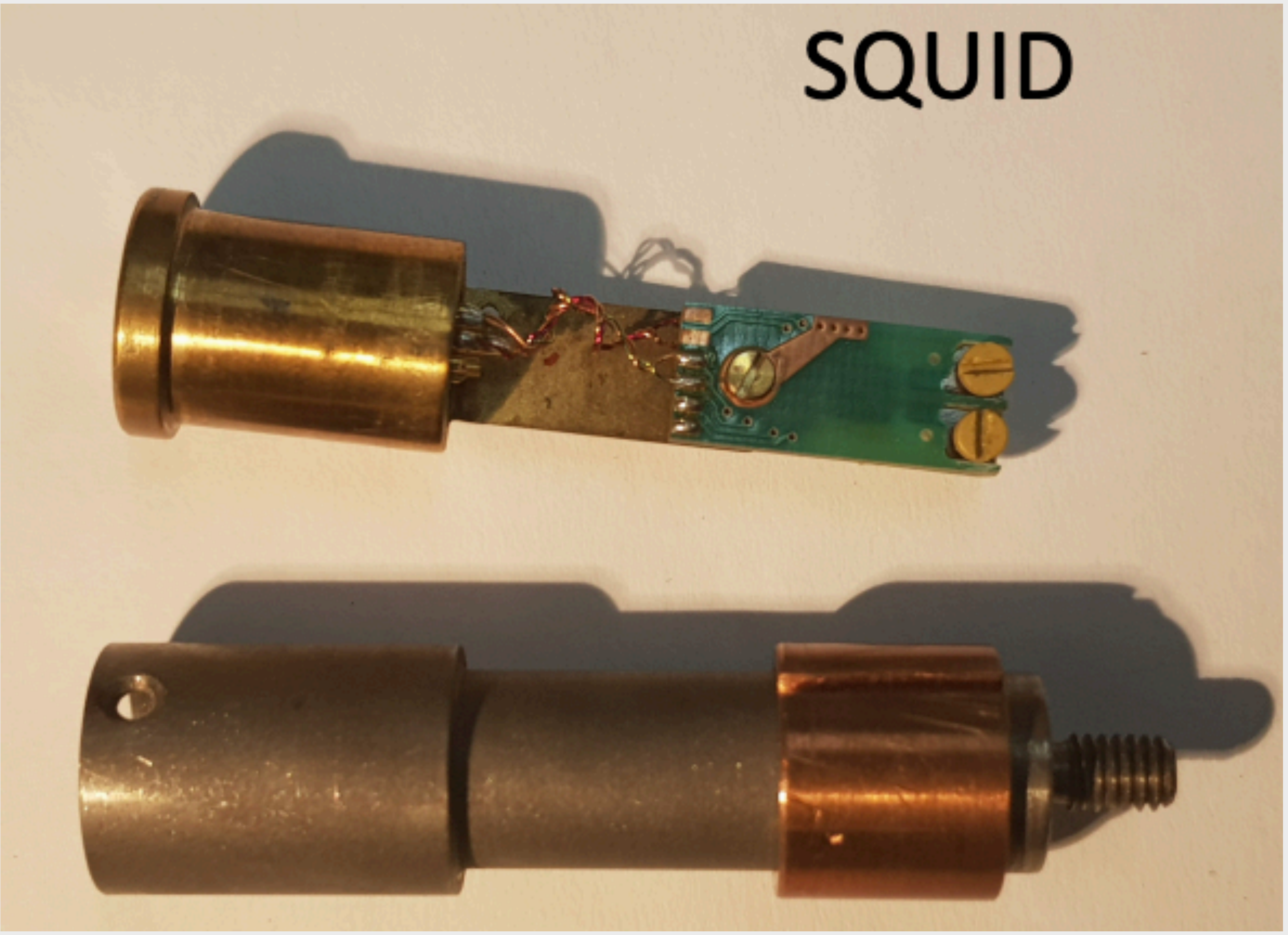

Two standalone lockin amplifiers
Two Signal generators
Locked to an H-maser
Temperature controller
SQUID control
Python data logging

Cryogenic Part

3.4K cryocooler
SQUID electronics

BAW and SQUID sit in a bulk Nb shield

EQUS
Australian Research Council
Centre of Excellence for
Engineered Quantum Systems

First Data

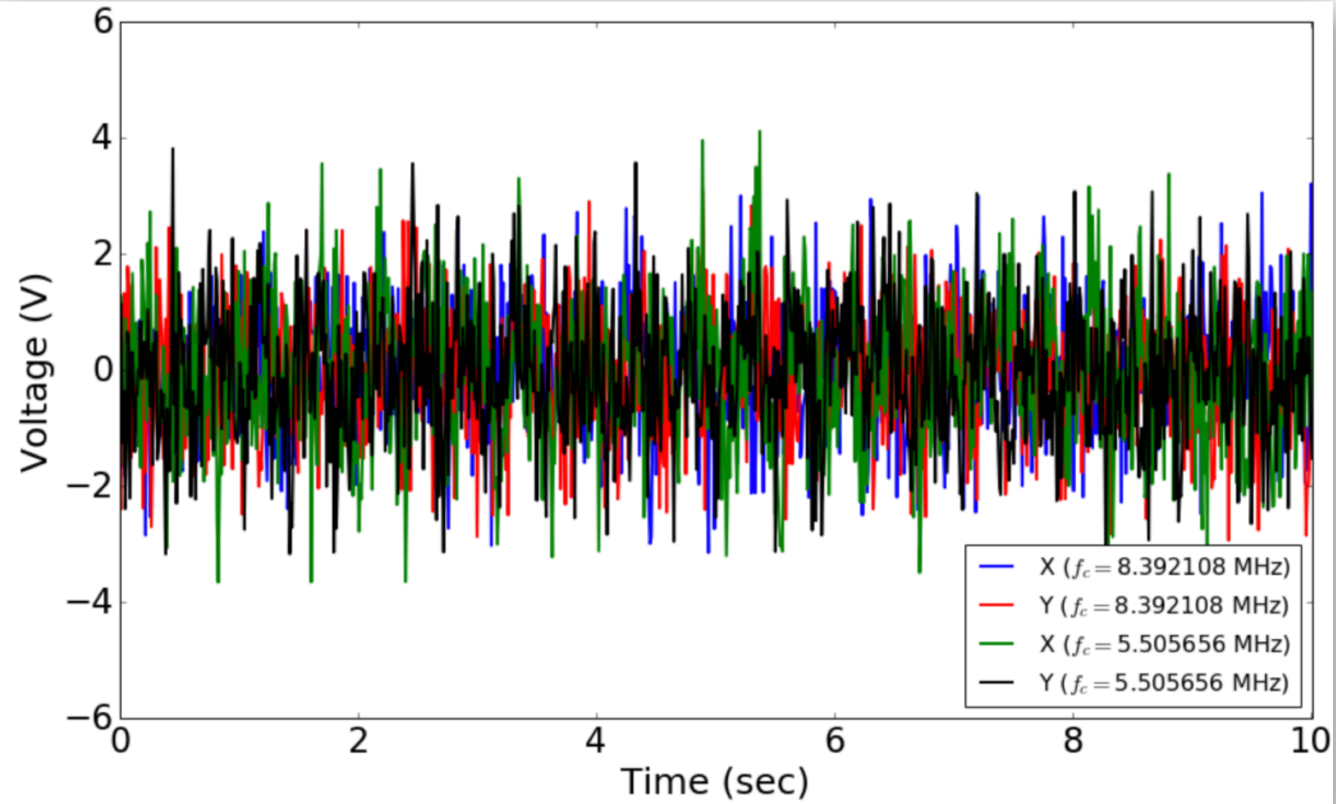

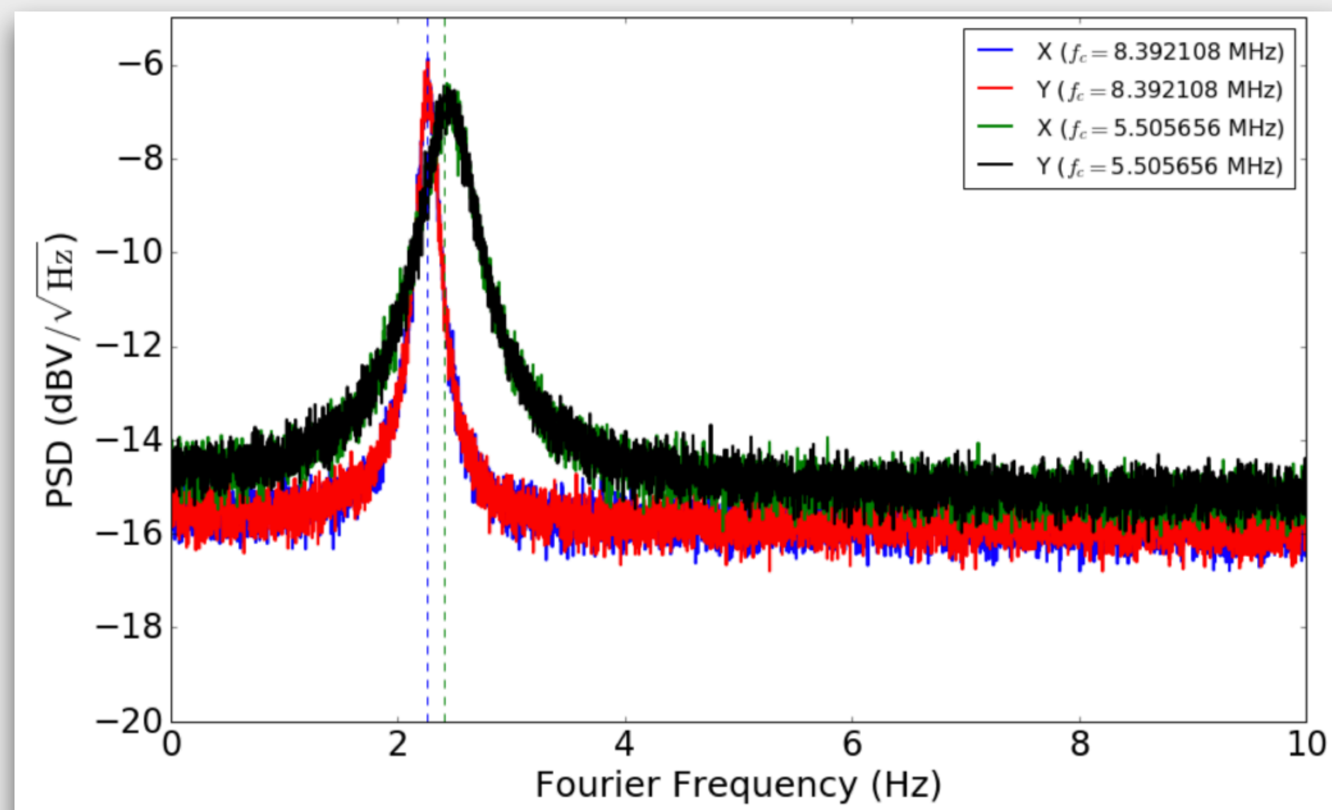

Data taking started: 15 Nov 2018

A few short and long (~1week) gaps

One cryocooler (3.4K), One crystal, 2 modes, 4 channels

1 week: 2 cryocoolers (3.4K + 20mK), 2 crystals, 4 modes, 8 channels

2 weeks: 2 cryocoolers (3.4K + 4K) , 2 crystals, 4 modes, 8 channels

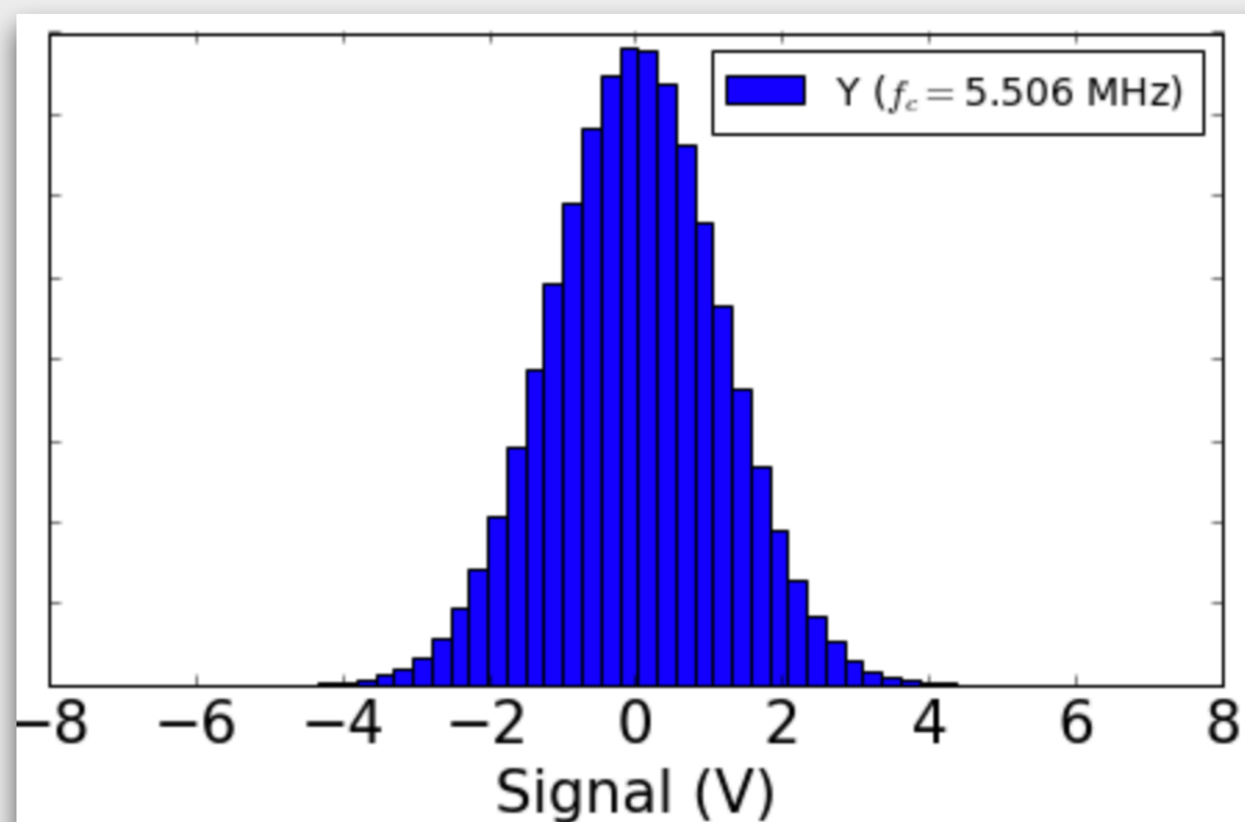

First Data

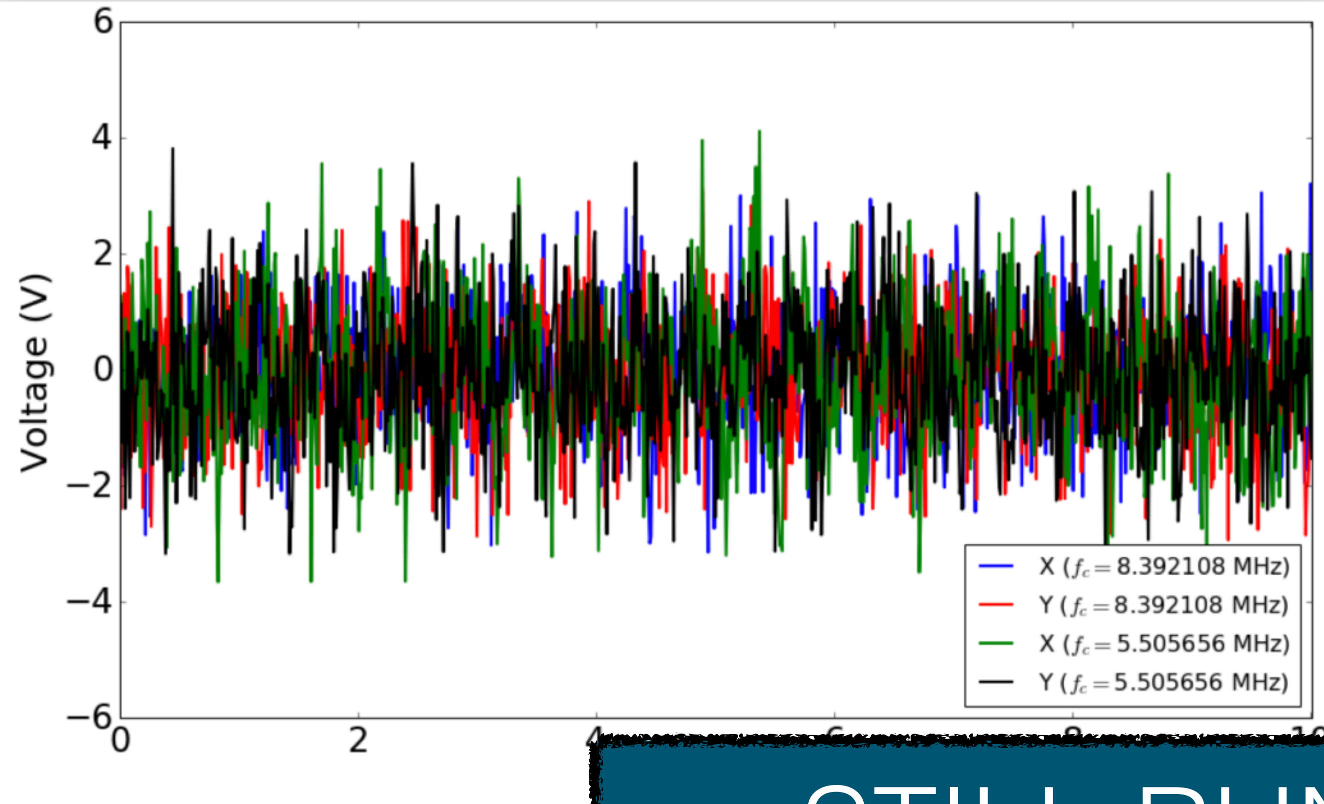

Data taking started: 15 Nov 2018

A few short and long (~1week) gaps

One cryocooler (3.4K), One crystal, 2 modes, 4 channels

1 week: 2 cryocoolers (3.4K + 20mK), 2 crystals, 4 modes, 8 channels

STILL RUNNING

ocoolers (3.4K + 4K) , 2 crystals, 4 modes, 8 channels

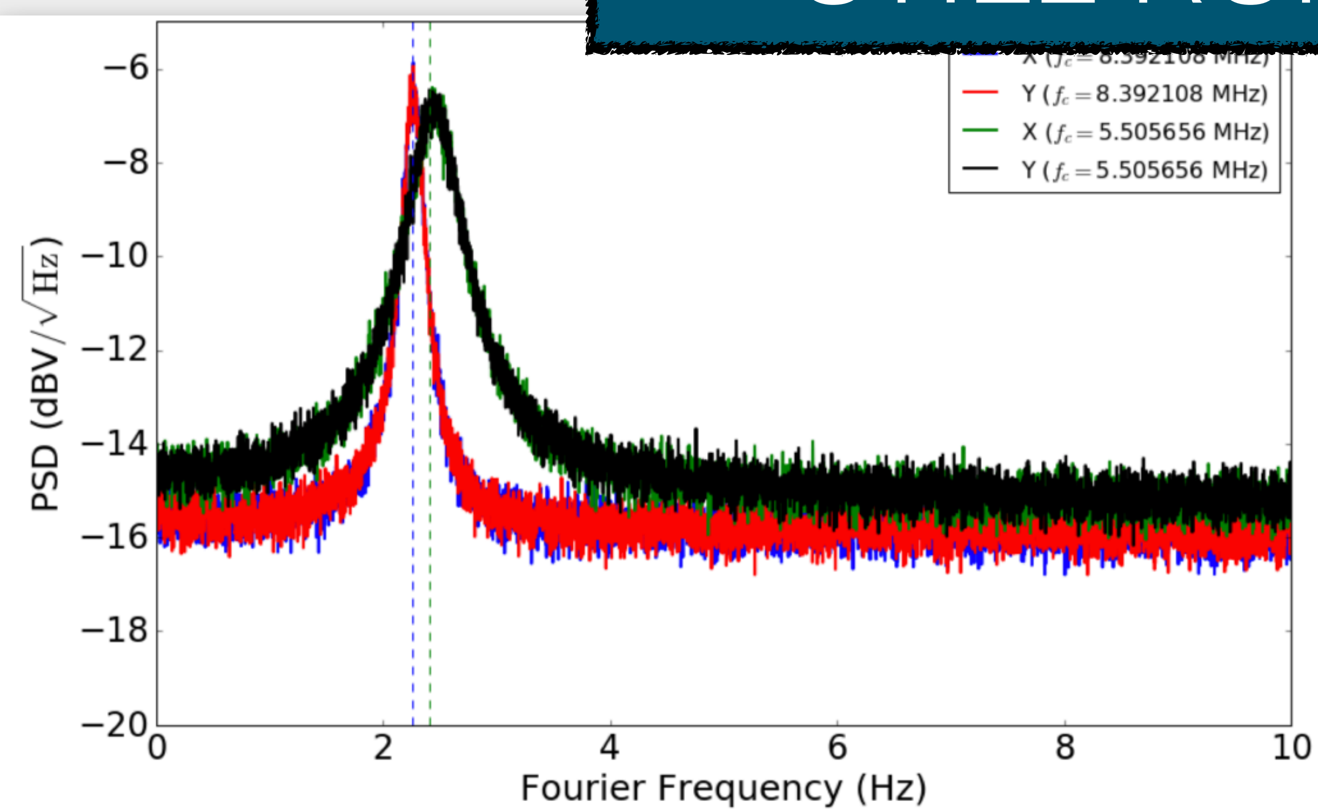

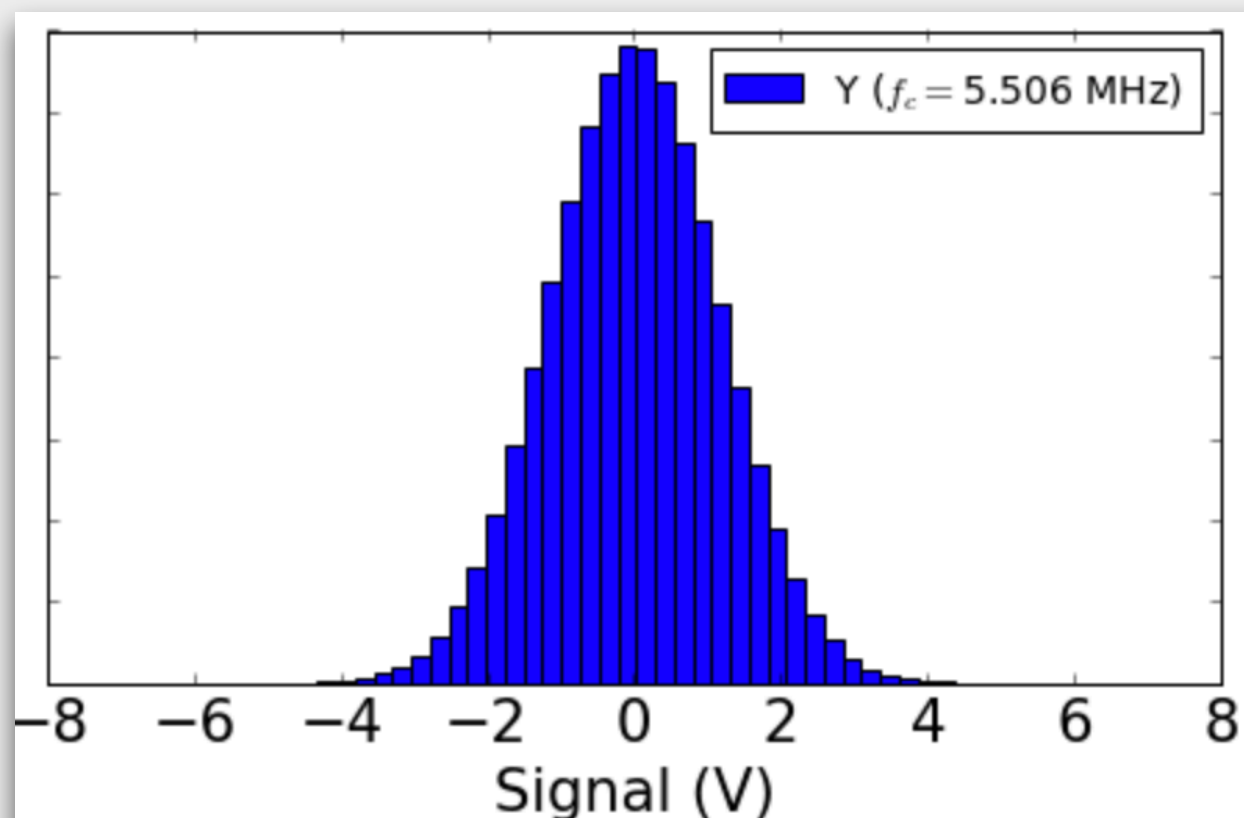

First 20mK Data

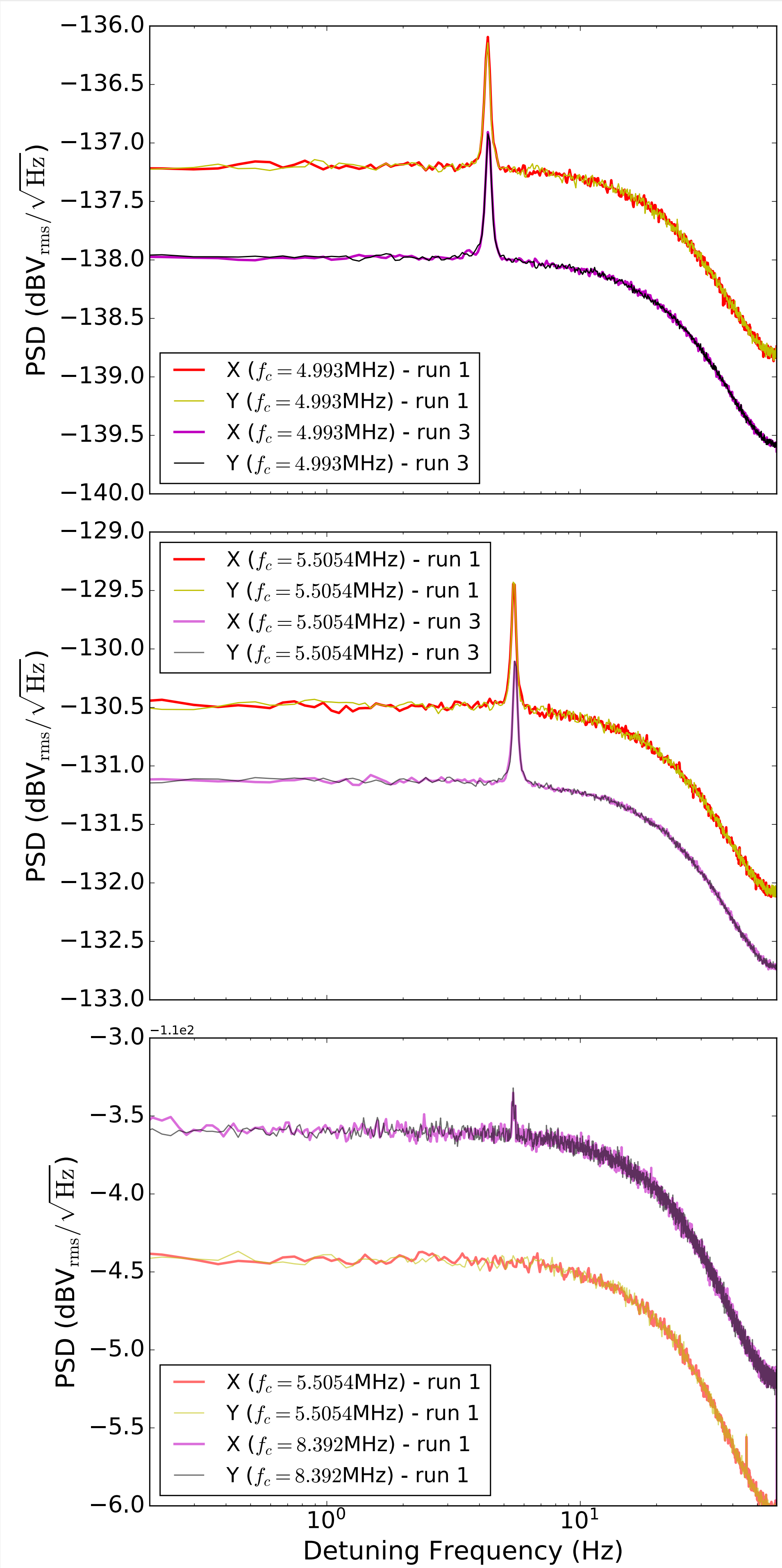

Data taking started: 15 Nov 2018

A few short and long (~1week) gaps

1 week: 2 cryocoolers (3.4K + 20mK), 2 crystals, 4 modes, 8 channels

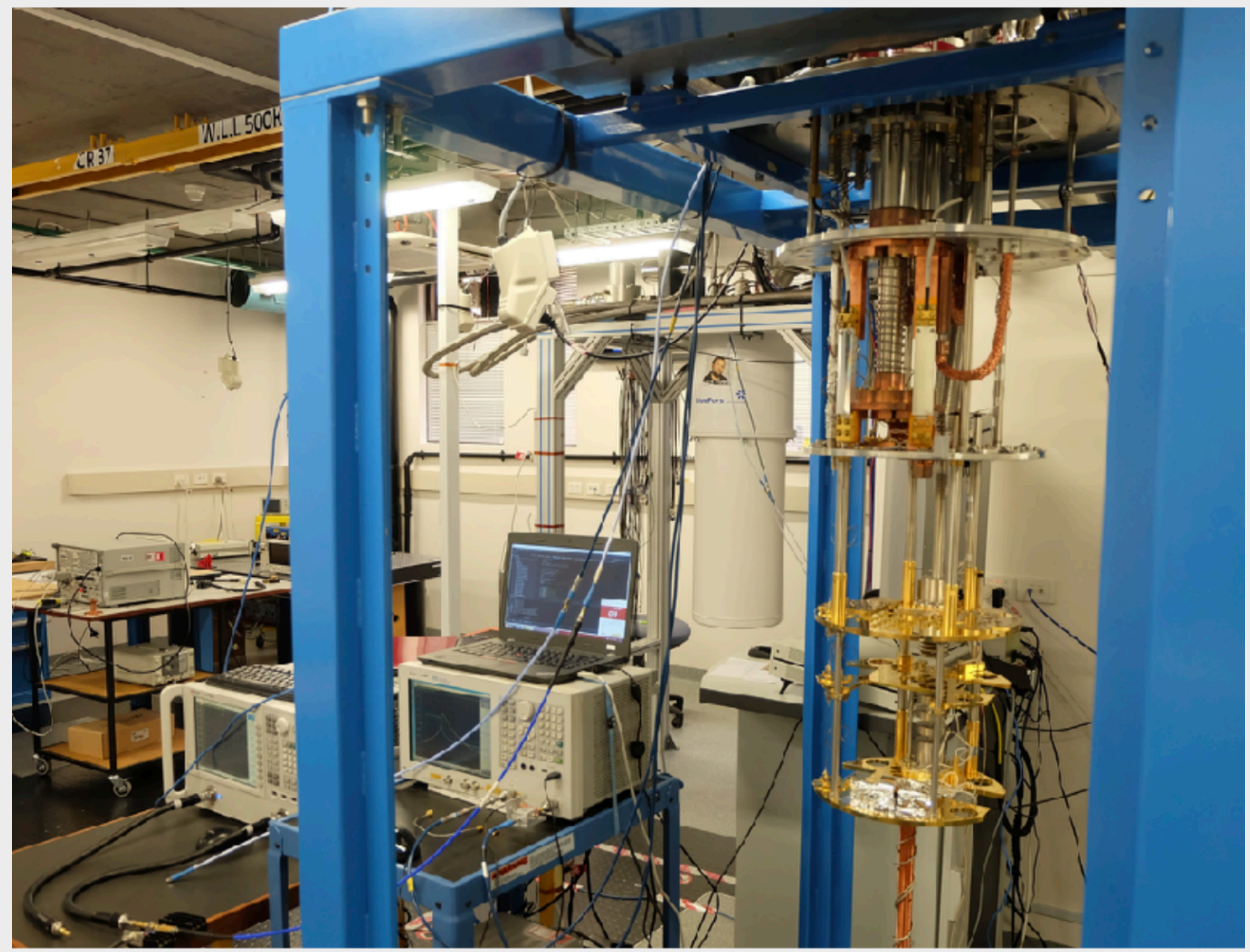

EQUS
Australian Research Council Centre of Excellence for Engineered Quantum Systems

Data Analysis

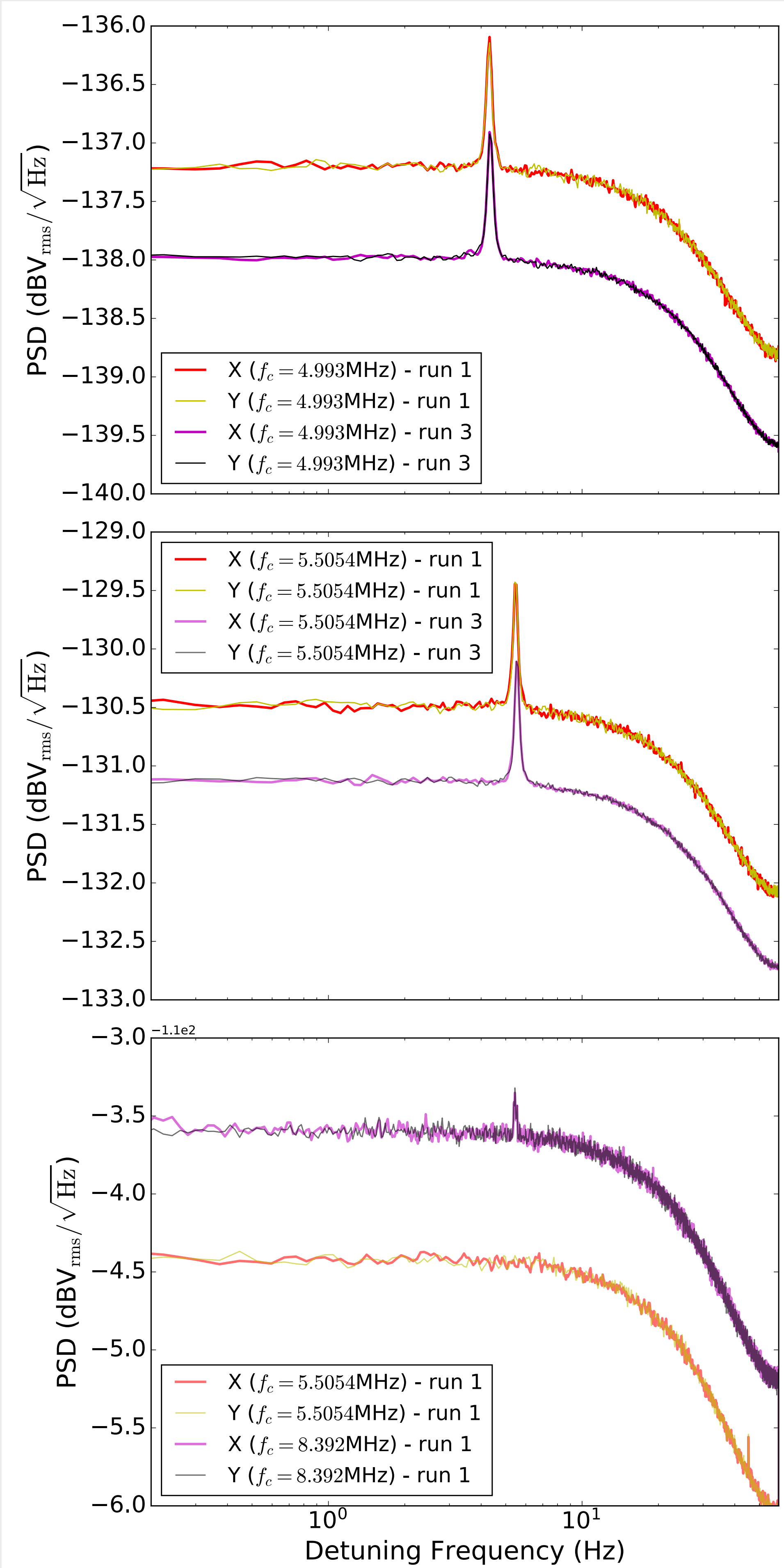

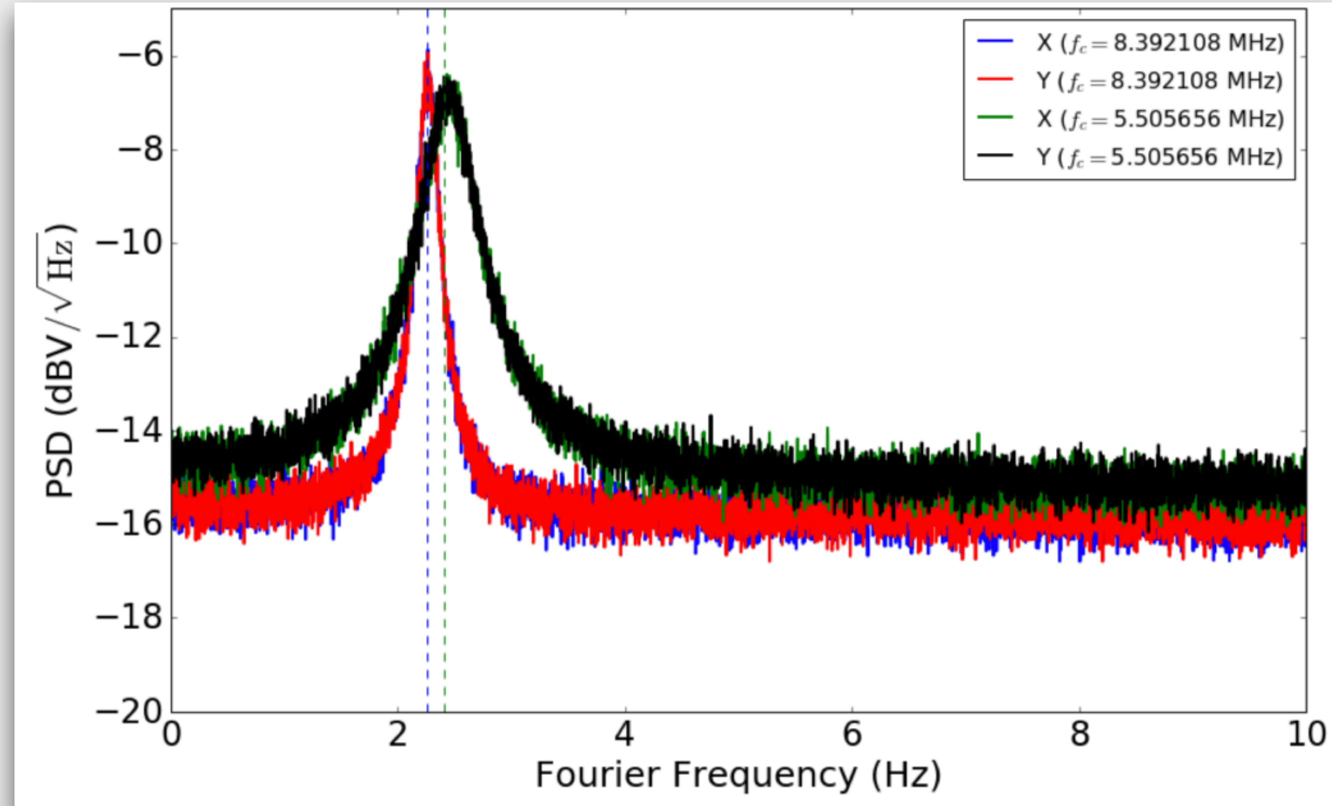

Ik Siong Heng
(University of Glasgo)

Outline

BAW Technology

BAW as a GW Antenna

Current Status and First Results

Perspectives

Test of Fundamental Physics @ UWA

Further Improvements

Easy

- Increase number of modes/channels/crystals
- Improvements in signal processing
- Shifting to 20 mK (dilution fridge)
- mK higher frequency SQUIDs

Hard

- Design of Dedicated BAW cavities
- Multisite Detection

Signal Processing

digital downconversion

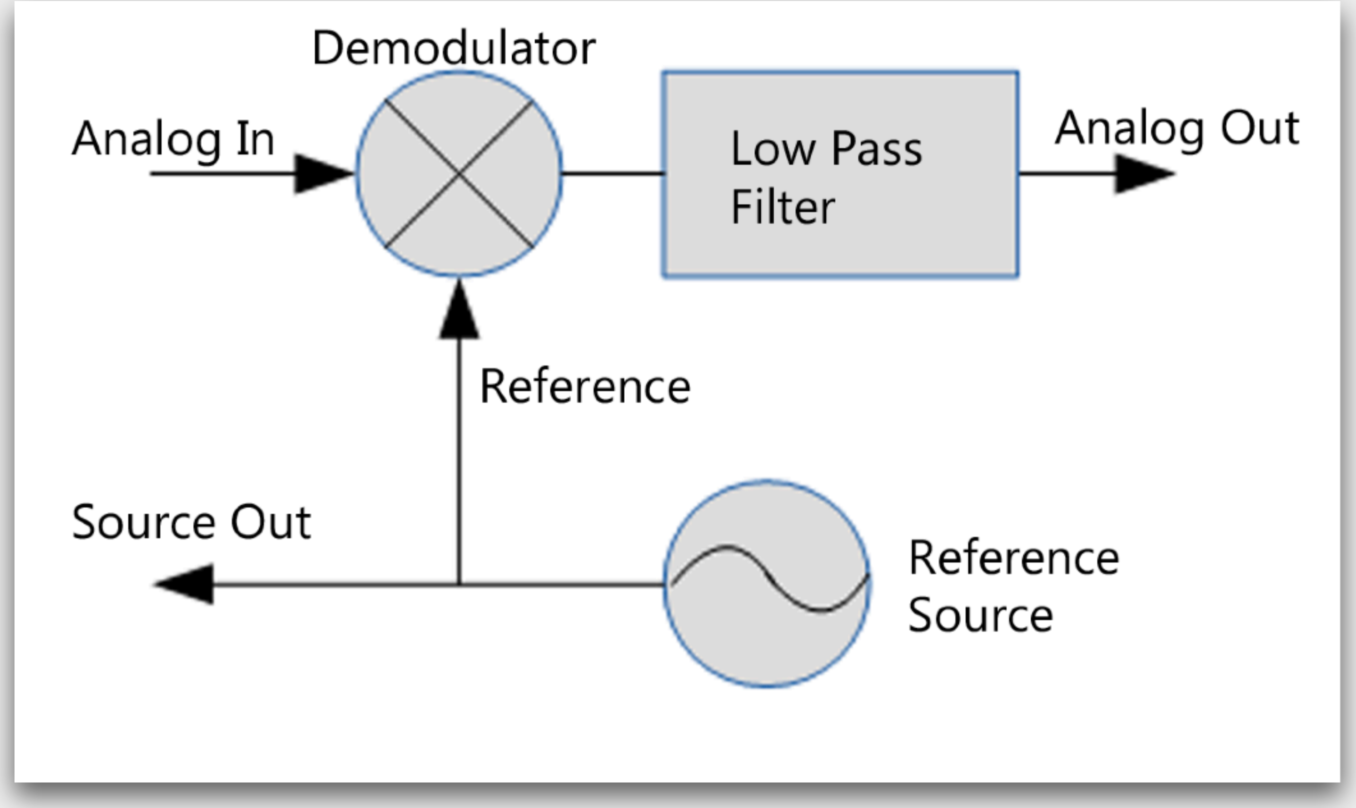

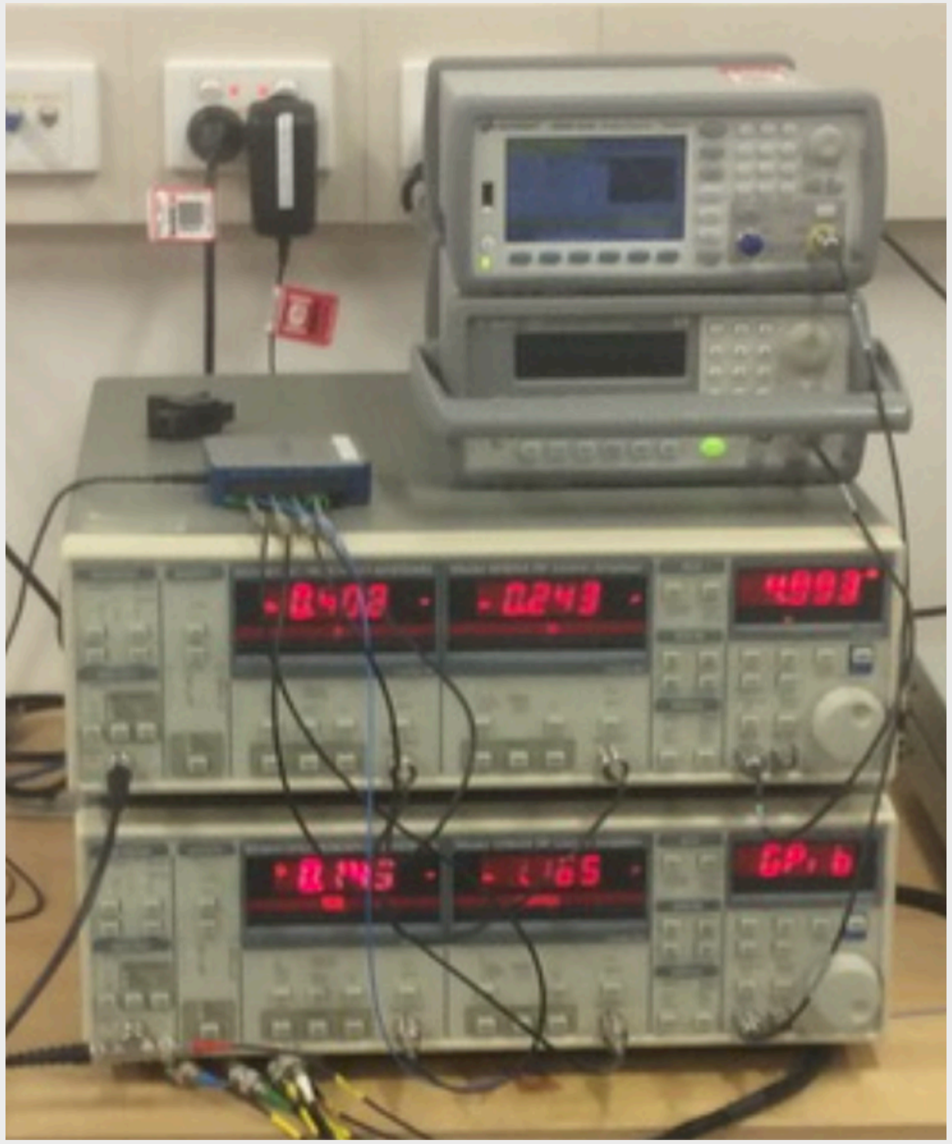

2 channels, up to 200MHz

Signal Processing

FPGA-based downconversion

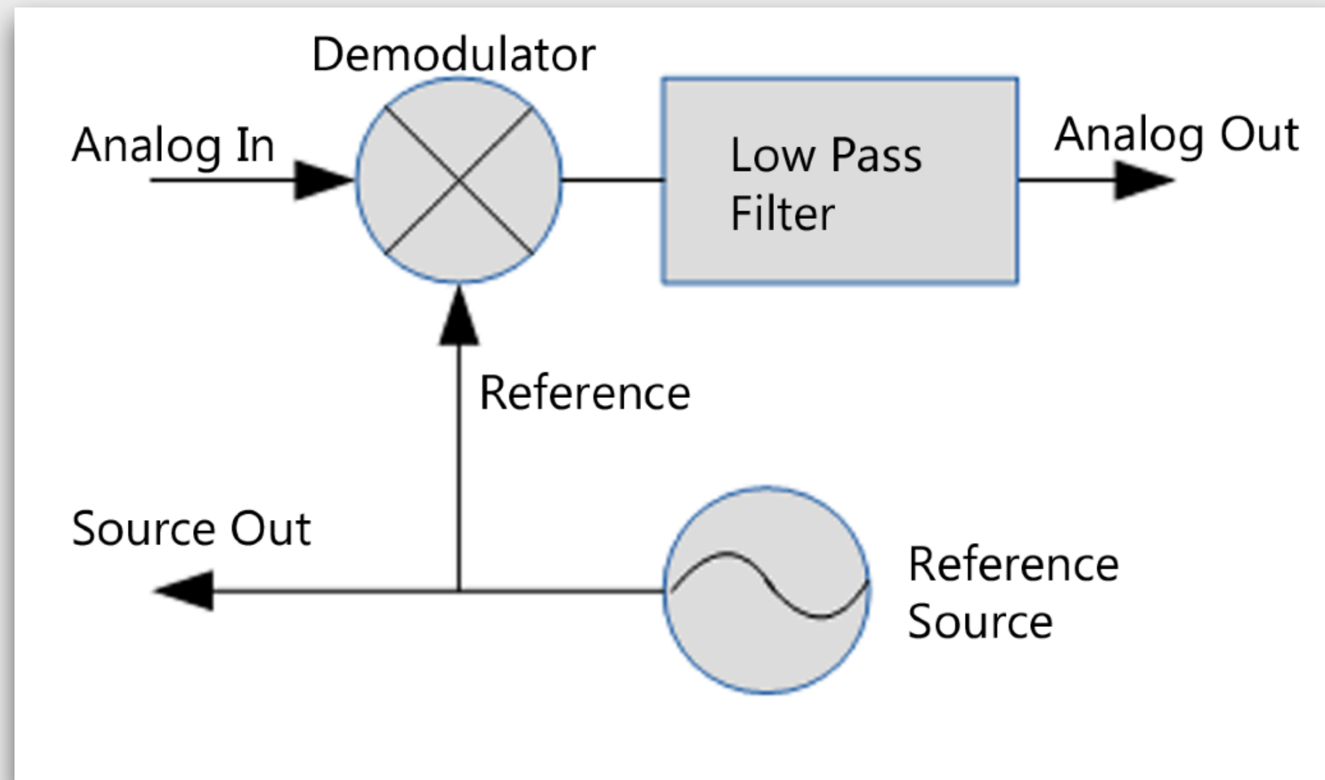

16 channels, up to 150MHz

no additional components

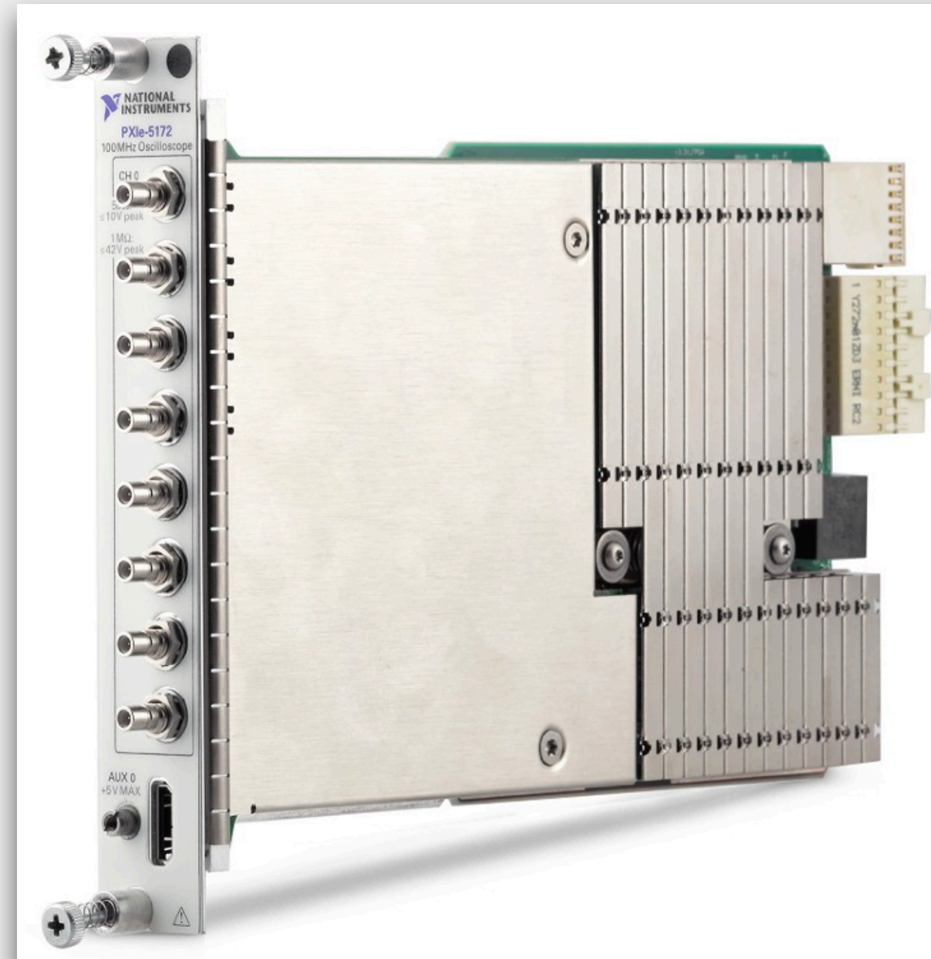

designed by Paul Altin (ANU)

EQUS
Australian Research Council Centre of Excellence for Engineered Quantum Systems

Further Improvements

Easy

- Increase number of modes/channels/crystals
- Improvements in signal processing
- Shifting to 20 mK (dilution fridge)
- mK higher frequency SQUIDs

Hard

- Design of Dedicated BAW cavities
- Multisite Detection

Outline

BAW Technology

BAW as a GW Antenna

Current Status and First Results

Perspectives

Test of Fundamental Physics @ UWA

ORGAN: Axion Haloscope Above 15GHz

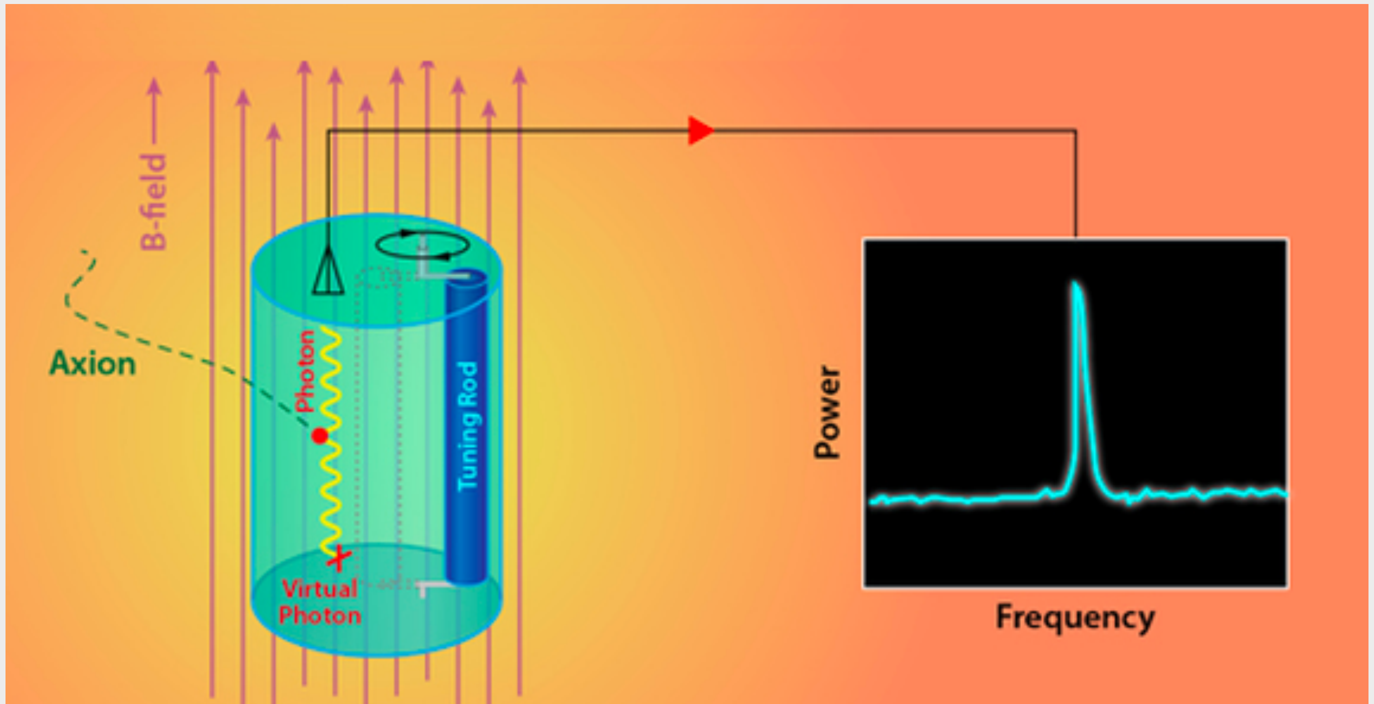

$$\mathcal{H}_{\text{int}} = \varepsilon_0 c g_{a\gamma\gamma}\theta\, \mathbf{E}\cdot\mathbf{B}$$

$$L_\theta = \frac{\alpha_s \theta}{8\pi} G^a_{\mu\nu}\widetilde{G}^{\mu\nu}$$

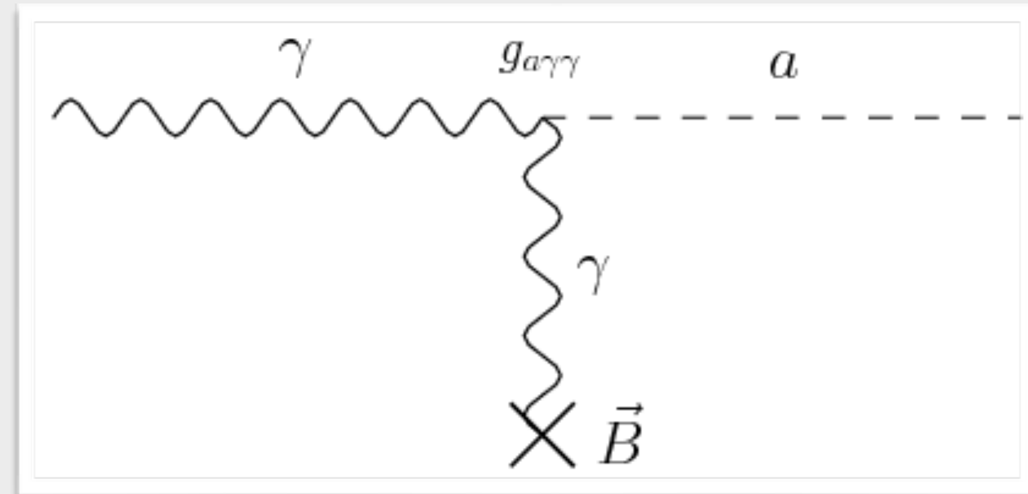

Inverse Primakoff effect

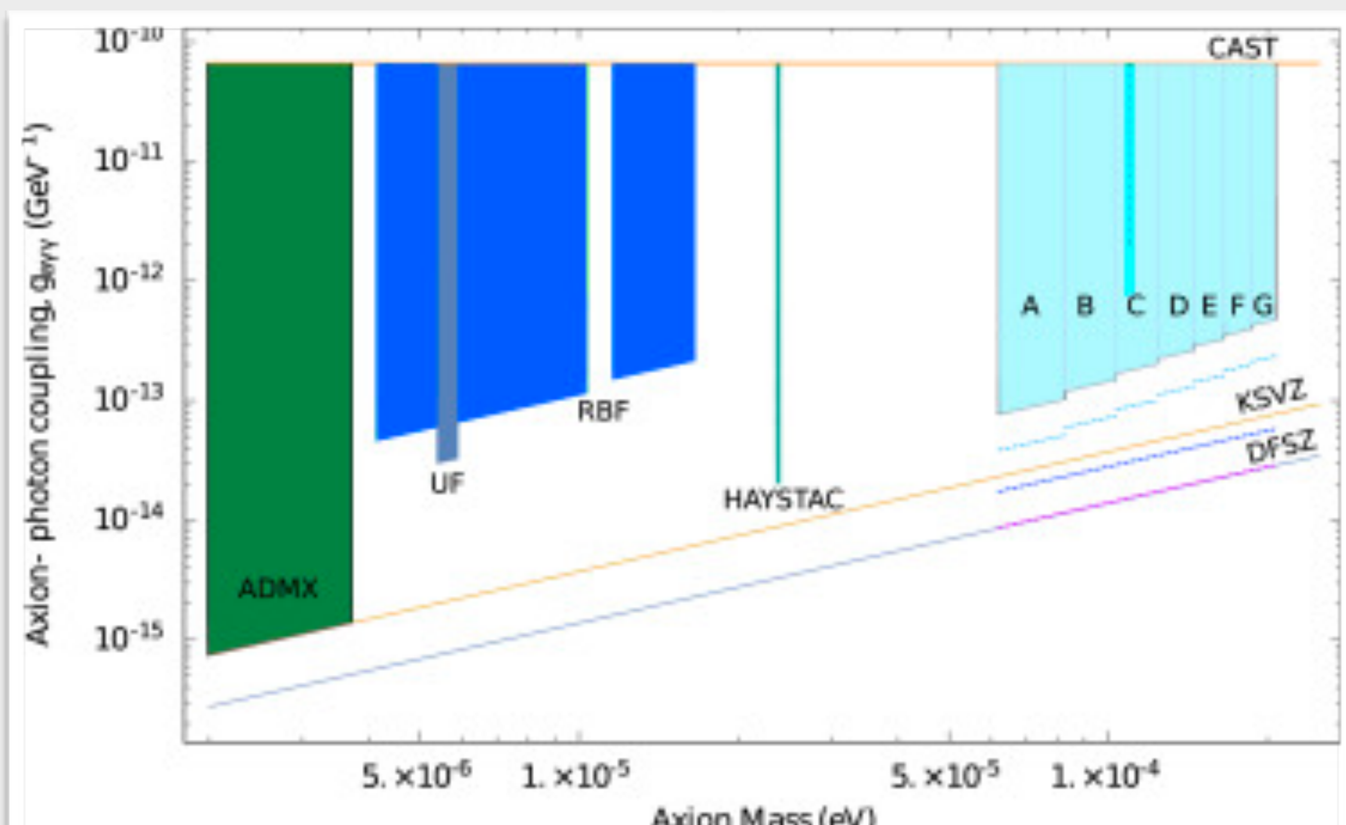

- Requires tuning
- Lowest possible temperatures (~20mK - dill fridge)
- Huge magnetic fields
- Low loss cavities
- Quantum limited amplification
- Huge mode volumes
- Mode design

Physics of the Dark Universe, Vol.18, 67-72 (2017)

EQUS
Australian Research Council Centre of Excellence for Engineered Quantum Systems

Ferromagnetic Haloscope

Electron-Axion Coupling

$$\hat{H} = -\frac{\hbar^2}{2m_e}\nabla^2 - \boxed{\frac{g_{aee}\hbar^2}{2m_e}\hat{\sigma}\cdot\nabla\mathbf{a},}$$

Axion Wind

$$a(\mathbf{r},t) = a_0 \sin\left(\omega_a t - \frac{m_a \mathbf{v_a}\cdot\mathbf{r}}{\hbar}\right)$$

System Hamiltonian

$$H = H_c + H_m + H_{\text{int}} + H_{aee}$$
$$H = \omega_c c^\dagger c + \omega_m b^\dagger b + g_{cm}(c^\dagger + c)(b^\dagger + b) + H_{aee},$$

Axion Induced Signal

$$P_{\text{out}}(\omega_a) = \frac{\hbar\omega_a\kappa_c^{\text{ext}} g_{cm}^2 \frac{S}{8}\gamma^2 B_{aee}^2 \sin^2(\phi)}{|\kappa_c\kappa_m\Delta_c\Delta_m - g_{cm}^2|^2}.$$

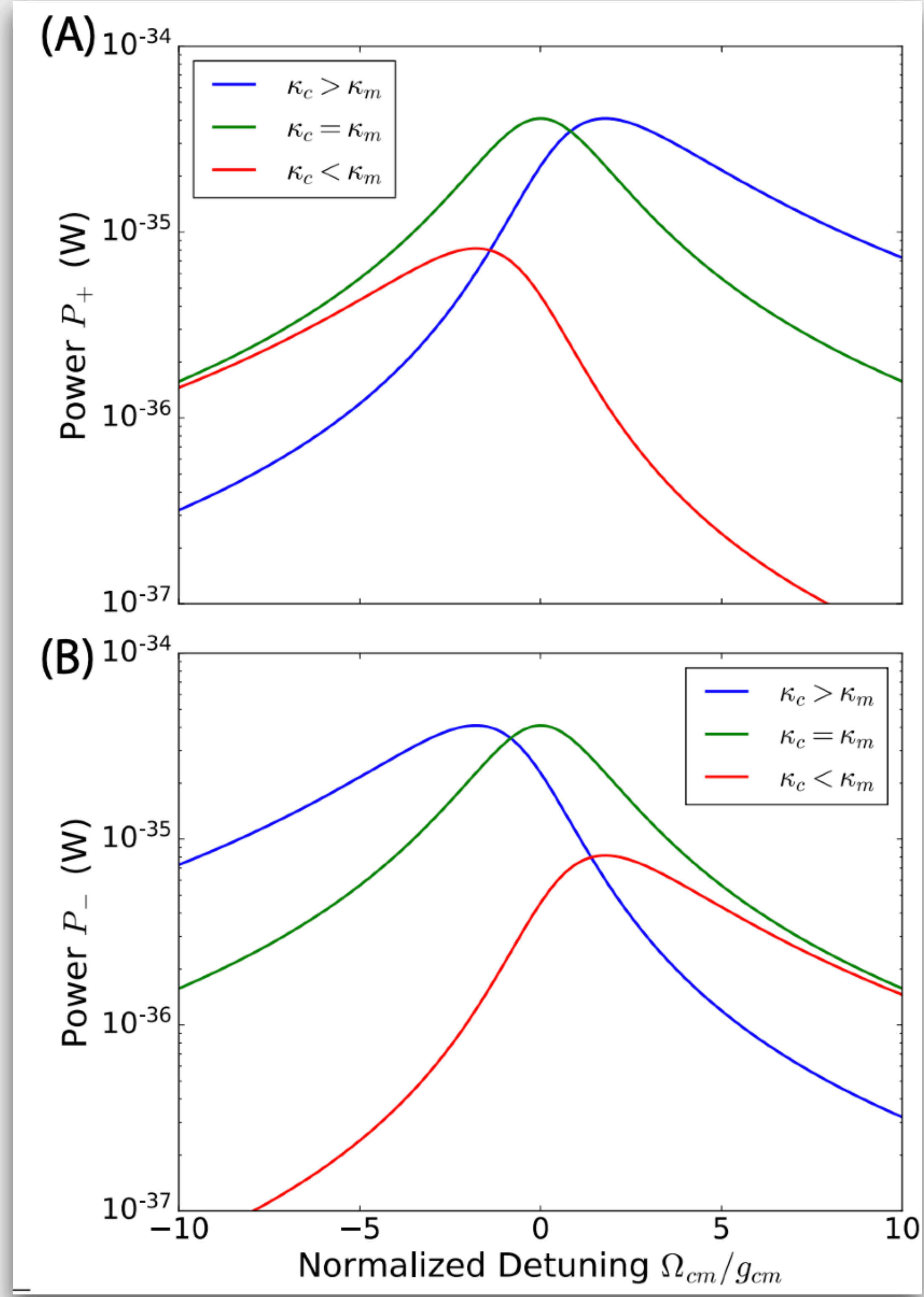

2mm diameter YIG sphere

Physics of the Dark Universe, Vol. 25, 100306 (2019)

EQUS
Australian Research Council
Centre of Excellence for
Engineered Quantum Systems

Ferromagnetic Haloscope

Dual Post Re-Entrant Cavity

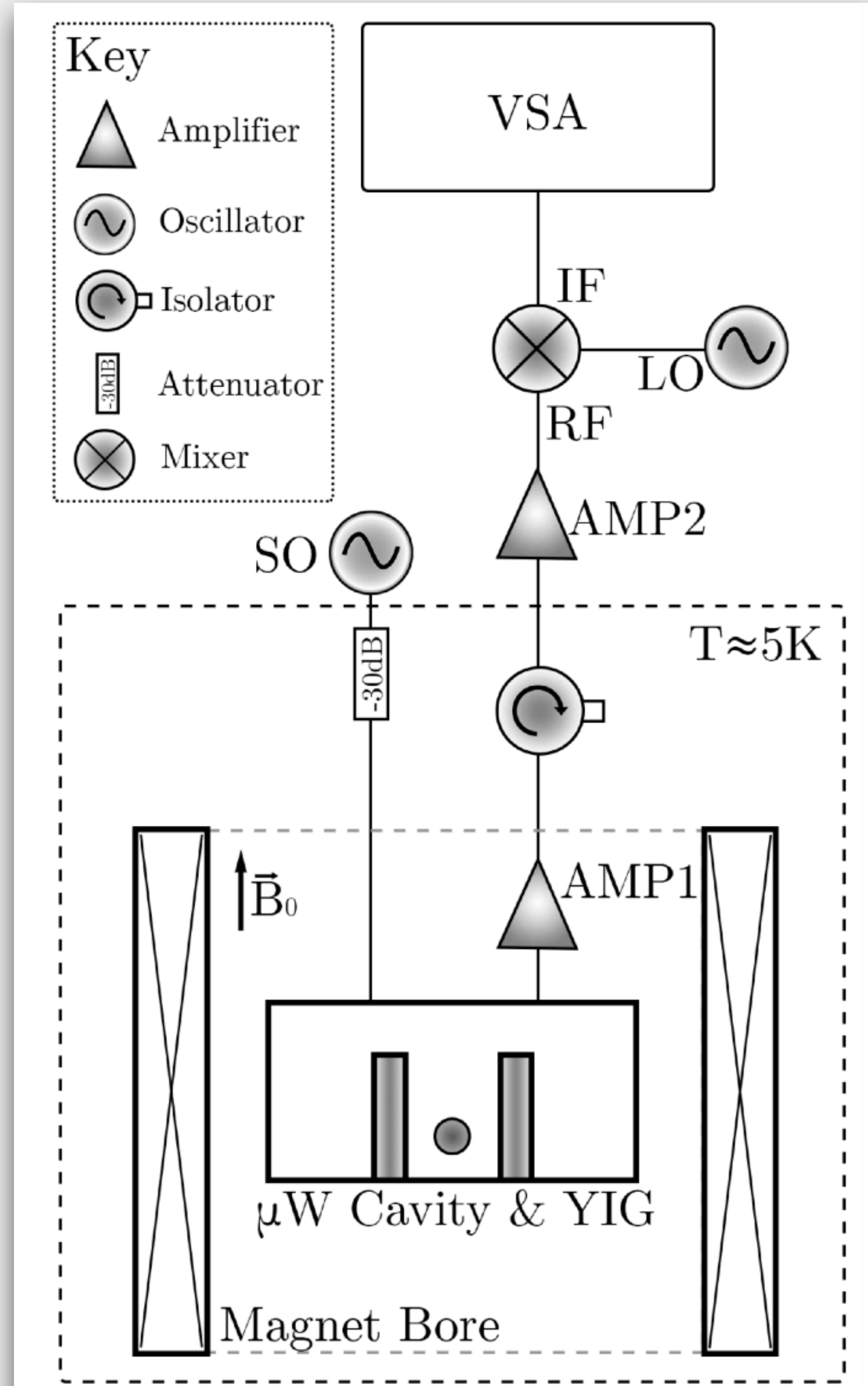

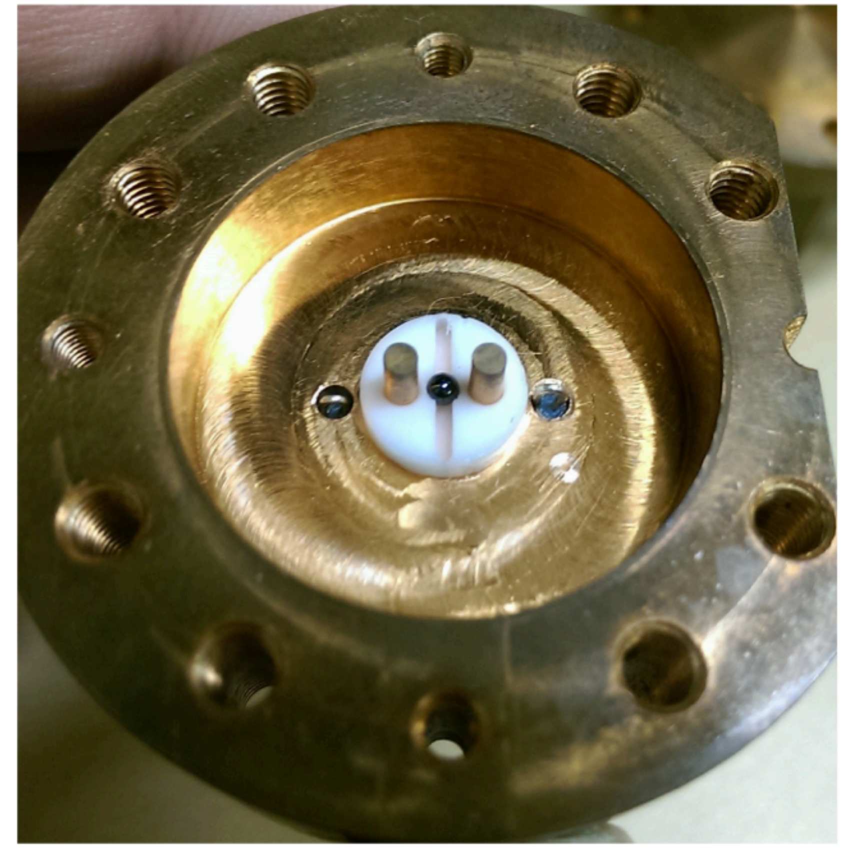

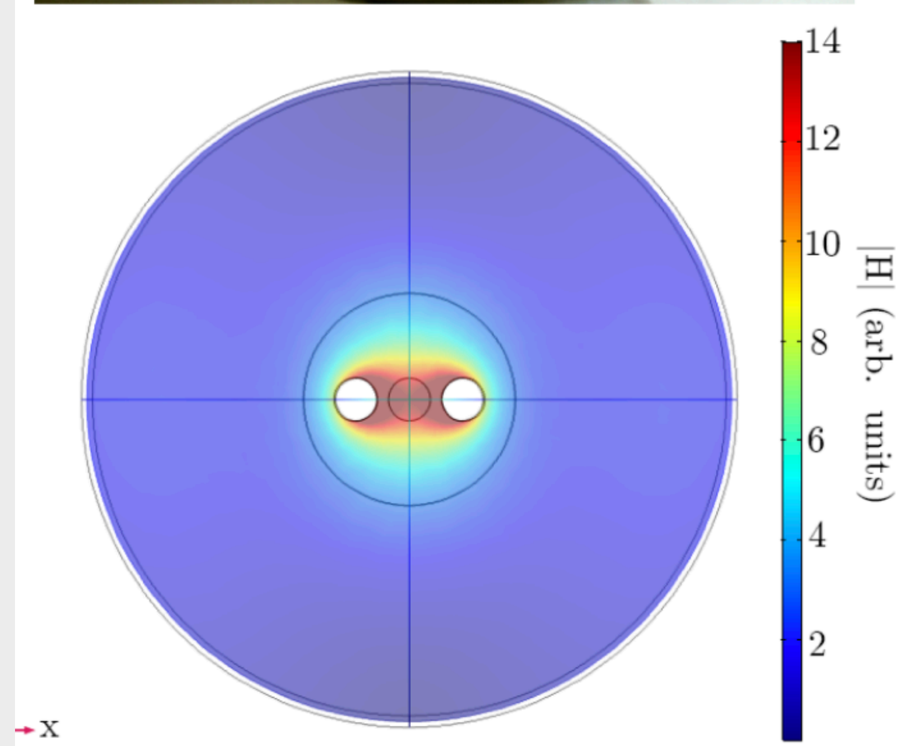

Physics of the Dark Universe, Vol. 25, 100306 (2019)

Ferromagnetic Haloscope

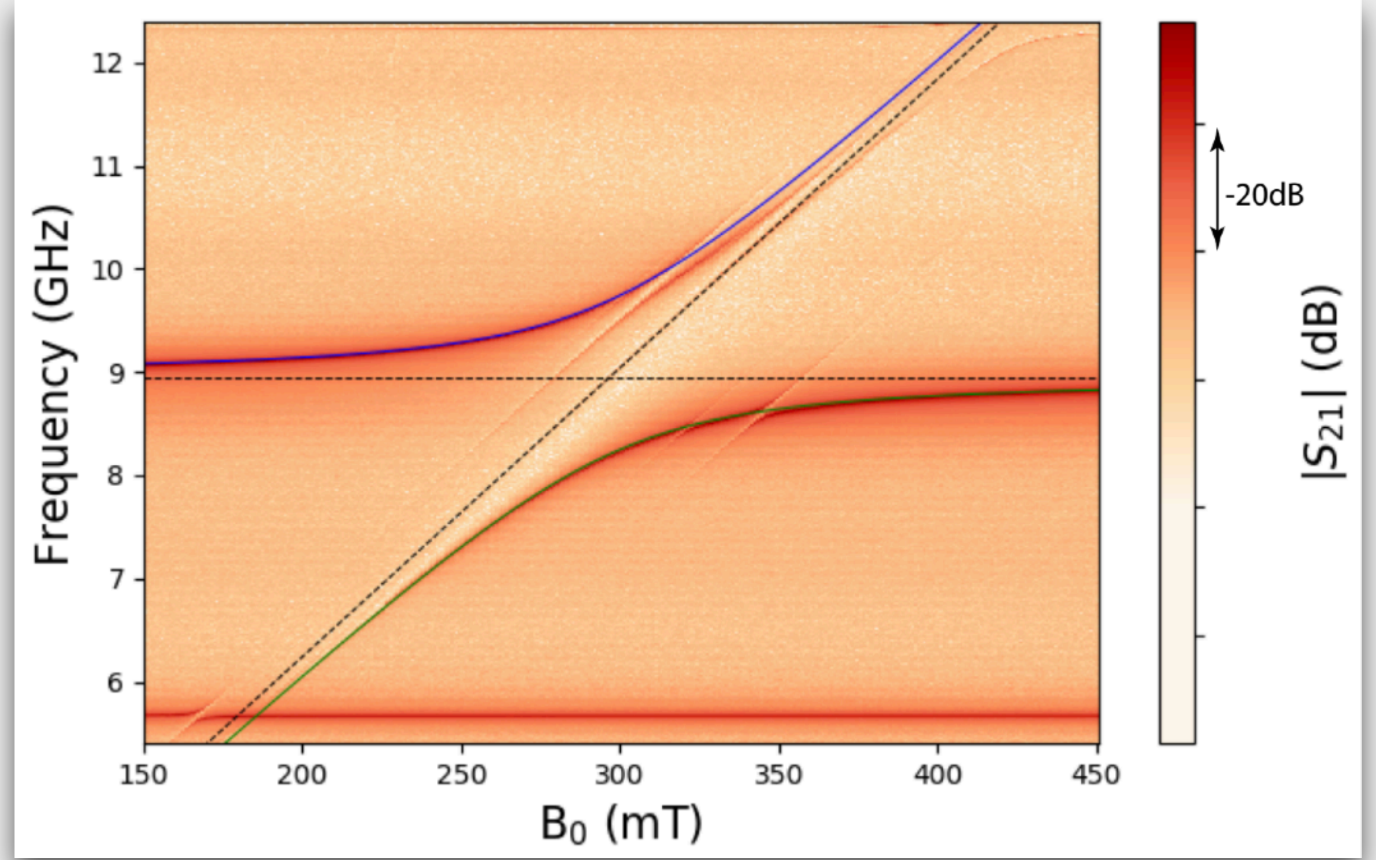

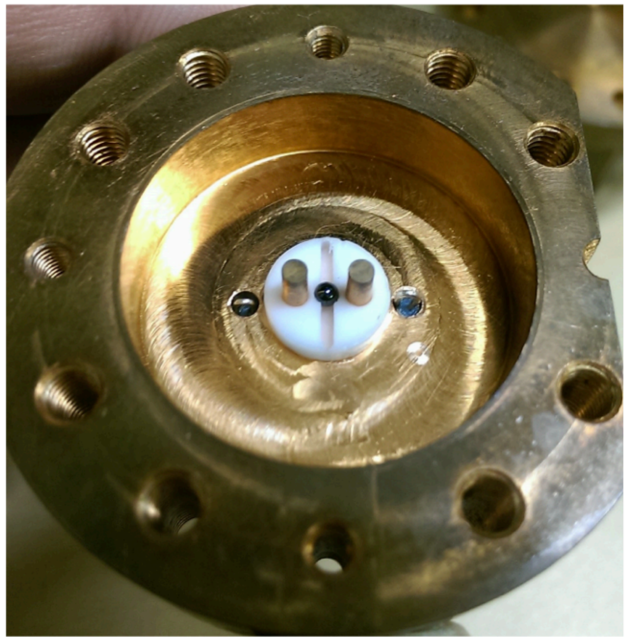

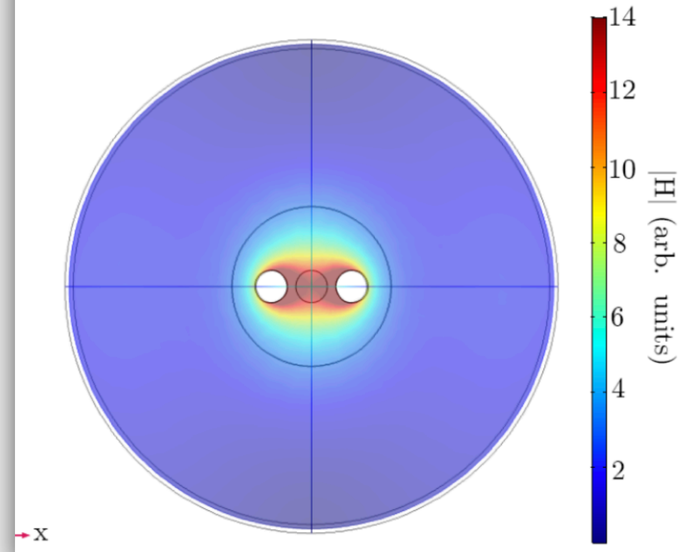

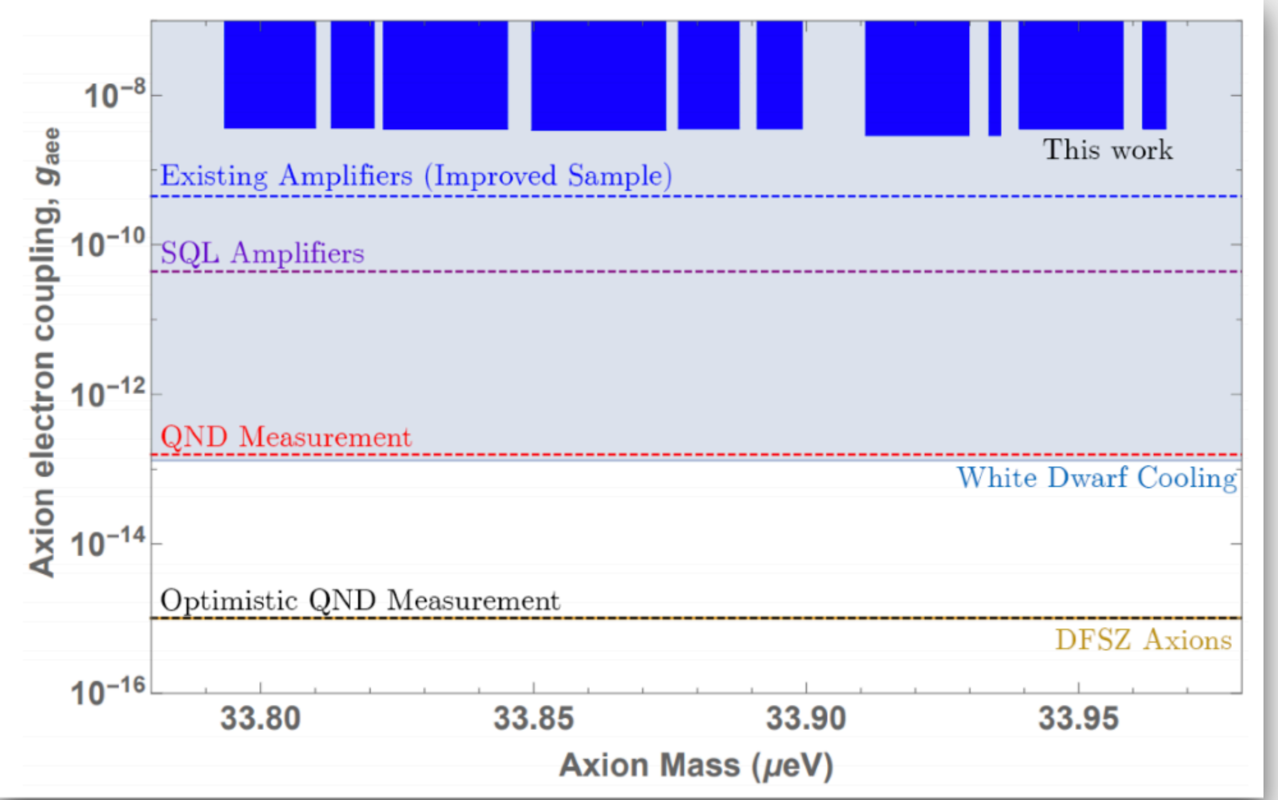

8 hours integration time (sensitive period)

2 hours integration time (insensitive period)

33.79 μeV$< m_a <$ 33.94 μeV with 95% confidence

Physics of the Dark Universe, Vol. 25, 100306 (2019)

EQUS
Australian Research Council Centre of Excellence for Engineered Quantum Systems

Ferromagnetic Haloscope

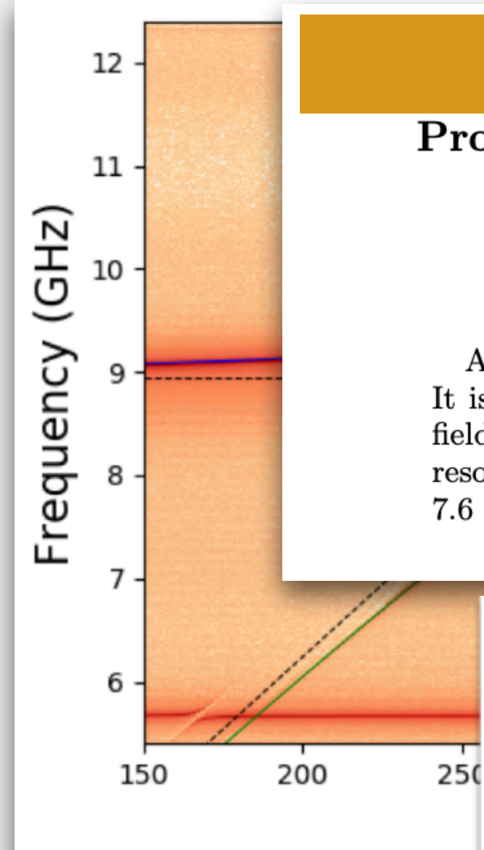

arxiv:1903.04843

KOBE-COSMO-19-01

Probing GHz Gravitational Waves with Graviton-magnon Resonance

Asuka Ito,* Tomonori Ikeda,† Kentaro Miuchi,‡ and Jiro Soda§

Department of Physics, Kobe University, Kobe 657-8501, Japan

(Dated: May 17, 2019)

A novel method for extending frequency frontier in gravitational wave observations is proposed. It is shown that gravitational waves can excite a magnon in the presence of an external magnetic field. Thus, gravitational waves can be probed by a graviton-magnon detector which measures resonance fluorescence of magnons. The sensitivity of the graviton-magnon detector reaches strains 7.6×10^{-22} [$\mathrm{Hz}^{-1/2}$] at 14 GHz and 1.2×10^{-20} [$\mathrm{Hz}^{-1/2}$] at 8.2 GHz, respectively.

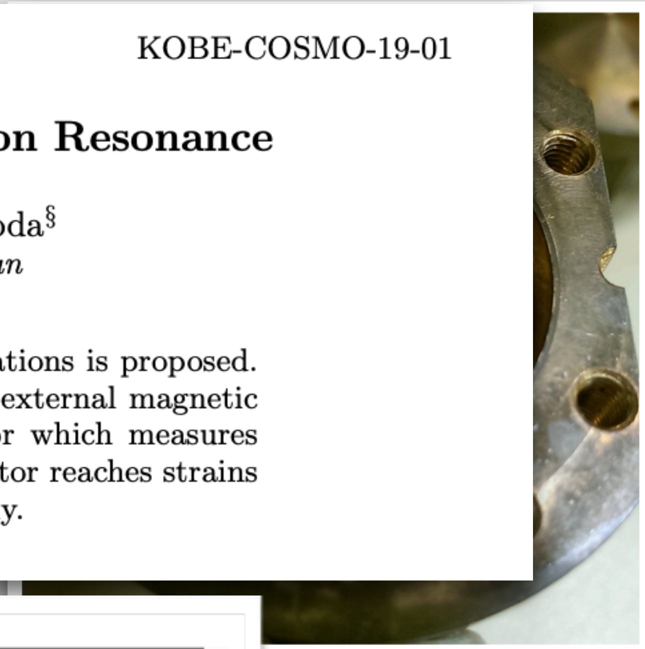

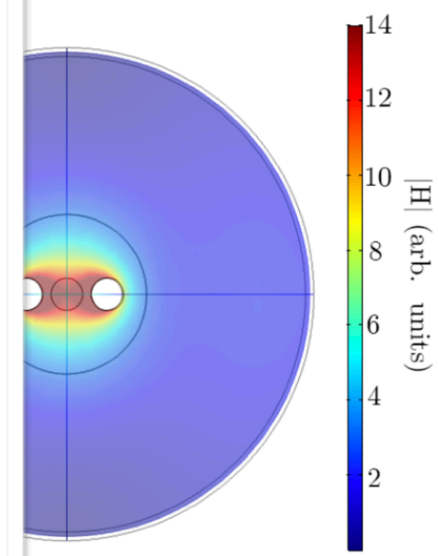

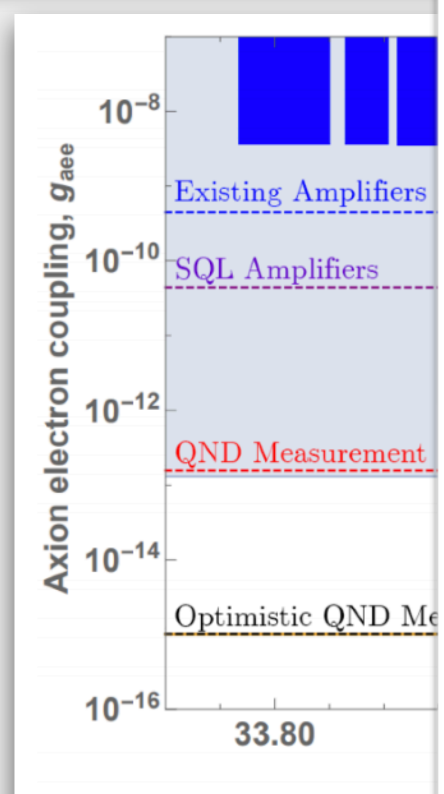

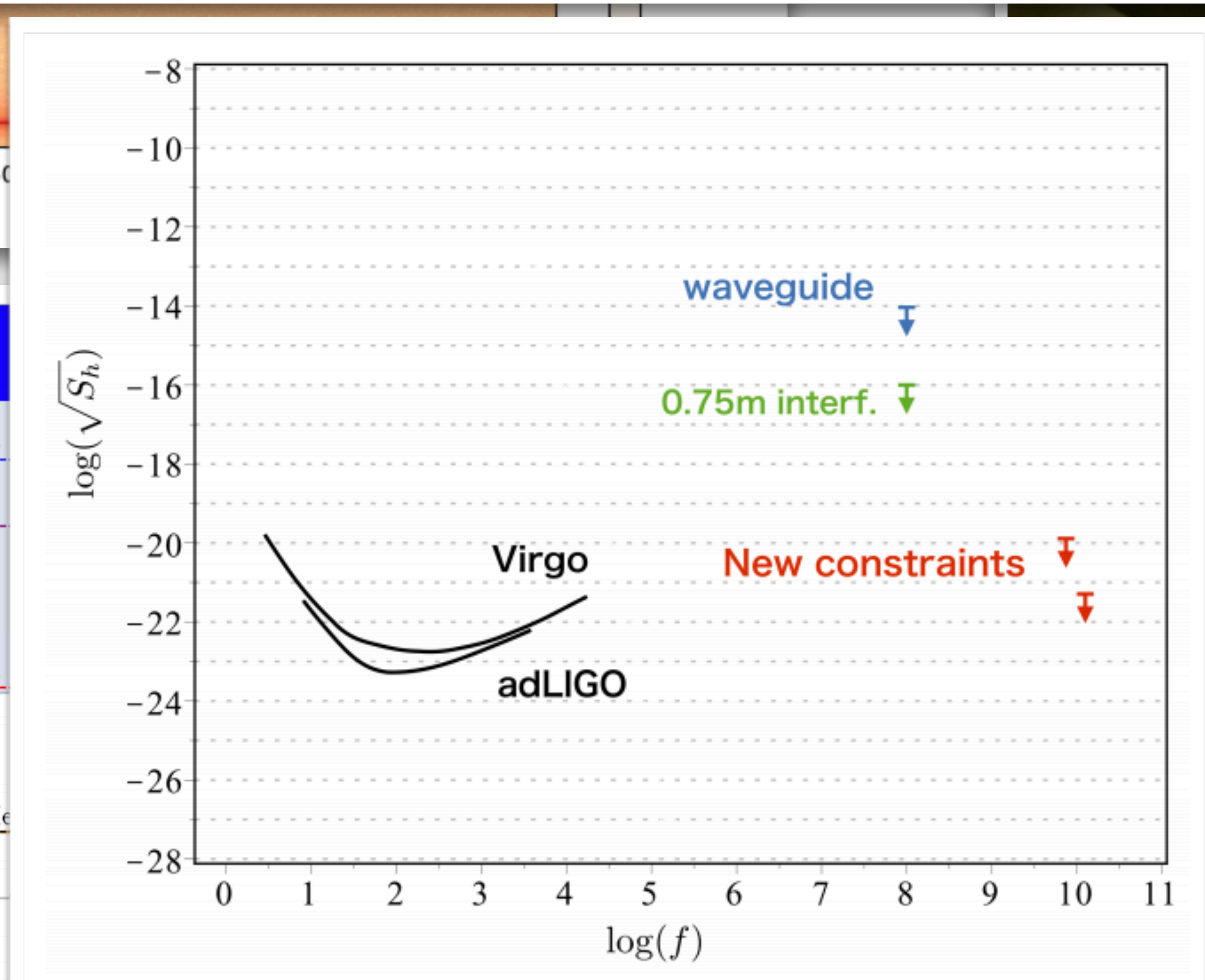

on time (sensitive period)

time (insensitive period)

.94 μeV with 95% confidence

Physics of the Dark Universe, Vol. 25, 100306 (2019)

Axion Detection with Frequency Metrology

$$\mathcal{H}_{\text{int}} = \varepsilon_0 c g_{a\gamma\gamma}\theta\ \mathbf{E}\cdot\mathbf{B}$$

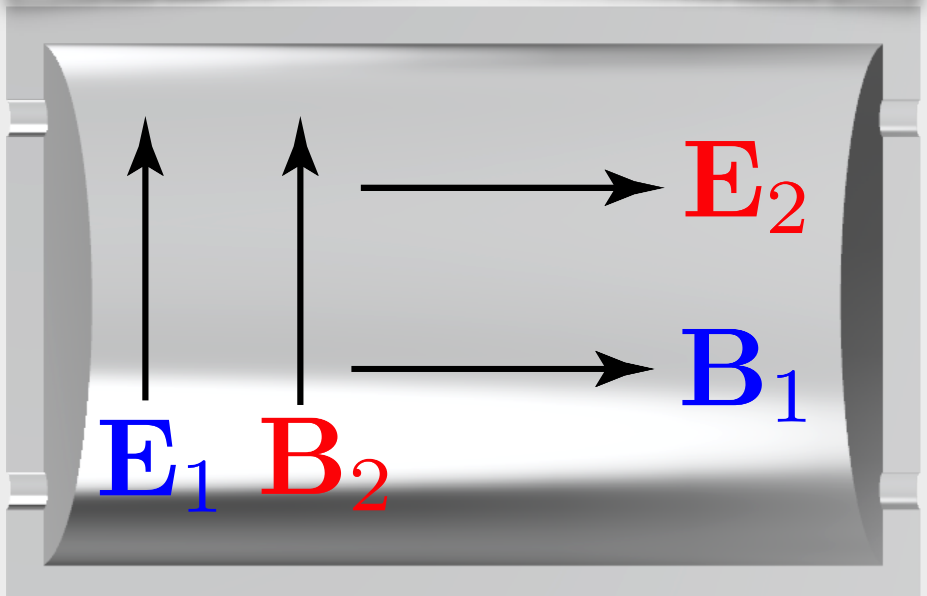

Axion UpConversion

$$\omega_a = \omega_2 - \omega_1$$

$$H_{\text{U}} = i\hbar g_{\text{eff}}\xi_-(a^* c_1 c_2^\dagger - a c_1^\dagger c_2)$$

Axion DownConversion

$$\omega_a = \omega_2 + \omega_1$$

$$H_{\text{D}} = i\hbar g_{\text{eff}}\xi_+(a c_1^\dagger c_2^\dagger - a^* c_1 c_2)$$

Axion induced phase fluctuations:

$$S_{\varphi,i}^{\text{U/D}}(f) = \left[1 + \frac{\gamma_i^2}{f^2}\right]\left(\frac{g_{\text{eff}}^2\xi_\pm^2}{f^2+\gamma_i^2}\left|\frac{\overline{x}_j}{\overline{x}_i}\right|^2 S_a(f) + S_\theta(f)\right)$$

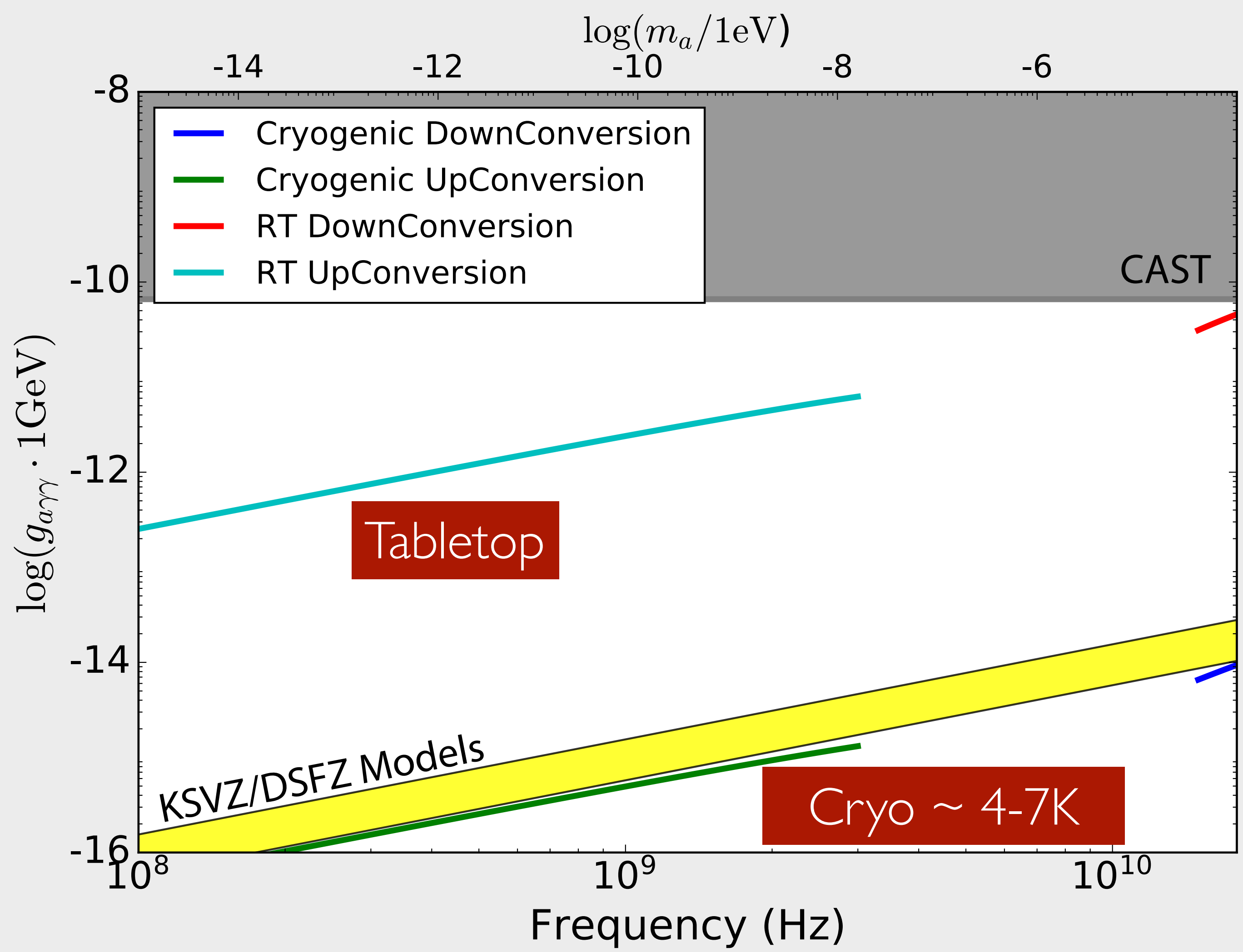

Physics of the Dark Universe, Vol. 26, 100345 (2019)

Physics of the Dark Universe, Vol. 23, 100244 (2019)

EQUS
Australian Research Council
Centre of Excellence for
Engineered Quantum Systems

Axion Modified Electrodynamics

Modified Axion Electrodynamics as Impressed Electromagnetic Sources Through Oscillating Background Polarization and Magnetization

Consequences for Low Mass Experiments

Michael Edmund Tobar, Ben T. McAllister, Maxim Goryachev

(Submitted on 5 Sep 2018 (v1), last revised 1 Aug 2019 (this version, v11))

We present a reformulation of axion modified electrodynamics with all modifications redefined within the constitutive relations between the D,H,B and E fields. This allows the interpretation of the axion induced background bound charge, polarization current and background polarization and magnetization satisfying the charge-current continuity equation. This representation is of similar form to photon sector odd-parity Lorentz invariance violating background fields. We show that when a DC B-field is applied an oscillating background polarization is induced at a frequency equivalent to the axion mass. In contrast, when DC E-field is applied, an oscillating background magnetization is induced at a frequency equivalent to the axion mass. We show that these terms are equivalent to impressed source terms, analogous to the way that voltage and current sources are impressed into Maxwell's equations in circuit and antenna theory. The impressed source terms represent the conversion of external energy into electromagnetic energy, and in the case of axion modified electrodynamics this is due to the inverse Primakoff effect converting energy from axions into photons. The axion induced oscillating polarization under a DC magnetic field is analogous to a permanent polarised electret oscillating at the axion Compton frequency, which sources an electromotive force from an effective impressed magnetic current source. In particular, it is shown that the impressed electrical DC current that drives the solenoidal magnetic DC field of an electromagnet, induces an impressed magnetic current parallel to the DC electrical c... so defines the boundary condition of the c...

Physics of the Dark Universe, Vol. 26, 100339 (2019)

$$\vec{E}_T = \vec{E} + \vec{E}_{aB}, \text{ where } \vec{E}_{aB} = -g_{a\gamma\gamma}\frac{c}{\epsilon_r}(a\vec{B}),$$

$$\vec{B}_T = \vec{B} + \vec{B}_{aE}, \text{ where } \vec{B}_{aE} = g_{a\gamma\gamma}\frac{\mu_r}{c}(a\vec{E}).$$

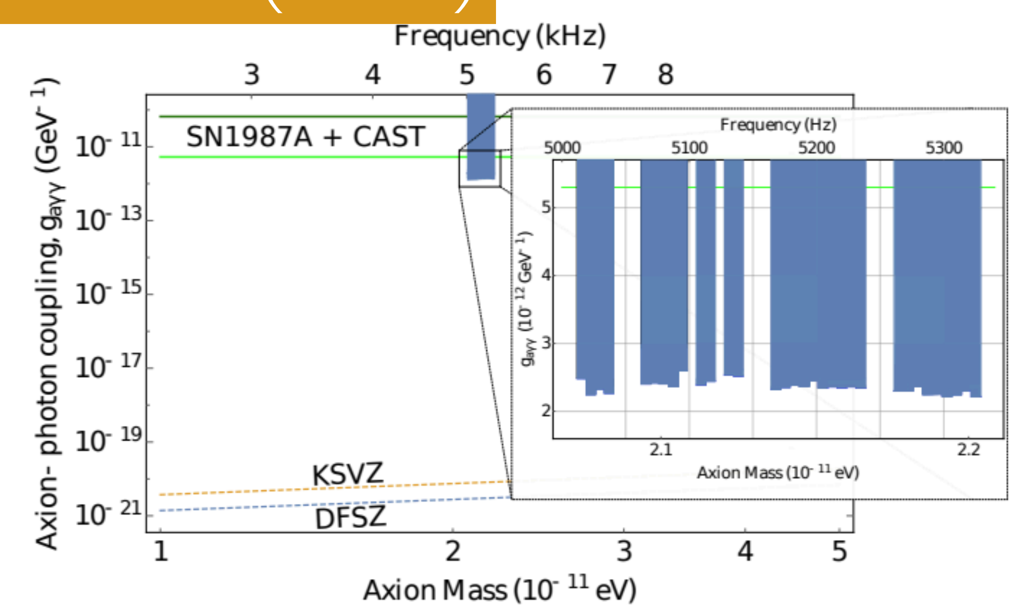

Broadband Axion Dark Matter Haloscopes via Electric Sensing

Ben T. McAllister, Maxim Goryachev, Jeremy Bourhill, Eugene N. Ivanov, Michael E. Tobar

(Submitted on 21 Mar 2018 (v1), last revised 26 Oct 2018 (this version, v4))

The mass of axion dark matter is only weakly bounded by cosmological observations, necessitating a variety of detection techniques over several orders of magnitude of mass ranges. Axions haloscopes based on resonant cavities have become the current standard to search for dark matter axions. Such structures are inherently narrowband and for low masses the volume of the required cavity becomes prohibitively large. Broadband low-mass detectors have already been proposed using inductive magnetometer sensors and a gapped toroidal solenoid magnet. In this work we propose an alternative, which uses electric sensors in a conventional solenoidal magnet aligned in the laboratory z-axis, as implemented in standard haloscope experiments. In the presence of the DC magnetic field, the inverse Primakoff effect causes a time varying permanent electric vacuum polarization in the z-direction to oscillate at the axion Compton frequency, which induces an oscillating electromotive force. We propose non-resonant techniques to detect this oscillating elctromotive force by implementing a capacitive sensor or an electric dipole antenna coupled to a low noise amplifier. We present the first experimental results and discuss the foundations and potential of this proposal. Preliminary results constrain $g_{a\gamma\gamma} >\sim 2.35\times10^{-12}$ GeV^{-1} in the mass range of 2.08×10^{-11} to 2.2×10^{-11} eV, and demonstrate potential sensitivity to axion-like dark matter with masses in the range of 10^{-12} to 10^{-8} eV.

arXiv:1803.07755

Lorentz Invariance Tests

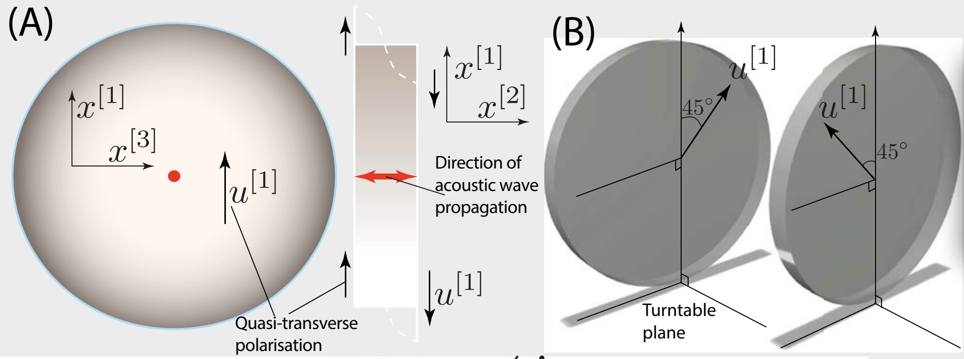

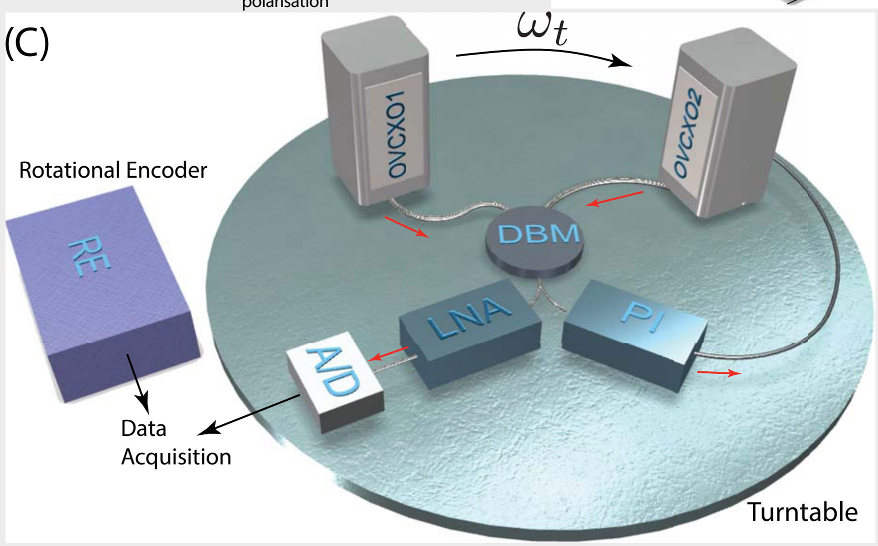

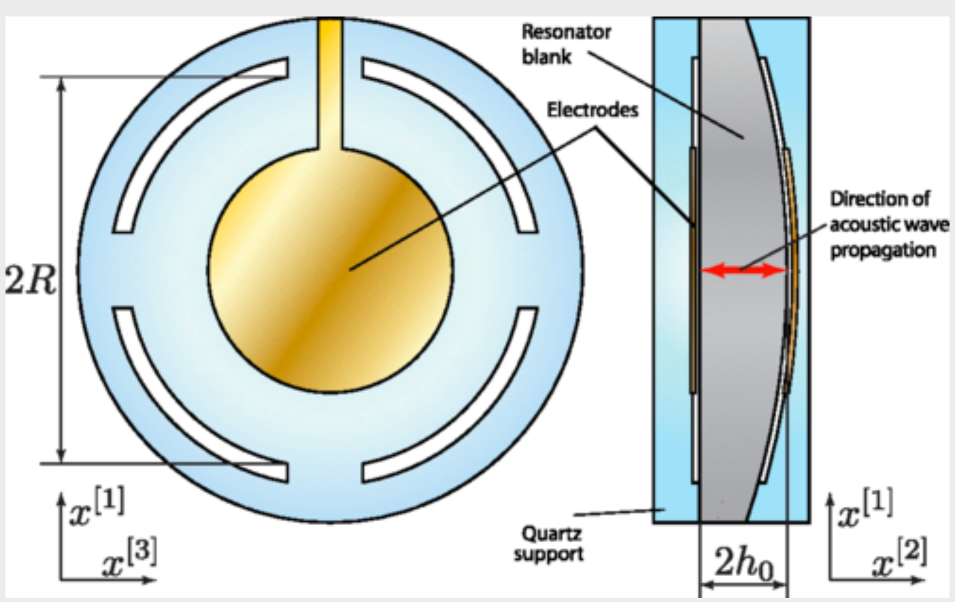

Acoustic Tests of Lorentz Symmetry Using Quartz Oscillators

Anthony Lo, Philipp Haslinger, Eli Mizrachi, Loïc Anderegg, Holger Müller, Michael Hohensee, Maxim Goryachev, and Michael E. Tobar

Phys. Rev. X **6**, 011018 – Published 24 February 2016

ABSTRACT

We propose and demonstrate a test of Lorentz symmetry based on new, compact, and reliable quartz oscillator technology. Violations of Lorentz invariance in the matter and photon sector of the standard model extension generate anisotropies in particles' inertial masses and the elastic constants of solids, giving rise to measurable anisotropies in the resonance frequencies of acoustic modes in solids. A first realization of such a "phonon-sector" test of Lorentz symmetry using room-temperature stress-compensated-cut crystals yields 120 h of data at a frequency resolution of 2.4×10^{-15} and a limit of $\tilde{c}_Q^n = (-1.8 \pm 2.2) \times 10^{-14}$ GeV on the most weakly constrained neutron-sector c coefficient of the standard model extension. Future experiments with cryogenic oscillators promise significant improvements in accuracy, opening up the potential for improved limits on Lorentz violation in the neutron, proton, electron, and photon sector.

Lowest Bound on anisotropy of Neutron Mass

Next Generation of Phonon Tests of Lorentz Invariance Using Quartz BAW Resonators

Publisher: IEEE

Abstract:
We demonstrate technological improvements in phonon sector tests of the Lorentz invariance that implement quartz bulk acoustic wave oscillators. In this experiment, room temperature oscillators with state-of-the-art phase noise are continuously compared on a platform that rotates at a rate of order of a cycle per second. The discussion is focused on improvements in noise measurement techniques, data acquisition, and data processing. Preliminary results of the second generation of such tests are given, and indicate that standard model extension coefficients in the matter sector can be measured at a precision of order 10^{-16} GeV after taking a year's worth of data. This is equivalent to an improvement of two orders of magnitude over the prior acoustic phonon sector experiment.

Phys. Rev. X 6, 011018 (2016)

IEEE TUFFC, Vol 65, 991-1000 (2018)

EQUS
Australian Research Council Centre of Excellence for Engineered Quantum Systems

Tests of Quantum Gravity

Testing of Generalized Uncertainty Principle With Macroscopic Mechanical Oscillators and Pendulums

P. A. Bushev, J. Bourhill, M. Goryachev, N. Kukharchyk, E. Ivanov, S. Galliou, M. E. Tobar, S. Danilishin

(Submitted on 8 Mar 2019 (v1), last revised 23 Aug 2019 (this version, v2))

Recent progress in observing and manipulating mechanical oscillators at quantum regime provides new opportunities of studying fundamental physics, for example, to search for low energy signatures of quantum gravity. For example, it was recently proposed that such devices can be used to test quantum gravity effects, by detecting the change in the [x,p] commutation relation that could result from quantum gravity corrections. We show that such a correction results in a dependence of a resonant frequency of a mechanical oscillator on its amplitude, which is known as amplitude-frequency effect. By implementing this new method we measure amplitude-frequency effect for 0.3 kg ultra high-Q sapphire split-bar mechanical resonator and for 10 mg quartz bulk acoustic wave resonator. Our experiments with sapphire resonator have established the upper limit on quantum gravity correction constant for $\beta_0 < 5\times10^6$ which is a factor of 6 better than previously detected. The reasonable estimates of β_0 from experiments with quartz resonators yield an even more stringent limit of 4×10^4. The data sets of 1936 measurement of physical pendulum period by Atkinson results in significantly stronger limitations on $\beta_0 \ll 1$. Yet, due to the lack of proper pendulum frequency stability measurement in these experiments, the exact upper bound on β_0 can not be reliably established. Moreover, pendulum based systems only allow testing a specific form of the modified commutator that depends on the mean value of momentum. The electro-mechanical oscillators to the contrary enable testing of any form of generalized uncertainty principle directly due to much higher stability and a higher degree of control.

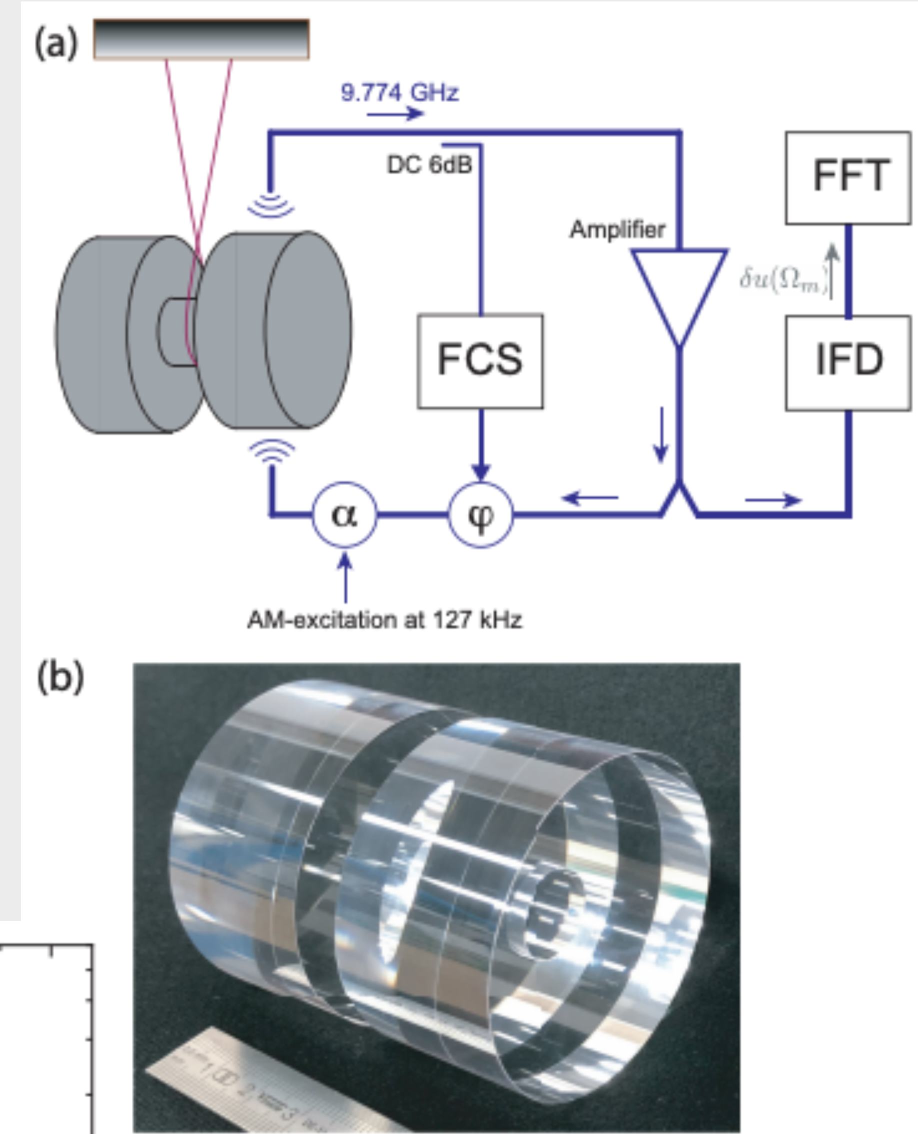

$$\Delta x \Delta p \geq \frac{\hbar}{2}\left[1 + \beta_0 \frac{\Delta p^2 + \langle p\rangle^2}{M_p^2 c^2}\right]$$

$$[\hat{x}, \hat{p}]_{\beta_0} = i\hbar\left[1 + \beta_0\left(\frac{\hat{p}}{M_p c}\right)^2\right],$$

$$\hat{H} \rightarrow \hat{H}_0 + \Delta\hat{H} = \left(\hat{p}^2/2m + m\Omega_0^2\hat{x}^2/2\right) + \beta_0\hat{p}^4/\left(3m(M_p c)^2\right)$$

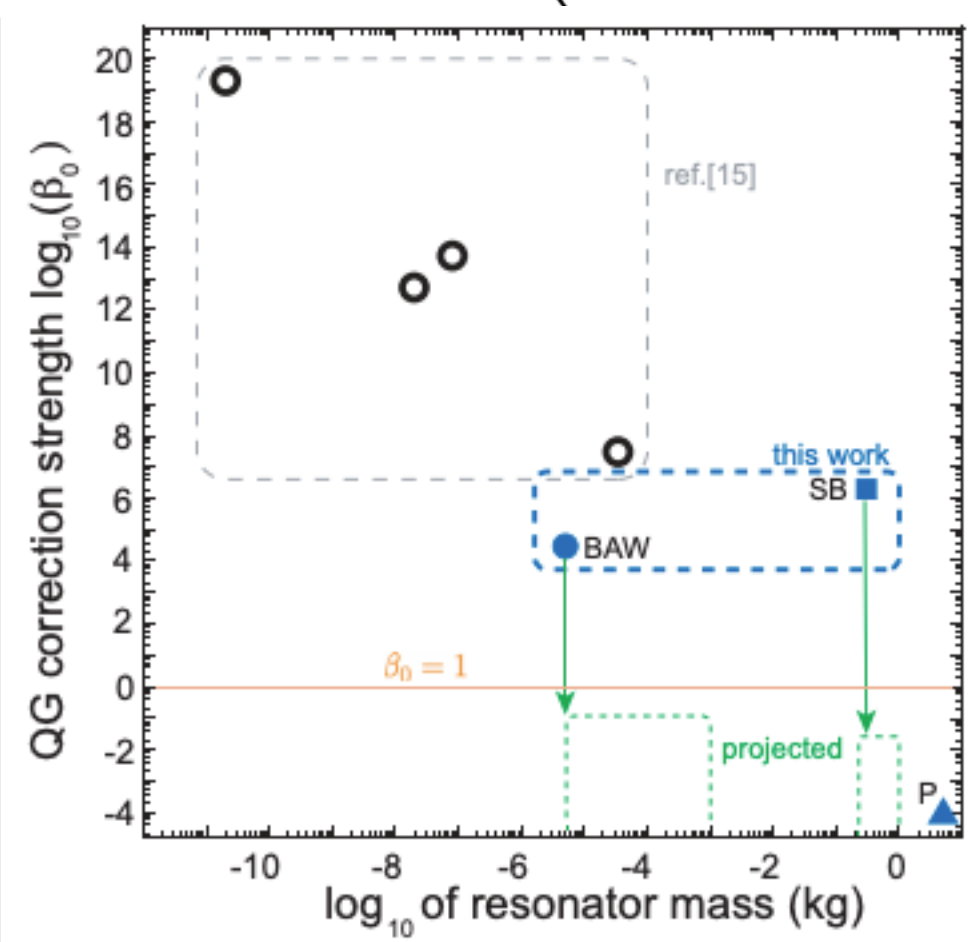

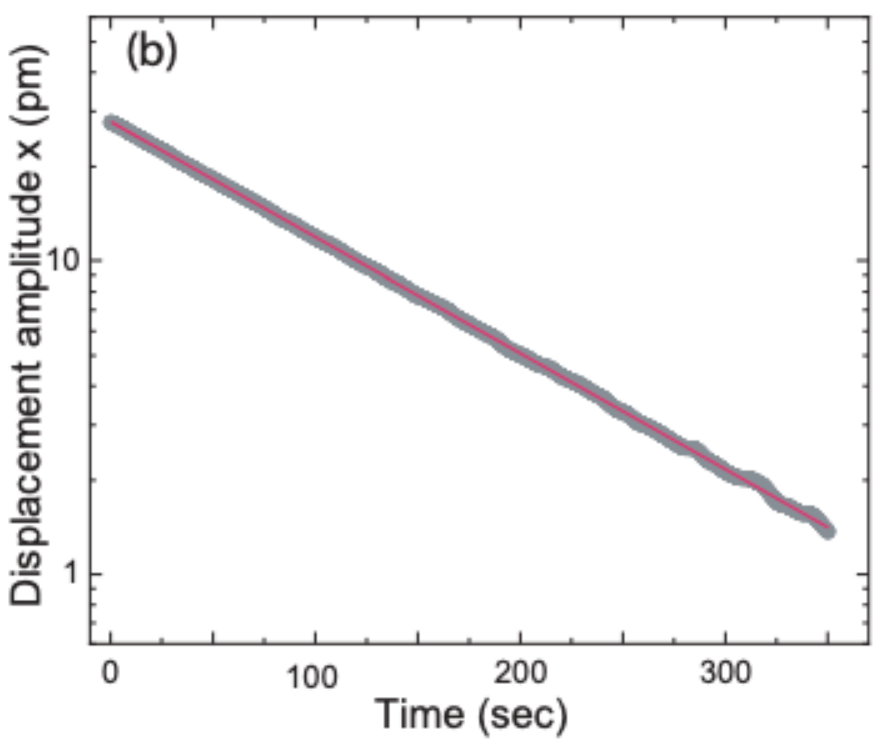

Phys. Rev. D 100, 066020 (2019)

EQUS
Australian Research Council Centre of Excellence for Engineered Quantum Systems

Advantages of BAW Technologies

Highest Qs in business
High Precision
Insensitive to external influences
Multi-Mode (1-100s MHz)
Piezoelectric Coupling to SQUIDs
Parametric coupling is possible
Reliable (mass production) technology
Small scale (~ 1 inch size)
Relatively inexpensive
Room for improvement!

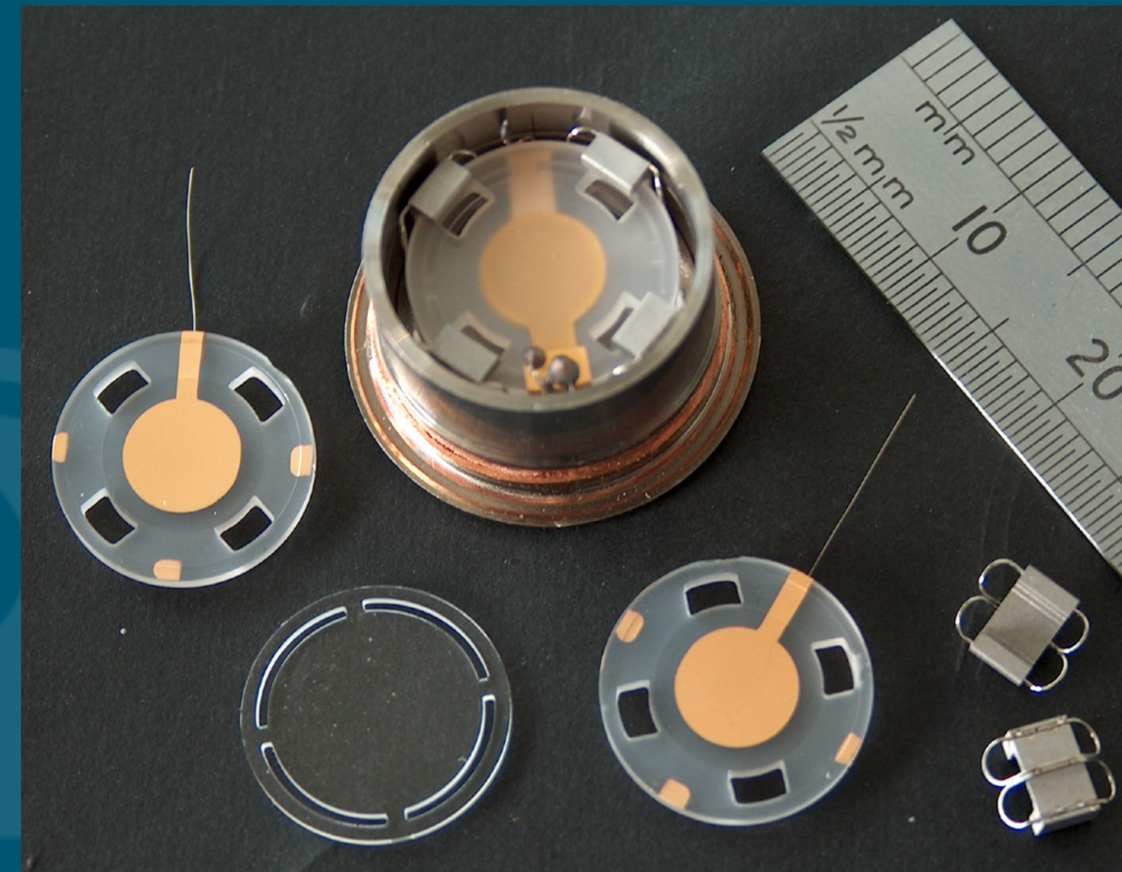

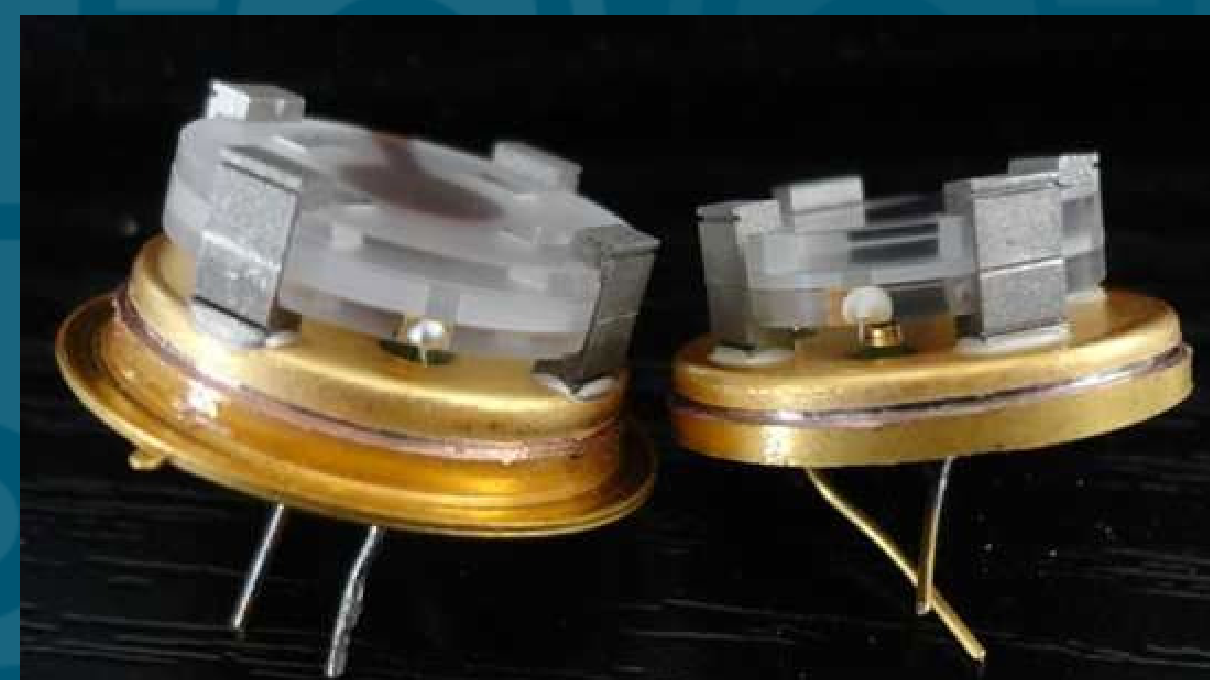

THE UNIVERSITY OF WESTERN AUSTRALIA

Phys.Rev.D 90, 102005 (2014)

Appl.Phys.Lett 105, 153505

EQUS
Australian Research Council
Centre of Excellence for
Engineered Quantum Systems